

X-17370

UNCLASSIFIED

BNL-178

Subject Category: PHYSICS

UNITED STATES ATOMIC ENERGY COMMISSION

**A SURVEY OF THREE HEAT EXCHANGERS
FOR A LIQUID METAL FUEL REACTOR**

By
M. Clark

DTIC QUALITY INSPECTED 2

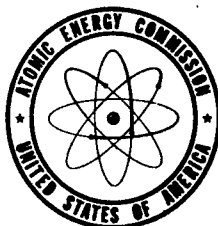
DISTRIBUTION STATEMENT A

Approved for public release
Distribution Unlimited

June 1952

Brookhaven National Laboratory
Upton, New York

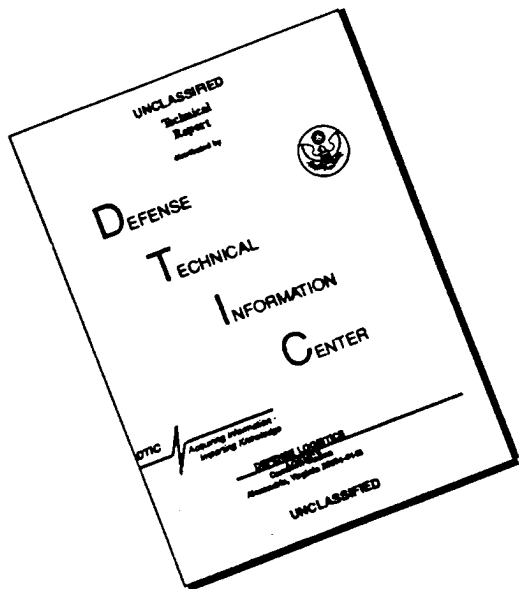
Technical Information Service, Oak Ridge, Tennessee



UNCLASSIFIED

19961016 461

DISCLAIMER NOTICE



**THIS DOCUMENT IS BEST
QUALITY AVAILABLE. THE COPY
FURNISHED TO DTIC CONTAINED
A SIGNIFICANT NUMBER OF
PAGES WHICH DO NOT
REPRODUCE LEGIBLY.**

Other issues of this report may bear the number LMFR-7.

Date Declassified: November 23, 1955.

This report was prepared as a scientific account of Government-sponsored work. Neither the United States, nor the Commission, nor any person acting on behalf of the Commission makes any warranty or representation, express or implied, with respect to the accuracy, completeness, or usefulness of the information contained in this report, or that the use of any information, apparatus, method, or process disclosed in this report may not infringe privately owned rights. The Commission assumes no liability with respect to the use of, or from damages resulting from the use of, any information, apparatus, method, or process disclosed in this report.

This report has been reproduced directly from the best available copy.

Issuance of this document does not constitute authority for declassification of classified material of the same or similar content and title by the same authors.

Printed in USA, Price 50 cents. Available from the Office of Technical Services, Department of Commerce, Washington 25, D. C.

BNL 178

A SURVEY OF THREE HEAT EXCHANGERS FOR A LIQUID METAL FUEL REACTOR

M. Clark

Work performed under Contract No. AT-30-2-Gen-16.

June 1952

Numerical Calculations:

Charles Eisenhauer
Leona Schloss
The author

Associated Universities, Inc.

BROOKHAVEN NATIONAL LABORATORY
Upton, N.Y.

CONTENTS

Notation - - - - -	6
Introduction - - - - -	7
Formulation of the Theory	
Tubular Heat Exchanger - - - - -	10
Spray Heat Exchanger - - - - -	15
Results	
Any Exchanger System - - - - -	23
Any Tubular Exchanger - - - - -	23
Tubular Exchanger Thermal Pumping - - - - -	23
Tubular Exchanger Mechanical Pumping - - - - -	24
Spray Exchanger Mechanical Pumping - - - - -	26
Summary of Results - - - - -	27
Acknowledgements - - - - -	31

Notation

a = inside radius of tube.
b = outer radius of tube walls.
c = a constant.
d = minimum distance between drops in spray heat exchanger.
f = heat transfer coefficient from liquid drops to salt (1.42 watts/cm²-°C).
g = acceleration due to gravitational force of the earth (980 cm/sec²).
h = power transfer coefficient from primary coolant to tube walls.
k = thermal conductivity of coolant (Bi: 0.15 watts/cm-°C).
l = length of each tube.
m = atoms of U per atom of Bi.
n = number of drops in heat exchanger.
p = Laplace transform variable replacing t.
 Δp = pressure drop.
q = radial distance from center of liquid drop.
r = radius of thermal legs.
 $s = \pi i \sqrt{P/k}$
 s_j = roots of a certain transcendental equation (equation (64)).
t = time taken by drop to fall to position z from point at which it was made.
u = speed of coolant in heat exchanger tubes.
v = speed of bismuth in drop-forming nozzles.
x = radius of header at point y along its axis.
y = distance along header from beginning of flare-out.
z = distance below plane where Bi drops are formed, at which the drop is located.
A = drop radius.
B = header height.
C = specific heat of coolant (Bi coolant: 0.148 joules/g-°C).
 C_0 = specific heat of salt (.92 joules/g-°C).
C' = a constant = 0.44.
D = $C_0 M_0 / CM$.
E = Young's modulus for tube walls (Croloy 2 1/4: 29×10^6 psi).
G = number of holes in drop-forming element near the top of the exchanger.
H = power flowing through each exchanger tube wall.
J = depth of Bi pool.
K = thermal conductivity of tube walls (0.26 watts/°C-cm).
L = total length of thermal legs, i.e. of piping connecting reactor with exchanger.
M = mass rate of flow of the primary coolant, viz. Bi.
 M_0 = mass rate of flow of salt.
N = number of tubes in heat exchanger.
P = power generated by reactor (450 Mw).
Q = volumetric flow rate of bismuth.
 Q_0 = volumetric flow rate of salt.
R = radius of the heat exchanger.
S = stress limit under operating conditions of tube walls (Croloy 2 1/4: 8000 psi).
 $T(A)$ = surface temperature of drop.
 $T_0(t)$ = salt temperature at position z = Ut.
 $T_0(0)$ = temperature of salt at its outlet.
 $T(q,t)$ = drop temperature at a radial distance q from its center at time t.
 $\bar{T}(r,t)$ = average temperature of drop.

A SURVEY OF THREE HEAT EXCHANGERS FOR A LIQUID METAL FUEL REACTOR

Introduction

Any power-producing reactor must be cooled. In the case of the liquid metal fuel reactor being considered by Brookhaven highly radioactive fuel, U, is dissolved in a primary coolant, Bi, of low cross section. The primary coolant transfers its heat by means of a heat exchanger to a secondary coolant, which operates at a low pressure. Finally, the secondary coolant transfers its heat by means of a second heat exchanger to a third thermodynamic medium operating at a high pressure. At the present stage in the art of designing reactors it is ill advised to operate the secondary coolant at a high pressure and to dispense with the tertiary coolant, because of the hazard of a leak into the primary coolant. Also, the secondary coolant may become excessively radioactive to be used as the final thermodynamic medium. All these transfers of heat from one coolant to another must take place with as little temperature degradation as possible in a system of great reliability⁽¹⁾.

The primary heat exchanger system should have as small a volume as is convenient in other respects in order to decrease the fuel investment. The problem of how to make a primary exchanger system of minimum volume or at least of small volume is the concern of this report. We do not consider the various other exchangers which may succeed the primary one, nor do we consider the refinements of even the primary exchanger. We are interested rather in surveying the effects of the many quantities that determine the exchanger system volume and general configuration. We shall try to avoid the fine points which would have to be considered in the design of an actual exchanger system. This work is motivated by the desire to get a better estimate of the doubling time and fuel investment in our liquid metal fuel reactor systems.

In this report we shall examine three heat exchanger systems that might be used in conjunction with the liquid fuel reactor described in a rudimentary manner in BNL-111⁽²⁾.

1. A conventional heat exchanger with many Croloy 2 1/4 tubes through which the primary reactor coolant, the bismuth-uranium fuel itself, flows countercurrently to the secondary coolant. The primary coolant circulates by reason of the density difference in that coolant between the hot and the cold legs connecting the heat exchanger and the reactor. The heat exchanger is located high enough above the reactor so that the primary coolant circulates at the requisite rate. We call this manner of circulating the coolant "thermal pumping."

(1) The author hopes that some day all this temperature degradation and complexity can be eliminated by some one magic coolant. Such a fluid must have a low neutron cross section, so that it can be used in the reactor itself and will not become significantly radioactive. In it the fuel will be dissolved or suspended; the two might be separated easily by some clever method. This one, prime coolant would drive turbines directly; the fissionable material would remain behind and be directly returned to the reactor. Heavy water or helium under high pressure might be a candidate for this position.

(2) D.H. Gurinsky, and others, "Preliminary Study of a Uranium-Bismuth Liquid Fuel Power Reactor," BNL-111, (1951).

2. The second system is the same as that in scheme 1, except that any thermal pumping is augmented by a mechanical pump. This method of circulating the coolant is called "mechanical pumping."
3. The third scheme uses a novel heat exchanger in which the very dense bismuth coolant is formed into drops near the top of the heat exchanger. The drops are allowed to fall through and in direct contact with a molten liquid salt of low density, viz., LiCl-KCl. This salt is introduced near the bottom of the heat exchanger and is collected at the top above the height at which the bismuth drops are formed. The bismuth drops agglomerate in a region below the point at which the liquid salt is introduced. The salt, in addition to purifying the bismuth-uranium fuel of all fission products⁽³⁾, acts as the secondary coolant. Thermal pumping appears to be out of the question with this scheme; we can consider only mechanical pumping. This system will be referred to as the "spray heat exchanger system." The other type of heat exchanger we shall call a "tubular heat exchanger." We shall see that the spray type of heat exchanger has many positive virtues, although it raises several problems.

The complete power system may be divided into a reactor, a heat exchanger which transfers energy from the primary, radioactive coolant used in the reactor to the secondary, non-radioactive coolant used as a thermodynamic medium, and the power-producing unit itself. We shall consider only the heat exchanger, the importance of various factors in the design of the primary heat exchanger system and their effect on the investment of uranium. We may characterize the reactor, for the purposes of this report, as a device producing a certain amount of power at a specific temperature differential between inlet and outlet, and requiring a certain constant pressure differential to drive the primary coolant. The header causes a loss in the kinetic energy of the coolant, especially in the flare-out.

The tubular heat exchanger is the source of both frictional losses and kinetic losses (especially at the flare-out). The heat energy in passing through the walls of the heat exchanger tube is degraded in temperature both as a result of the gradient through the walls and of the drop across the laminar film between the coolant and the tube walls. The remaining film drop between the outside of the tubes and the secondary coolant is left to the consideration of the engineer designing the other parts of the system which will utilize the heat energy. Masses of uranium are invested in the legs, the header, and the heat exchanger. The investment in the header is trivial, however, compared to the investment elsewhere.

For reasons of convenience we choose as the independent variables the inner radius of the heat exchanger tubes, their wall thickness, the number of tubes in the heat exchanger, the speed in the thermal legs, the temperature drop across the tube walls and the laminar film between the walls and the bismuth, and the fractional kinetic energy loss parameters. From these arbitrarily chosen quantities we find the radius of the thermal legs, the speed in the heat exchanger tubes, the heat transfer coefficient, the length of the heat exchanger tubes, the volume of the heat exchanger system, and the mass of uranium invested in it. In the case of thermal pumping, we calculate the length of the thermal legs. In the case of mechanical pumping, this leg length is an independent variable; we compute the pumping power and pressure differential the pump must create.

⁽³⁾D. Bareis, "A Continuous Fission Product Separation Process," BNL-125, (1951).

The advantages of a spray exchanger have been manifest for many years: the uranium investment is relatively small, and the energy is available at but a small degradation in temperature. In this exchanger the energy is degraded in temperature by the film between the bismuth drops and the salt and by the gradient in the drops themselves. In any horizontal plane the salt is considered to be isothermal because of the mixing and because of the fact that the drops fall uniformly on the plane. In this exchanger, the bismuth loses all its kinetic energy in being formed into drops at the top of the exchanger and also suffers a modified head loss in falling as drops through the exchanger. These pressure losses preclude the use of thermal pumping.

Again for reasons of convenience we take the radius of the drops, the speed at which the salt flows through the heat exchanger, the height of the heat exchanger and the ratio of the mass rates of flow of salt to bismuth as the independent variables. From these we compute the speed at which the drops fall, the difference between the inlet and outlet salt temperatures, the volumetric and mass flow rates of the bismuth and the salt, the closest spacing of the grid forming the drops, the number of drops, the radius of the heat exchanger, the number of nozzles needed to form the drops, the investment in uranium and in bismuth, the pressure drop, and the pumping power.

Several of the various parameters seem arbitrarily chosen. We are considering the heat exchanger system for case F in Table A-1 of BNL-111 and make the assumptions of Appendix 1 of that report. In point of fact, there is really nothing fixed about the power developed by the reactor, or the pressure drop and temperature differential across it. They could be very different from the numbers selected here.

In the next section we formulate a theory for tubular heat exchangers and for spray heat exchangers. In the third section we present the results for the heat exchangers considered in this report.

Formulation of the Theory

Tubular Heat Exchanger

The primary coolant, bismuth, flows as the heatant inside circular tubes over whose external surfaces the secondary coolant flows countercurrently. A schematic

diagram is shown in Figure 1. If the fluid is pumped thermally, then the heat exchanger must be high enough above the reactor to provide a pressure differential between the hot and cold legs sufficient to circulate the bismuth at the rate needed.

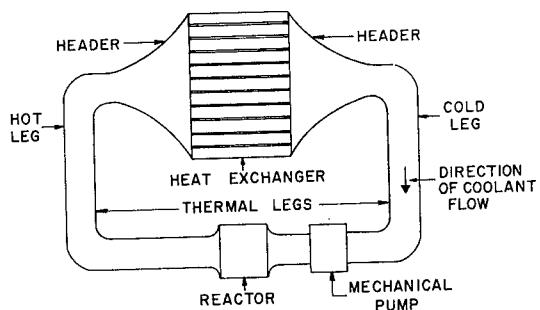


Figure 1.

The mass rate, M , of flow of primary coolant, bismuth, is fixed by the statement that the heat removed from the coolant in the exchanger is equal to the heat given to it by the reactor:

$$P = CM\Delta T , \quad (1)$$

where P = the power (450 Mw in our case) produced by the reactor,

C = the specific heat of the coolant (0.148 joules/g-°C),

ΔT = the temperature difference (170°C in our case) between the hot and cold thermal legs, each of which is assumed isothermal, i.e., no heat losses occur.

The temperature drop, ΔT_1 , across the film is given by the power, H , flowing through each tube wall:

$$H = 2\pi a l h \Delta T_1 , \quad (2)$$

$$= P/N , \quad (3)$$

where a = inside radius of tube,

l = length of each tube,

h = heat transfer coefficient from primary coolant to tube wall,

N = number of tubes in the heat exchanger.

The temperature drop, ΔT_2 , across the tube wall is also given by the power H flowing through each tube:

$$H = \frac{2\pi l \Delta T_2 K}{\ln b/a} , \quad (4)$$

where K = thermal conductivity of tube walls (.26 watts/°C-cm),

b = outer radius of tube walls,

ΔT_2 = temperature drop across tube wall.

The heat transfer coefficient, h , is found⁽⁴⁾ from the following relation:

$$2ha/k = 7 + 0.025 (2Capu/k)^{0.8}, \quad (5)$$

where k = thermal conductivity of primary coolant (.15 watts/cm⁻¹°C),

ρ = density of primary coolant (9.91 g/cm³),

u = speed of coolant in heat exchanger tubes.

The speed, u , is given by mass conservation:

$$N\pi a^2 u\rho = \pi r^2 V\rho, \quad (6)$$

where r = radius of thermal legs,

V = speed of coolant in thermal legs.

The total temperature drop $\Delta T_1 + \Delta T_2$ which can be tolerated usually limits the amount of power flowing through each tube. Under some conditions, however, the stress the tubes can endure may be limiting. For thin walls the stress, S , due to the thermal gradient is given by⁽⁵⁾

$$H = \frac{4\pi S(1-\nu)Kl}{\eta E \left[1 - \frac{2a^2}{b^2-a^2} \ln b/a \right]}, \quad (7)$$

$$\approx \frac{4\pi S(1-\nu)Kl(b+a)}{\eta E(b-a)} \quad (8)$$

where ν = Poisson's ratio (0.28),

η = thermal coefficient of expansion ($16 \times 10^{-6}/^\circ\text{C}$),

E = Young's modulus (29×10^6 lbs/in²).

We need to take into account the fissionable material invested in the two headers. We consider a header shaped so that the momentum of the primary coolant changes uniformly with distance. (See Figure 2. We shall show later that any reasonable shape of the header gives the same total mass in the heat exchanger systems.) The shape of a header is then given by

$$y = c \left[V - M/\pi\rho x^2 \right], \quad (9)$$

where y = distance along axis of header from point where header starts flaring out,

x = radius of header at point y ,

c = constant.

The value c may be determined from the condition that

⁽⁴⁾R.N. Lyon, Liquid Metals Handbook. Atomic Energy Commission, Department of the Navy, Washington, 1950. Ch. 6, p. 130 ff.

⁽⁵⁾S. Timoshenko, Theory of Elasticity. McGraw-Hill Book Co., 1934. para. 114.

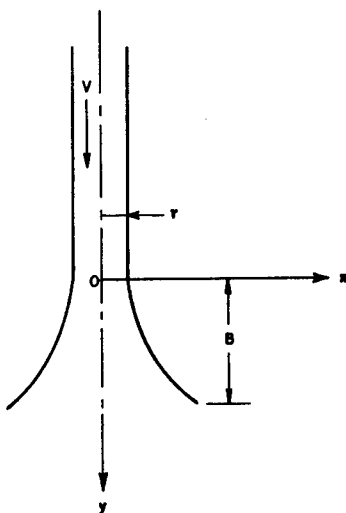


Figure 2.

$$\left. \frac{dy}{dx} \right|_{y=0} = \tan 3.5^\circ = 2cM/\pi\rho r^3, \quad (10)$$

which is the condition that the kinetic losses be minimized. The volume of the header is given by the expression

$$\int_0^B \pi x^2 dy, \quad (11)$$

where B = header height.

Finally, B may be determined from the condition that the header cross-sectional area must be the same as the area of all the tubes inside the heat exchanger:

$$\pi x_0^2 = N\pi a^2, \quad (12)$$

where

$$x_0 = x \text{ at } y = B.$$

(We neglect the small header volume entailed in the expansion from the total cross-sectional area of the heat exchanger itself.) The mass rate of flow, M , is given by

$$M = \pi r^2 \rho V. \quad (13)$$

We can now very easily find the volume of each header to be

$$0.19 r^3 \left| \ln (\sqrt{N} a/r) \right|. \quad (14)$$

The volume of the thermal legs is

$$\pi r^2 L, \quad (15)$$

where L = total length of thermal legs.

The volume within all heat exchanger tubes is:

$$N\pi a^2 l. \quad (16)$$

The total volume of primary coolant in the heat exchanger system is:

$$2 \times 0.19 r^3 \left| \ln (\sqrt{N} a/r) \right| + \pi r^2 L + \pi a^2 N l. \quad (17)$$

The mass of uranium tied up in the heat exchanger system is easily calculated to be:

$$\frac{18.3}{(1.6 + m)} m \left[0.19 \times 2r^3 \left| \ln (\sqrt{N} a/r) \right| + \pi r^2 L + \pi a^2 N l \right], \quad (18)$$

where m = atomic fraction of U to Bi.

The length, L , of the pipes connecting the reactor with the exchanger must be long enough to go from one to the other. We assume a shield 200 cm thick between the reactor and heat exchanger, and an unblanketed reactor of only 100 cm radius and of 150 cm height. We assume further the total cross-sectional area of the exchanger to be four times as great as the area within the exchanger tubes alone. The radius of the exchanger is

$$R = 2 \sqrt{N} a . \quad (19)$$

The minimum active pipe length is, then, from Figure 1:

$$L \geq 2 [2 \sqrt{N} a + 100 + 200] \quad (20)$$

$$\geq 4 \sqrt{N} a + 600 . \quad (21)$$

The minimum passive length is

$$|l - 150| , \quad (22)$$

where we have neglected the header length. Probably the pipes should be rather longer than our optimistic, minimum estimates.

The pressure drop due to the frictional losses in the heat exchanger tubes is given by⁽⁶⁾:

$$\Delta p = 1.52 \times 10^{-6} \rho u^{1.8} / a^{1.2} , \quad (23)$$

where Δp = pressure drop in psi, l and a are expressed in cm, u is in cm/sec. The pressure drop due to frictional losses in the thermal legs is given by

$$\Delta p = 1.52 \times 10^{-6} L V^{1.8} / r^{1.2} . \quad (24)$$

The pressure drop due to kinetic energy losses is very much harder to compute. Such losses occur primarily in the flare-out from the inlet header and from the flare-out of each heat exchanger tube into the outlet header. We circumvent calculating the kinetic losses in characterizing them by parameters α and β : β , the fraction of the kinetic energy per unit volume of the thermal legs lost in the headers and in the legs themselves, and α , the fraction of the kinetic energy per unit volume in a heat exchanger tube lost in the entrance and exit to that tube. Were the kinetic energy of the liquid in the heat exchanger tubes to be totally lost the pressure drop would be $\rho u^2 / 2$. The total pressure drop due to kinetic losses is then characterized by:

$$\Delta p = 7.25 \times 10^{-6} [\alpha \rho u^2 + \beta \rho V^2] . \quad (25)$$

The pressure generated by the density difference of the coolant between the hot and cold thermal legs is given approximately by:

⁽⁶⁾E.R. Gilliland, D. Bareis, G. Feick, in the Science and Engineering of Nuclear Power, Addison Wesley, 1949, Vol. II, Ch. 10, p. 173.

$$\Delta p = \rho L \xi \Delta T g / 2 , \quad (26)$$

$$= .00711 \rho \xi \Delta T L , \quad (27)$$

where ξ = density expansion coefficient of the primary coolant, Bi (1.22×10^{-3} g/cm³·°C).

This expression would be exact if $L/2$ were the altitude difference between the horizontal parts of the pipes joining the heat exchanger and reactor as shown in Figure 1. If these horizontal parts are short, then the expression will be a good approximation. These horizontal runs should be as short as is reasonably convenient to keep the fuel investment low. Let us assume the mechanical pump creates a pressure difference of Π in the direction of the pressure created by the thermal legs. After substitution for the properties of bismuth, the pressure balance equation then becomes:

$$\begin{aligned} \Pi + 1.47 \times 10^{-3} L &= 1.52 \times 10^{-6} LV^{1.8}/r^{1.2} + 1.52 \times 10^{-6} \iota u^{1.8}/a^{1.2} + \\ 7.19 \times 10^{-5} (\alpha u^2 + \beta V^2) &+ 0.43 + 1.52 \times 10^{-6} V^{1.8} | \iota - 150 | / r^{1.2} . \end{aligned} \quad (28)$$

We are now in a position to set up the procedure for study of the heat exchanger design. The choice of convenient, independent variables is governed by equation (28). It is found that a , $b-a$, N , V , α , β , and $\Delta T_1 + \Delta T_2$ are the most convenient set of independent variables. In the case of mechanical pumping we may choose L in addition provided it satisfies the inequality (21). Then from equations (1) and (13) r may be determined as:

$$r = .0357 (P/V)^{1/2} , \quad (29)$$

where P is measured in watts and V in cm/sec. We combine equation (6) and (29) to get u :

$$u = 1.27 \times 10^{-3} (P/Na^2) . \quad (30)$$

The heat transfer coefficient is next determined from equation (5):

$$h = \frac{.541}{a} + .0203 \frac{u^{.8}}{u^{.8}} , \quad (31)$$

where a is taken in cm, u in cm/sec, and h in watts/cm²·°C. From equations (2), (3), and (4), we can determine the length of heat exchanger tubes needed to transmit the power desired:

$$\iota = \frac{.159 (1 + 3.85 h a \ln b/a) P}{(\Delta T_1 + \Delta T_2) N a h} . \quad (32)$$

Nevertheless, the stress limit of the material (Croloy 2. 1/4) of the tube walls must not be exceeded. From equation (7) we learn that the ι found from equation (33) must satisfy the following inequality:

$$\iota \geq .0229 \frac{P}{N} \left(1 - \frac{2a^2}{b^2 - a^2} \ln b/a \right) . \quad (33)$$

If this inequality is not satisfied, then the equality of (33) is used to determine ι .

In the case of thermal pumping, the total length of the thermal legs necessary to circulate the coolant at the requisite rate can be found from equation (28) by putting $\Pi = 0$:

$$L = \frac{.43 + 1.52 \times 10^{-6} \frac{V^{1.8}}{r^{1.2}} |_{l=150} + 1.52 \times 10^{-6} \frac{u^{1.8}}{a^{1.2}} + 7.19 \times 10^{-5} \beta V^2 + 7.19 \times 10^{-5} \alpha u^2}{1.47 \times 10^{-3} - 1.52 \times 10^{-6} \frac{V^{1.8}}{r^{1.2}}} . \quad (34)$$

However, in all cases the independent variables must be adjusted so that L is at least as great as the minimum necessary length given by equation (21). An especially convenient parameter to adjust in this connection is V .

In the case of mechanical pumping, the length of the pipes connecting the reactor with the heat exchanger is given by equation (21). Equation (28) reveals that the pressure which must be created by the mechanical pump is given by:

$$\Pi = 0.43 + \left[1.52 \times 10^{-6} \frac{V^{1.8}}{r^{1.2}} - 1.47 \times 10^{-3} \right] L + 1.52 \times 10^{-6} \frac{u^{1.8}}{a^{1.2}} + 7.19 \times 10^{-5} (\alpha u^2 + \beta V^2) + 1.52 \times 10^{-6} \frac{V^{1.8}}{r^{1.2}} |_{l=150} . \quad (35)$$

The pumping power is the work done per unit time, W , in circulating the coolant by the mechanical pump:

$$W = M\Pi/\rho , \quad (36)$$

$$= 2.76 \times 10^{-5} \Pi P , \quad (37)$$

where W and P are measured in watts and Π in psi. The latter equation is a consequence of (1).

In either case, the volume of the heat exchanger system is

$$0.383 r^3 |_{ln(\sqrt{N} a/r)} + 3.14 \left[N a^2 l + r^2 (L + |_{l=150}) \right] , \quad (38)$$

and the mass of uranium is

$$m = .00661 \times \text{volume.} \quad (39)$$

Spray Heat Exchanger

We turn now to the quantitative evaluation of the spray heat exchanger. Drops of liquid bismuth fall through a tank full of KCl-LiCl that slowly moves upward. See Figure 3 for a schematic diagram.

If the liquid drops of Bi are assumed to fall at a constant speed through the salt, the calculation is greatly simplified. This approximation is a good one. The speed of fall, U , is given⁽⁷⁾ by Newton's law:

⁽⁷⁾ J. H. Perry, Chemical Engineer's Handbook, McGraw-Hill Book Co., 1950. 3rd ed., p. 1017 ff.

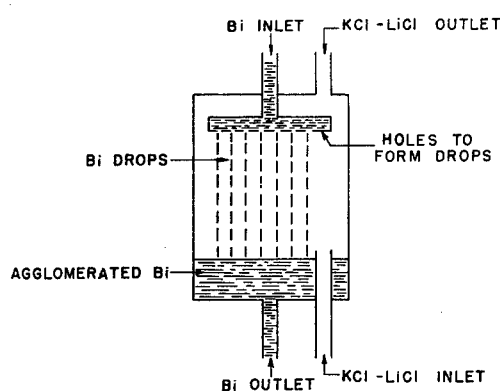


Figure 3. Spray heat exchanger.

$$U = -U_0 + \sqrt{\frac{8gA}{3C'}} \left(\frac{\rho}{\rho_0} - 1 \right), \quad (40)$$

$$= -U_0 + 176.0 \sqrt{A}, \quad (41)$$

where U_0 = salt velocity (in cm/sec),
 ρ_0 = salt density (1.60 g/cm^3),
 C' = a constant (0.44),
 ρ = Bi density (9.91 g/cm^3),
 A = Bi drop radius (in cm).

The heat balance equation between the Bi drops and the salt states that the heat transferred through the laminar film surrounding a Bi drop per unit time is the same as the heat gained by the salt per unit time:

$$4\pi A^2 f [T(A,t) - T_0(t)] \frac{\Delta z}{U} \frac{n\Delta z}{\lambda} = -C_0 \rho_0 \left(\pi R^2 - \frac{4}{3} \pi A^3 \frac{n}{\lambda} \right) \frac{U_0}{U} \Delta z \Delta T_0(t), \quad (42)$$

where f = heat transfer coefficient from liquid drops to salt ($1.42 \text{ watts/cm}^2 \cdot {}^\circ\text{C}$),
 $T(A,t)$ = temperature of drop at its surface $q = A$ at time t ,
 λ = active length of spray heat exchanger,
 n = number of drops in heat exchanger,
 C_0 = specific heat of salt ($0.92 \text{ joules/g} \cdot {}^\circ\text{C}$),
 T_0 = salt temperature,
 z = distance below horizontal plane where drops are formed,
 R = radius of the heat exchanger.

Let the initial uniform drop temperature be taken as zero. The drop temperature at any later position is given⁽⁸⁾ by:

$$T(q,t) = \frac{-2\pi k}{\rho C A q} \sum_{j=1}^{\infty} (-)^j j \int_0^t d\zeta \exp(kj^2 \pi^2 (\zeta - t)/\rho C A^2) T(A, \zeta) \sin(\pi j q/A), \quad (43)$$

where $T(q,t)$ = drop temperature at point q from its center at a time t ,
 t = time taken by drop to fall to a position z from point at which it was made,
 k = thermal conductivity of Bi ($0.15 \text{ watts/cm} \cdot {}^\circ\text{C}$).

Note that

$$z = Ut. \quad (44)$$

To avoid making mistakes it is most essential that equation (43) be converted to a uniformly convergent series. Upon integrating by parts, we get such a series:

$$T(q,t) - T(A,t) = \frac{2A}{\pi q} \sum_{j=1}^{\infty} \frac{(-)^j}{j} \int_0^t d\zeta \exp(kj^2 \pi^2 (\zeta - t)/\rho C A^2) \frac{dT(A, \zeta)}{d\zeta} \sin(\pi j q/A), \quad (45)$$

⁽⁸⁾H. S. Carslaw and J. C. Jaeger, Conduction of Heat in Solids. Oxford, 1947. para. 91.

where we have used the familiar relation:

$$\sum_{j=1}^{\infty} \frac{(-)^j}{j} \sin(j\pi q/A) = -\pi q/2A . \quad (46)$$

The heat in the drops in excess of that in them at zero of temperature is

$$4\pi\rho C \int_0^A T(q,t)q^2 dq \quad (47)$$

$$= \frac{4}{3}\pi\rho CA^3 T(A,t) - \frac{8\rho CA^3}{\pi} \sum_{j=1}^{\infty} \frac{1}{j^2} \int_0^t \exp(kj^2\pi^2(\zeta-t)/\rho CA^2) \frac{dT(A,\zeta)}{d\zeta} d\zeta . \quad (48)$$

The heat energy leaving a drop per unit time must equal the heat absorbed by the salt per unit time:

$$-4\pi\rho C \frac{\partial}{\partial t} \int_0^A T(q,t)q^2 dq = -C_0 \frac{\lambda}{n} \frac{M_0}{U} \frac{dT_0(t)}{dt} , \quad (49)$$

where M_0 = mass rate of salt flow,

$$M_0 = \rho_0 U_0 \left(\pi R^2 - \frac{4}{3}\pi A^3 \frac{n}{\lambda} \right) . \quad (50)$$

This last relationship may be immediately integrated. In conjunction with (48) we get:

$$-C_0 \frac{\lambda}{n} \frac{M_0}{U} [T_0(t) - T_0(0)] = -4\pi\rho C \int_0^A T(q,t)q^2 dq , \quad (51)$$

$$= -\frac{4}{3}\pi A^3 \rho C T(A,t) + \frac{8\rho CA^3}{\pi} \sum_{j=1}^{\infty} \frac{1}{j^2} \int_0^t d\zeta \exp(kj^2\pi^2(\zeta-t)/\rho CA^2) \frac{dT(A,\zeta)}{d\zeta} , \quad (52)$$

where $T_0(0)$ = salt temperature at exit.

Equation (42) may be solved for $T(A,t)$:

$$T(A,t) = T_0(t) - \frac{C_0 \lambda M_0}{4\pi A^2 n f U} \frac{dT_0}{dt} . \quad (53)$$

By substitution of (53) into (52) we can get a simple integral equation in $T_0(t)$ alone:

$$DT_0(0) + (1-D)T_0(t) - \left[\frac{\rho C_0 M_0 A}{3 M f} + \frac{\pi^2}{15 \kappa} \right] \frac{dT_0(t)}{dt} + \frac{6}{\pi^2 \kappa} \frac{dT_0(0)}{dt} \sum_{j=1}^{\infty} \frac{e^{-\kappa n^2 t}}{j^4} +$$

$$+ \sum_{j=1}^{\infty} \left[\frac{6}{\pi^2 \kappa} \frac{1}{j^4} + \frac{2 A \rho C_0 M_0}{\pi^2 f M} \frac{1}{j^2} \right] \int_0^t d\zeta e^{\kappa n^2 (\zeta-t)} \frac{d^2 T_0(\zeta)}{d\zeta^2} = 0 , \quad (54)$$

where

$$D = C_0 M_0 / CM, \quad (55)$$

M = mass rate of Bi flow,

$$= \frac{4}{3} \pi A^3 \rho \frac{n}{\lambda} U, \quad (56)$$

$$\kappa = k \pi^2 / \rho C A^2. \quad (57)$$

The integral equation, (54), may be solved by the Laplace transform method: (p is the variable conjugate to t .)

$$\frac{DT_0(0)}{p} + (1-D)\bar{T}_0(p) - \left[\frac{\rho C_0 M_0 A}{3Mf} + \frac{\pi^2}{15\kappa} \right] \left[p\bar{T}_0(p) - T_0(0) \right] + \frac{6}{\pi^2 \kappa} \frac{dT_0(0)}{dt} \sum_{j=1}^{\infty} \frac{1}{j^4(p+\kappa j^2)} +$$

$$+ \sum_{j=1}^{\infty} \left[p^2 \bar{T}_0(p) - pT_0(0) - \frac{dT_0(0)}{dt} \right] \left[\frac{1}{p+\kappa j^2} \right] \left[\frac{6}{j^4 \pi^2 \kappa} + \frac{2A\rho C_0 M_0}{\pi^2 f M j^2} \right] = 0. \quad (58)$$

We use

$$\sum_{j=1}^{\infty} \frac{1}{j^2(p+\kappa j^2)} = \frac{\pi^2}{6p} + \frac{\kappa}{2p^2} - \frac{\pi}{2p} \sqrt{\frac{\kappa}{p}} \coth \left(\pi \sqrt{\frac{p}{\kappa}} \right), \quad (59)$$

$$\sum_{j=1}^{\infty} \frac{1}{j^4(p+\kappa j^2)} = \frac{\pi^4}{90p} - \frac{\pi^2 \kappa}{6p^2} - \frac{\kappa^2}{2p^3} + \frac{\pi \kappa^{3/2}}{2p^{5/2}} \coth \left(\pi \sqrt{\frac{p}{\kappa}} \right). \quad (60)$$

to evaluate several series. The Laplace transform of the salt temperature may now be found:

$$\bar{T}_0(p) = \frac{D \left[1 - \kappa/fA \right] \frac{T_0(0)}{p} + \frac{\rho C A}{\pi f} D T_0(0) \sqrt{\frac{\kappa}{p}} \coth \pi \sqrt{\frac{p}{\kappa}}}{D \left[1 - \kappa/fA \right] + \frac{3\kappa}{\pi^2 p} - \frac{3}{\pi} \sqrt{\frac{\kappa}{p}} \coth \pi \sqrt{\frac{p}{\kappa}} + \frac{kD}{fA} \pi \sqrt{\frac{p}{\kappa}} \coth \sqrt{\frac{p}{\kappa}}}, \quad (61)$$

upon using the fact that $T(a, 0) = 0$ in equation (53) to evaluate $dT_0(0)/dt$ in terms of $T_0(0)$. The salt temperature is found from the inverse of (61). Let

$$s = \pi i \sqrt{p/\kappa}. \quad (62)$$

If $D \neq 1$:

$$\frac{T_0(t)}{T_0(0)} = \frac{D}{D-1} - 6D \sum_{j=1}^{\infty} \frac{e^{-\kappa s_j^2 t / \pi^2}}{\left[\left(3 - 2D + \frac{kD}{fA} s_j^2 \right) \left(3 + \frac{kD}{fA} s_j^2 \right) - 3D + D^2 \left(1 + \frac{k}{fA} \right) s_j^2 \right]}, \quad (63)$$

where s_j are the nonzero solutions of

$$s_j \cot s_j = 1 - \frac{1}{\frac{k}{fA} + \frac{3}{Ds_j^2}} \quad (64)$$

If $D = 1$, there exists a double pole in (61) at $p = 0$. The salt temperature is then given by:

$$\frac{T_0(t)}{T_0(0)} = 1 + \frac{3}{7 \left(1 + 5 \frac{k}{fA}\right)^2} + \frac{15 kt}{\rho CA^2 \left(1 + \frac{5k}{fA}\right)} - 6 \sum_{j=1}^{\infty} \frac{e^{-\kappa s_j^2 t / \pi^2}}{s_j^2 \left[1 + \frac{5k}{fA} + \left(\frac{k}{fA}\right)^2 s_j^2\right]} \quad (65)$$

The surface temperature of the metal is found from (63) and (53). If $D \neq 1$:

$$\frac{T(A,t)}{T_0(0)} = \frac{D}{D-1} - 6D \sum_{j=1}^{\infty} \frac{\left[1 + \frac{Dks_j^2}{3fA}\right] e^{-\kappa s_j^2 t / \pi^2}}{\left[\left(3-2D + \frac{kD}{fA} s_j^2\right) \left(3 + \frac{kD}{fA} s_j^2\right) - 3D + D^2 (1+k/fA)s_j^2\right]} \quad (66)$$

Equation (45) may be used to find $T(q,t)$ if desired. However, the average temperature, $\bar{T}(q,t)$, is of more interest. The use of equation (51) leads to considerably simpler results than the more straightforward method, viz.:

$$\frac{\bar{T}(q,t)}{T_0(0)} = \frac{\frac{4\pi\rho C}{3} \int_0^A T(q,t) q^2 dq}{\frac{4}{3} \pi A^3 \rho C}, \quad (67)$$

$$= D(T_0(t) - T_0(0)), \quad (68)$$

into which (63) may be substituted if desired.

Let us turn for a moment to a consideration of the roots of (64). First, let us look at a rough plot of the right hand side and left hand side of (64) in Figures 4a and 4b. The following points are to be noted:

1. The $s \cot s$ lines go through the odd half integer points with increasing steepness as s gets larger.
2. Both the right side and left side of the equation start out at $s = 0$ with unit value and zero slope.
3. The $1 - 1/\left[\frac{k}{fA} + \frac{3}{Ds^2}\right]$ function approaches $1 - \frac{fA}{k}$ asymptotically.
4. The first purely real root occurs at $s > \pi$ if $D < 1$ but at $s < \pi$ if $D > 1$.
5. The roots are spaced at least π apart, but this spacing approaches exactly π as s increases and the roots become very nearly a half odd integer $x\pi$ as s gets larger.

Let us look for pure imaginary roots now in Figures 4c and 4d. If $D > 1$ it is easy to see from the second derivative of both sides of equation (64) that there are no purely imaginary roots. If $D < 1$, by the same method, we can see there is exactly one purely imaginary root.

It is readily seen that the series in expressions (63) and (66) converge with extreme rapidity. For any reasonable accuracy under almost any conditions, the first root is the only root really needed; the sums break down into but one term.

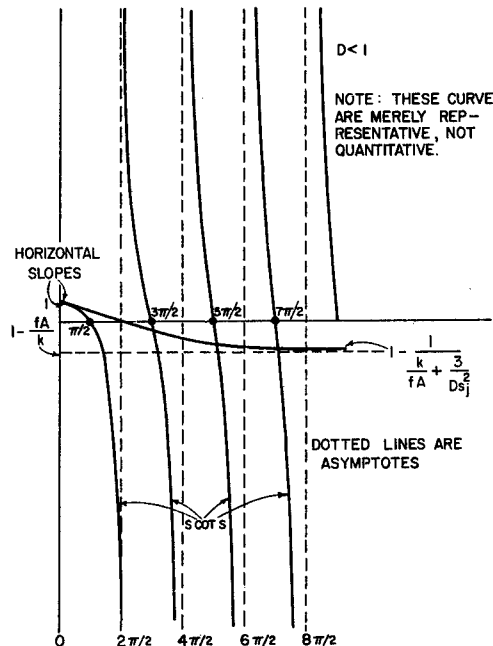


Figure 4a.

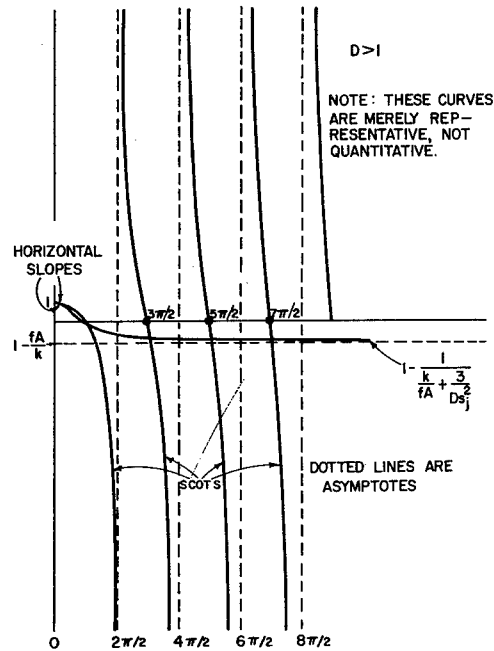


Figure 4b.

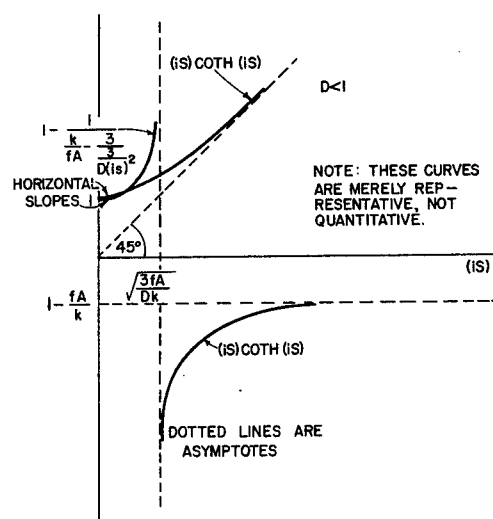


Figure 4c.

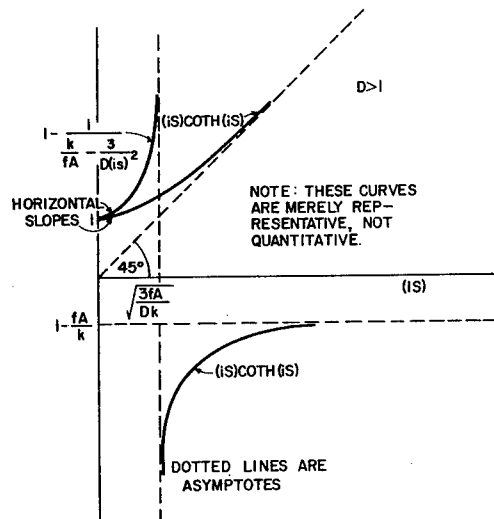


Figure 4d.

As yet we have not considered whether there may be complex roots. If equation (64) be expanded in a power series, it can be reduced to

$$\sum_{j=0}^{\infty} \frac{1}{j!} \left(\frac{\pi^2 p}{\kappa} \right)^j \left[\frac{j!(2j+2)}{(2j+3)!} \right] \left[\frac{4k}{ha} j^2 + \left(\frac{6k}{ha} + 2 \right) j + 3 - \frac{3}{D} \right] = 0. \quad (69)$$

We now note that the zeros of

$$\frac{4k}{ha} z^2 + \left(\frac{6k}{ha} + 2 \right) z + 3 - 3/D \quad (70)$$

are all real for the discriminant is always positive. If $D < 1$, one root is positive and the other is negative. If $D > 1$, both roots are negative. From a slight generalization of several theorems derived by Laguerre relating to the zeros of integral functions, we can conclude⁽⁹⁾ that in the p plane the roots of the transcendental equation are all real. Further, in the p plane if $D < 1$, one root is positive and all the others are negative, and if $D > 1$, all roots are negative. The summation in equation (63) is to be carried over all roots of (64) in the p plane. This statement means that we sum (63) over all non-zero, negative roots s_j of (64). Because (64) is even between positive and negative values, we may alternatively sum (63) over just the positive solutions of (64). If $D < 1$, we have, of course, to sum (63) over the one imaginary root of (64), also.

We may now evaluate all other quantities of interest in sequence: U is found from equation (36). The mass flow rate, M , of bismuth is:

$$M = P/C \delta T, \quad (71)$$

where δT = the differential between the inlet and outlet bismuth temperatures ($170^\circ C$),

$$\delta T = \overline{T(q,t)}. \quad (72)$$

The volumetric flow rate, Q , of the bismuth is:

$$Q = M/\rho. \quad (73)$$

The mass flow rate, M_0 , of the salt is

$$M_0 = D(C/C_0)M. \quad (74)$$

The volumetric flow rate of the salt is

$$Q_0 = M_0/\rho_0. \quad (75)$$

The minimum distance, d , between drops is

$$d = \left(\frac{4}{3} \pi \right)^{1/3} \left(\frac{UQ_0 + 1}{U_0 Q} \right)^{1/3} A. \quad (76)$$

The number of drops, n , is

⁽⁹⁾E.C. Titchmarsh, The Theory of Functions, 2nd edition, para. 8.61 - 8.63.

$$n = 3\lambda Q / 4\pi A^3 U. \quad (77)$$

The radius, R , of the heat exchanger, based on the assumption that the drops are spaced on a square lattice the minimum distance apart, is:

$$R = (nd^3/\pi\lambda)^{1/2}. \quad (78)$$

The number of holes, G , in the top plate is:

$$G = \pi R^2/d^2. \quad (79)$$

Again if we assume a shield of 200 cm thickness, a reactor of 100 cm radius and of 200 cm height, the total length of pipe connecting the best exchanger and reactor cannot be less than

$$L = 600 + 2R + |J + \lambda - 200|, \quad (80)$$

where J = depth of the bismuth pool. The mass, μ , of bismuth in the spray heat exchanger is

$$\mu = Mt, \quad (81)$$

and the mass, χ , of uranium in the exchanger is

$$\chi = (233/209)\mu m. \quad (82)$$

The mass of bismuth in the pool where the drops are agglomerated at the bottom of the heat exchanger is πJR^2 .

Again, the mass of bismuth in the pipes connecting the reactor and heat exchanger is $\pi r^2 L$.

The masses of uranium in the pool and in the pipes are respectively $[18.3/(1.60+m)] m \pi JR^2$, and $[18.3/(1.60+m)] m \pi r^2 L$.

If we assume the drops are of the same diameter as the nozzles or hole which formed them, the speed, v , in the nozzle is approximately

$$v = Q/G\pi A^2. \quad (83)$$

Consequently, the pressure, Π , that must be created by a mechanical pump if we neglect any thermal pumping is:

$$\Pi = 1.45 \times 10^{-5} \left[\frac{1}{2} \rho v^2 + g\lambda(\rho - \rho_0) + \beta \rho V^2/2 \right] + 1.52 \times 10^{-6} \frac{V^{1.8}}{r^{1.2}} L, \quad (84)$$

where Π is in psi, but all other quantities are in the cgs system of units. Finally,

$$W = \Pi Q. \quad (85)$$

Results

The results of our numerical work are presented in graphical form in Figures 5 through 34. The results may be broken down into:

1. any of the heat exchanger systems,
2. any tubular exchanger system,
3. only tubular exchangers with thermal pumping,
4. only tubular exchangers with mechanical pumping,
5. only spray exchangers.

We summarize our results below.

Any Exchanger System

Radius of Piping Connecting Reactor with Exchanger: Figure 5.

1. Decreases as (speed in piping) $^{-1/2}$. It is desirable to use as high a speed as is convenient to cut down the fuel investment.

Any Tubular Exchanger

Speed in Heat Exchanger Tubes: Figures 6a, b.

1. Decreases rapidly as (number of tubes) $^{-1}$.
2. Decreases rapidly as (radius of exchanger tubes) $^{-2}$.

Power Transfer Coefficient: Figures 7a, b, c.

1. Decreases rapidly as tube radius increases. Turbulence decreases.
2. Increases as speed in tubes increases, but more slowly than linearly.
3. Decreases as number of tubes increases, but slower than (number of tubes) $^{-1}$. Speed in tubes decreases.

Length of Heat Exchanger Tubes: Figures 8a, b.

1. Decreases more slowly than (number of tubes) $^{-1}$ if the temperature drop across inner laminar film + wall is limiting; decreases as (number of tubes) $^{-1}$ if the stress the tubes can endure limits (large temperature drops).
2. Decreases somewhat as radius of tubes increases if the stress limits. Only slight decrease if temperature drop limits.
3. Decreases as walls become thinner.

Tube Wall/Inner Laminar Film Temperature Drop: Figures 9a, b.

1. Decreases moderately as tubes become larger.
2. Decreases as number of tubes increases.
3. Decreases as walls become thinner.

Tubular Exchanger Thermal Pumping

Total Active Length of Pipes Connecting Reactor with Exchanger: Figures 10a, b, c,d.

1. Decreases extremely rapidly as number of tubes increases up to 10,000 and then levels off.

2. Decreases very rapidly as radius of tubes increases up to 1.0 cm, then levels off.
3. Increases very rapidly as speed in piping increases, approaching an asymptote at $480 \text{ cm/sec} = 16. \text{ ft/sec}$ beyond which friction exceeds density difference.
4. Thinner walls, higher temperature drops and less kinetic energy loss are of secondary importance.

Volume of, Bismuth Weight in, Uranium Investment in Whole Heat Exchanger System:
Figures 11a, b, c, d.

1. Decrease extremely rapidly as number of tubes increases up to 10,000 because piping length decreases rapidly and then levels off.
2. Decrease very rapidly with tube radius to a minimum at 1.0 cm radius, then increases substantially. At first, length of piping decreases very rapidly, but then surface-to-volume ratio decreases.
3. From a broad minimum at 300 cm/sec increase rapidly to ∞ at 480 cm/sec as speed in piping increases. Low speeds imply a large pipe diameter and high speeds high friction; in between there is an optimum.
4. Increase as tubes grow fatter, temperature drop grows smaller, and as kinetic energy losses increase.
5. Header volume is negligible.

Volume of, Bismuth Weight in, and Uranium Investment in Heat Exchanger Proper:
Figures 12a, b.

1. Increases rapidly as radius of tubes increases because of lower surface-to volume ratio.
2. Increase moderately as number of tubes increases if temperature limits, but remain constant if stress limits.
3. Decrease as walls get thinner and as temperature drop grows larger.
4. This volume is important.

Volume of, Bismuth Weight in, and Uranium Investment in Piping Connecting Reactor with Exchanger: Figures 13a, b, c, d.

1. Decrease extremely rapidly as number of tubes in exchanger increases, leveling off at 10,000, because piping length decreases.
2. Decrease very rapidly as tube radius increases, because piping length decreases, and level out at 1.0 cm radius.
3. From a minimum near 300 cm/sec, increase rapidly to ∞ at 480 cm/sec because of friction.
4. Decrease as temperature drop increases, as walls become thinner, and as kinetic losses are lowered.
5. This volume is important.

Tubular Exchanger Mechanical Pumping

Length of Piping Connecting Reactor with Exchanger: Figures 14a, b.

1. Decreases rapidly with increase in number of tubes to a broad minimum at 10,000 tubes.
2. Longer the fatter the tube walls, especially for small radii.
3. Shorter the larger the temperature drop, especially for small tubes.
4. Shallow minimum as tube diameter is altered.
5. This is the weakest part of the calculation because one may want to add many things between the reactor, its shield and the exchanger, and because of the

crudity of our estimate of exchanger radius.

Total Pressure Drop: Figures 15a, b, c, d, e.

1. Decreases extremely rapidly as number of tubes increases, levelling out at 10,000 tubes.
2. Decreases very rapidly as tubes grow in size to a broad minimum at 1.5 cm radius.
3. Increases rapidly with speed in the piping.
4. Decreases a little for thinner walls, especially for tubes of small radius, for higher temperature drops, for shorter piping, and for lower kinetic energy losses.
5. It would appear that pressure limitations are reached before pumping power limitations.

Pressure Drop Caused by Exchanger Tube Friction: Figures 16a, b, c.

1. Decreases extremely rapidly as number of tubes increases.
2. Decreases very rapidly as tubes get larger.
3. Decreases a little for thinner tubes and higher temperature drops.
4. This pressure drop is important.

Pressure Drop Caused by Kinetic Energy Loss in Heat Exchanger Tubes: Figures 17a, b.

1. Decreases extremely rapidly as number of tubes increases.
2. Decreases very rapidly as radius of tubes increases.
3. Pressure drop is of minor importance.

Pressure Drop Caused by Friction in Active Part of Piping Connecting Reactor with Exchanger: Figures 18a, b, c.

1. Increases rapidly as speed in piping increases.
2. Increases as heat exchanger tube radius increases because of larger diameter exchanger. Increases for pressure generated.
3. Increases a little as the number of exchanger tubes increases. The pressure generated behaves similarly.
4. This pressure drop is of minor importance.

Pressure Drop Caused by Kinetic Energy Loss in Piping Connecting Reactor with Exchanger: Figure 19.

1. Increases rapidly as $(\text{speed in piping})^2$.
2. This pressure drop is a major contribution to the total drop.

Pressure Drop Caused by Friction in Passive Part of Piping Connecting Reactor with Exchanger: Figures 20a, b, c, d.

1. Decreases rapidly as number of tubes increases.
2. Increases rapidly as speed in piping increases.
3. Decreases moderately as size of exchanger tubes increases.
4. Increases moderately as length of piping increases.
5. Decreases as tubes becomes thinner and as temperature drop increases.
6. This pressure drop is minor.

Volume of, Bismuth Weight in, and Uranium Investment in Heat Exchanger System: Figures 21a, b, c, d.

1. Decrease rapidly as number of tubes in increased til a minimum is reached at about 10,000 tubes.

2. Increase rapidly as the radius of the exchanger tubes increases because of the lower surface-to-volume ratio. The lower limit on tube size is fixed by limits on the frictional pressure drop and by requirements of rigidity.
3. Increase as tubes walls become fatter and as temperature drop decreases.
4. Increase linearly with length of piping.
5. Decrease a little as speed in piping increases.

Volume of, Bismuth Weight in, and Uranium Investment in Piping Connecting Reactor with Exchanger: Figures 22a, b, c.

1. Decrease as (speed in piping)⁻¹.
2. Decrease somewhat as number of exchanger tubes increases and reach a broad minimum at about 10,000 tubes.
3. Go through a shallow minimum at roughly 0.75 cm as the tube radius is increased.
4. Increase as tube walls become thicker and as temperature drop decreases.

Volume of Bismuth Weight in, and Uranium Investment in Heat Exchanger Proper: Figures 23a, b.

1. Increase rapidly as the tube radius increases.
2. Increase somewhat as the number of exchanger tubes increases if the temperature drop limits, but remains constant if the stress limits.
3. Increase somewhat as the wall thickness increases and as the temperature drop increases.

Volume of, Bismuth Weight in, and Uranium Investment in Headers: Figures 24a, b, c.

1. This volume is strictly of minor importance.

Spray Exchanger Mechanical Pumping

Before summarizing the results, it should be stated that a weakness in our calculations lies in the fact that the power transfer coefficient has conservatively been assumed to be 1.42 watts/cm²·°C, instead of having been calculated from the relative drop and salt speed, the drop size, and the properties of bismuth and LiCl-KCl. Measurements will be started to rectify this situation.

Temperature Drop From Bismuth to Salt, Hot Pipes: Figures 25a, b, c, d.

1. Decreases as the time of fall of bismuth drops increases.
2. Decreases rapidly as the heat absorption ratio decreases. The heat absorption ratio is the ratio of heat absorbed by salt per degree to the heat absorbed by bismuth per degree.
3. Decreases rapidly as the drop size decreases especially for low heat absorption ratios.

Inlet Salt Temperature: Figures 26a, b, c, d, e.

1. Increases as the time of drop fall increases.
2. Increases as the drop size decreases for small times but not for large time.
3. Increases as heat absorption ratio increases.
4. Large drops come into thermal equilibrium after 2 sec but small drops come into thermal equilibrium essentially immediately.

Height of Active Part of Heat Exchanger: Figures 27a, b, c.

1. Increases moderately as time of fall increases.
2. Increases as the drop size increases.
3. Decreases as salt speed increases.
4. Note the active part of the exchanger is very shallow.

Minimum Radius of Heat Exchanger: Figures 28a, b.

1. Decreases a little as drop size increases, as heat absorption ratio decreases, and, for the larger drops, as salt speed increases.

Number of Holes in Distribution Plate: Figures 29a, b.

1. Decreases rapidly as the drop size increases. The maximum number of holes fixes the smallest drop size allowable.
2. Is almost constant as the salt speed changes and as the heat absorption ratio changes.

Total Pressure Drop: Figures 30a, b, c, d, e, f.

1. Increases rapidly as the speed in the piping increases.
2. Increases somewhat as the drop size increases.
3. Increases as time of fall increases.
4. Decreases somewhat as the salt speed increases.
5. Is almost constant as the heat absorption ratio changes.

Volume of, Bismuth Weight in, and Uranium Investment in Heat Exchanger: Figures 31a, b, c, d, e, f, g, h.

1. Increase somewhat as drop sizes decrease.
2. Increase somewhat as time of fall of drops increases.
3. Increase a little as heat absorption ratio increases.
4. Is almost independent of salt speed.
5. Decrease a little as speed in piping increases.

Volume of, Bismuth Weight in, and Uranium Investment in Piping Connecting Reactor with Exchanger: Figures 32a, b, c, d.

1. Decrease a little as drop size increases.
2. Increase but little as the heat absorption ratio increases.
3. Is almost independent of time of drop fall.

Volume of, Bismuth Weight in, and Uranium Investment in Pool: Figures 33a, b.

1. Decrease somewhat as drop radius increases.
2. Decrease as salt speed increases.
3. Decrease a little as heat absorption ratio increases.

Volume of, Bismuth Weight in, and Uranium Investment in Active Part of Heat Exchanger: Figure 34.

1. Increase markedly with time of drop fall.

Summary of Results

We summarize our results in Table 1 by comparing a reasonable design of each of the three exchanger systems. We note the superiority of the spray exchanger over the tubular exchanger with mechanical pumping and of the latter over the tubular

Table 1: Design Characteristics for Three Exchanger Systems (Reactor Power: 450 Mw)

	Tubular Exchanger	Thermal Pumping	Mechanical Pumping	Spray Exchanger	Mechanical Pumping
Heat Exchanger Dimensions					
Tube size	1.00 cm	.750 cm	.25 cm	.250 cm	.250 cm
Radius (inner)	.787 in	.590 in	.25 in	.197 in	.197 in
Diameter (inner)	.25 cm = .098 in	.25 cm = .098 in		2.0 sec	
Tube wall thickness				193 cm = 6.33 ft	
Tube length	370 cm = 12.1 ft	399 cm = 13.1 ft		136 cm = 4.45 ft	
Number of tubes	10,000	10,000	No. of distribution plate holes	30 cm = .984 ft	
Speed in tubes	57 cm/sec = 1.9 ft/sec	100 cm/sec = 3.3 ft/sec	Speed of drop fall	270,000	
Power transfer coefficient	1.06 w/cm ² -°C = 1870 Btu/hr-ft ² -°F	1.59 w/cm ² -°C = 2810 Btu/hr-ft ² -°F	Speed of salt rise	68 cm/sec = 2.2 ft/sec	
Tube stress	<8000 psi	<8000 psi	Power transfer coefficient drops to salt	20 cm/sec = .66 ft/sec	
Temperatures					
Wall and inner film drop	35°C = 63°F	35°C = 63°F	Bi/salt drop (hot sides)	11°C = 19°F	
Wall/film temperature drop	.91	1.3	Temperature rise of salt	170°C = 306°F	
Temperature drop of bismuth	170°C = 306°F	170°C = 306°F	Temperature drop of bismuth	170°C = 306°F	
Mean Bi temperature	4000°C = 7520°F	4000°C = 7520°F	Mean Bi and salt temperature	4000°C = 7520°F	
Piping Dimensions					
Pipe size	44 cm	38 cm	Pipe size	34 cm	
Radius (inner)	2.9 ft	2.5 ft	Radius (inner)	2.2 ft	
Diameter (inner)			Diameter (inner)		
Lengths	1370 cm = 45 ft	450 cm = 15 ft	Length		
Active half-length			Active half + passive half-length	500 cm = 16 ft	
Passive total length	220 cm = 7.2 ft	250 cm = 8.2 ft			
Speed in piping	300 cm/sec = 9.8 ft/sec	400 cm/sec = 13 ft/sec	Speed in piping	500 cm/sec = 16 ft/sec	
Pressures and Pumping Power					
Heat exchanger			Pressures and Pumping Power		
Friction	.83 psi	3.5 psi	Heat exchanger		
Kinetic (40% energy loss)	.095 psi	.30 psi	Head	1.6 psi	
Piping and headers			Kinetic (40% energy loss)	.08 psi	
Friction			Piping and headers		
Active part	1.3 psi	.84 psi	Friction	1.6 psi	
Passive part	.10 psi	.23 psi			
Kinetic (20% energy loss)	1.3 psi	2.30 psi	Kinetic (20% energy loss)	3.6 psi	

<u>Reactor</u>	<u>.43 psi</u>	<u>.43 psi</u>	<u>Reactor</u>	<u>.43 psi</u>
Total pressure drop	4.0 psi	7.7 psi	Total pressure drop	22 psi
Generated	4.0 psi	1.3 psi		
Net supplied by pump	0.00 psi	6.3 psi		
Pumping power	0.00 kw	79 kw		
Net pressure generated per unit length	1.00×10^{-3} psi/cm	$95 \text{ kw (if no aid)}$	Pumping power	270 kw
	3.05×10^{-2} psi/ft	5.35×10^{-4} psi/cm	Friction per unit length of piping	1.60×10^{-3} psi/cm = .0488 psi/ft
<u>Volumes</u>				
Heat exchanger	11.6 kL	7.05 kL	Heat exchanger	3.61 kL
Header	.03 kL	.01 kL	Pool	3.51 kL
Piping	17.8 kL	5.19 kL	Piping	3.62 kL
Total	29.5 kL	12.2 kL	Total	10.7 kL
Piping per unit length	.00602 kL/cm = .183 kL/ft	.00451 kL/ft = .138 kL/ft	Piping per unit length	.00351 kL/cm = .107 kL/ft
<u>Bismuth Masses</u>			<u>Bismuth Masses</u>	
Heat exchanger	115 metric tons	69.9 metric tons	Heat exchanger	35.7 metric tons
Header	127 short tons	77.0 short tons	Pool	39.4 short tons
	.3 metric tons	.1 metric tons	Piping	34.7 metric tons
	.3 short tons	.1 short tons	Total	38.3 short tons
Piping	177 metric tons	51.4 metric tons		35.8 metric tons
	195 short tons	56.6 short tons		39.5 short tons
Total	292 metric tons	121 metric tons		106. metric tons
	322 short tons	134. short tons		117 short tons
Piping per unit length	.0596 metric tons/cm = 2.00 short tons/ft	0.447 metric tons/cm = 1.50 short tons/ft	Piping per unit length	.0348 metric tons/cm = 1.17 short tons/ft
<u>Uranium Masses</u>			<u>Uranium Masses</u>	
Uranium concentration	598 ppm (atomic)	598 ppm (atomic)	Uranium concentration	598 ppm (atomic)
Heat exchanger	77.1 kg	46.6 kg	Heat exchanger	23.9 kg
Header	.2 kg	.1 kg	Pool	23.2 kg
Piping	118 kg	34.3 kg	Piping	23.9 kg
Total	195 kg	81.0 kg	Total	71.0 kg
Piping per unit length	.0398 kg/cm = 1.21 kg/ft	.0298 kg/cm = .909 kg/ft	Piping per unit length	.0232 kg/cm = .707 kg/ft
<u>Properties of Croloy 2 1/4 Tubes</u>			<u>Properties of LiCl-KCl</u>	
Thermal conductivity	$.26 \text{ w/oC-cm} = 15 \text{ Btu/hr-}^{\circ}\text{F-ft}$		Composition	55% (59% M)
Thermal expansion coefficient	$16 \times 10^{-6}/^{\circ}\text{C} = 29 \times 10^{-6}/^{\circ}\text{F}$		KCl (by weight)	45% (41% M)
Creep stress limit	8000 psi		LiCl (by weight)	1.60 g/cm ³ = 99.9 lb/ft ³
Young's modulus	29×10^6 psi		Density	.92 joules/g- $^{\circ}\text{C}$ =
Poisson's ratio	.28		Specific heat	.22 Btu/lb- $^{\circ}\text{F}$
<u>Properties of Bi</u>				
Thermal conductivity	.15 w/cm- $^{\circ}\text{C} = 8.9 \text{ Btu/hr-}^{\circ}\text{F-ft-}^{\circ}\text{F}$			
Specific heat	.15 joules/g- $^{\circ}\text{C} = .035 \text{ Btu/lb-}^{\circ}\text{F}$			
Density	$9.91 \text{ g/cm}^3 = 61.8 \text{ lb/ft}^3$			

exchanger with thermal pumping. Because the length of piping is very uncertain we quote the net pressure created per unit length and the investment per unit length. These quantities allow us to take into account bends, which were omitted from consideration, the effects of inserting various components which were not considered, and consequences of changing the reactor pressure drop from the very hypothetical .43 psi to some more realistic value.

It may be noted in the spray exchanger that if the temperature drop from the bismuth to salt is increased to 21°C the time of fall is cut to 1 sec and the heat exchanger investment is cut in half. Remaking the pool from a right cylinder into a trumpet will materially decrease the pool investment. The spray exchanger then looks even more advantageous. (It must be remembered that one film + wall temperature drop with the tubular exchangers is 35°C, whereas the total drop may be about 50°C.) There are few other parameters which may as effectively lower the investment (although a higher value for the power transfer coefficient of the drops will also decrease the spray exchanger investment). The disadvantages of the spray exchanger system are: (1) difficulties with emergency cooling, (2) difficult corrosion problems, (3) possible admixing of bismuth and salt, (4) somewhat higher pumping powers (not serious), (5) number of holes in the distribution plate.

Kinetic energy losses in the heat exchangers proper are of negligible importance. Header volumes are of negligible importance.

Acknowledgements

The author wishes to acknowledge the aid or advice of many people and to thank them for it.

This problem had its origins in discussions with Dr. Warren E. Winsche, Mr. William R. Page and Mr. David W. Bareis. These people were of very considerable assistance to the author in the early stages of the work. Later Dr. Orrington E. Dwyer gave useful advice.

Mr. Charles Eisenhauer and most especially Miss Leona Schloss were of very great assistance with a large part of the numerical work.

Mrs. Jean Dominy was of great assistance in beautifully typing the manuscript, including all the numerous graphs.

The author would like to thank Dr. Irving Kaplan for valuable criticisms of the work.

Finally, the author would like to acknowledge and to thank the many anonymous members of the Technical Information Division for the enormous amount of painstaking and tedious work involved in bringing out a report such as this.

Any Exchanger System

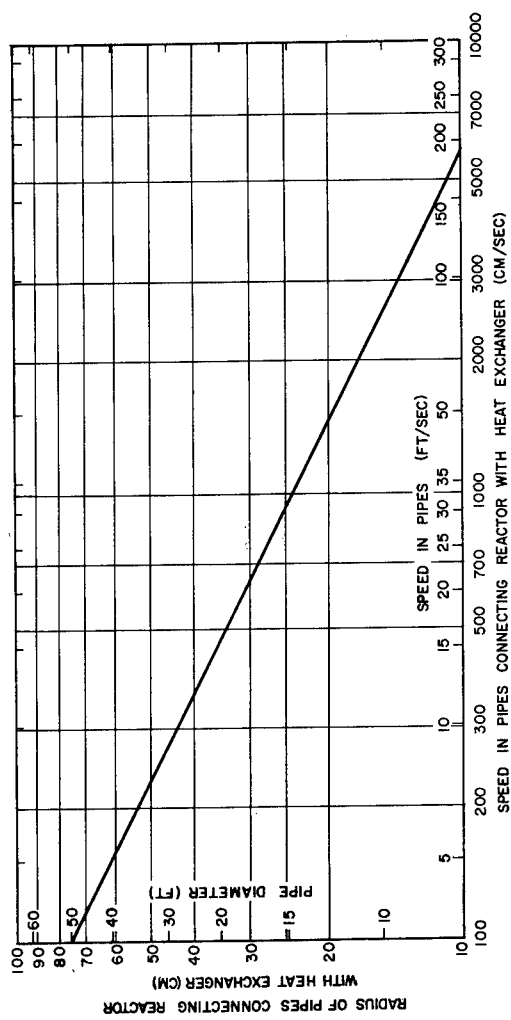


Figure 5. Radius of pipes connecting reactor with heat exchanger vs speed in pipes.

Any Tubular Exchanger

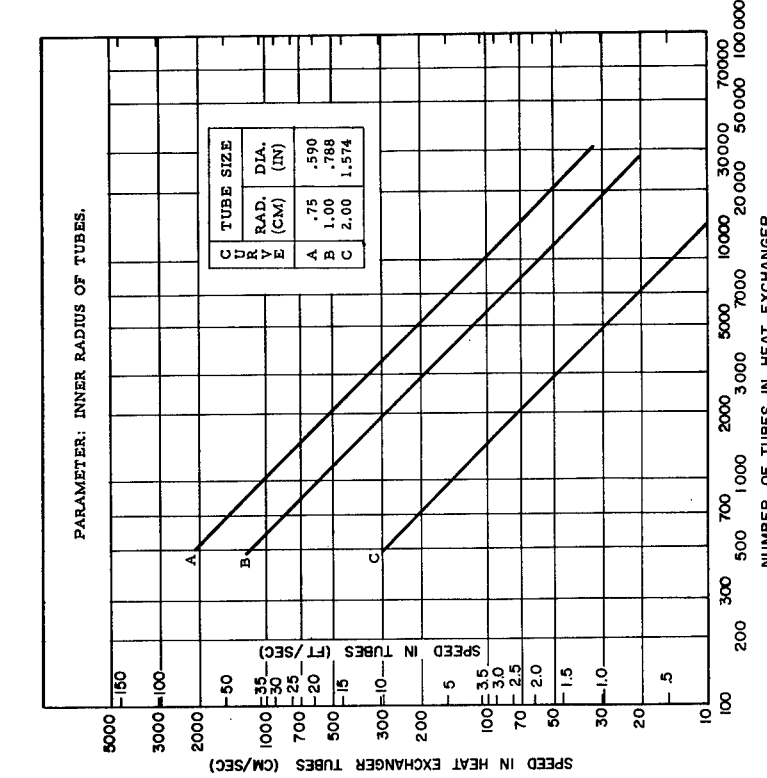


Figure 6a. Speed in heat exchanger tubes vs number of exchanger tubes.

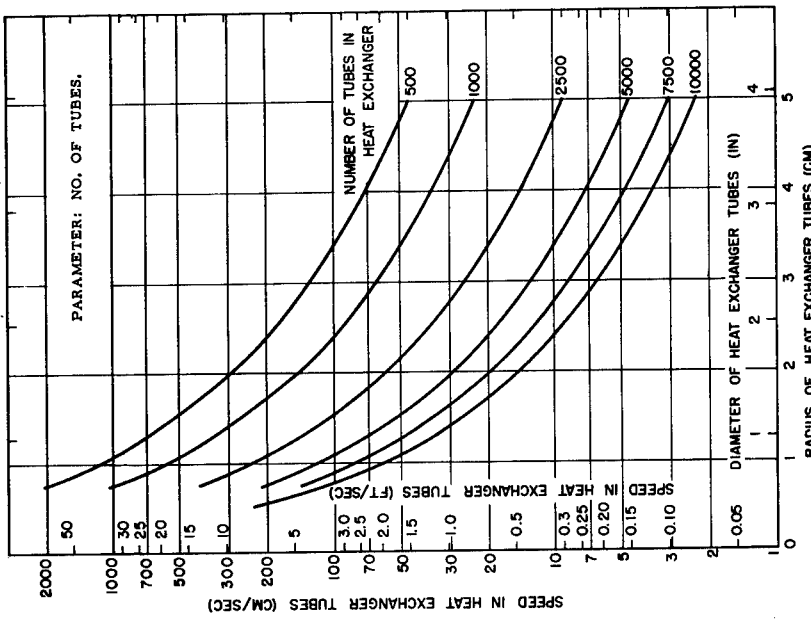


Figure 6b. Speed in heat exchanger tubes vs radius of heat exchanger tubes.

Any Tubular Exchanger

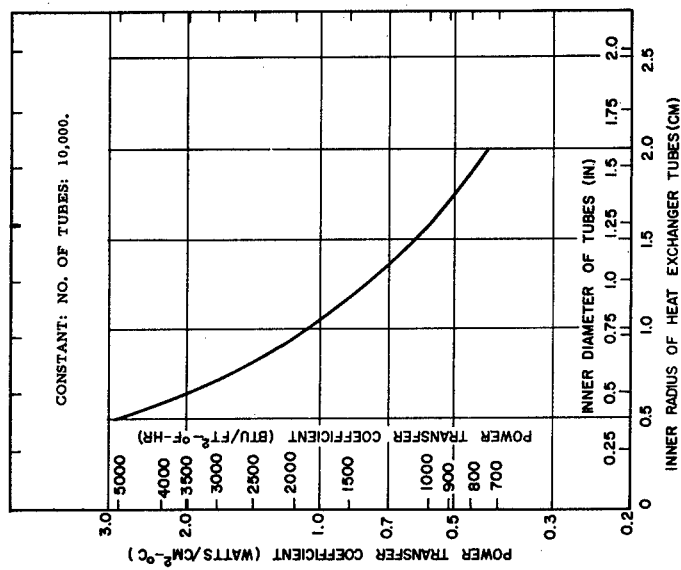


Figure 7a. Power transfer coefficient
vs inner radius of heat exchanger tubes.

Any Tubular Exchanger

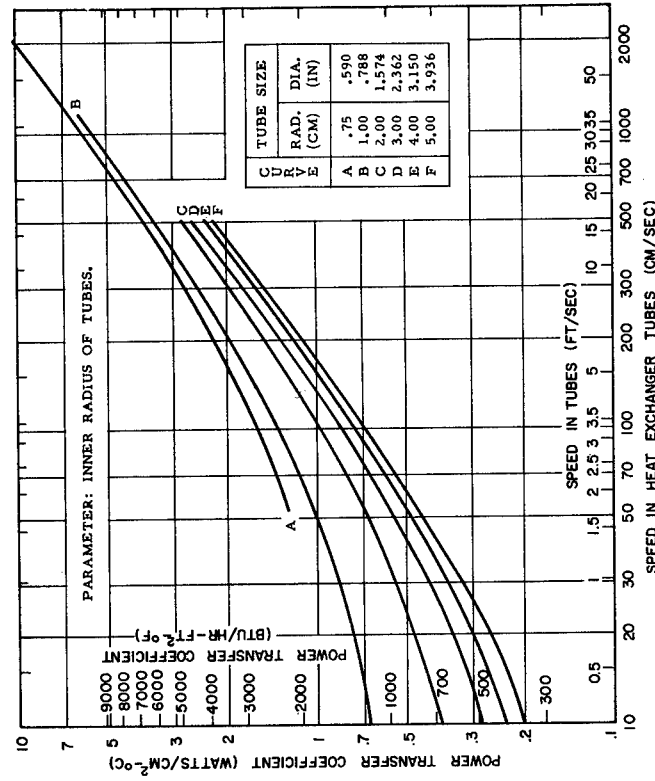


Figure 7b. Power transfer coefficient vs speed in heat exchanger tubes.

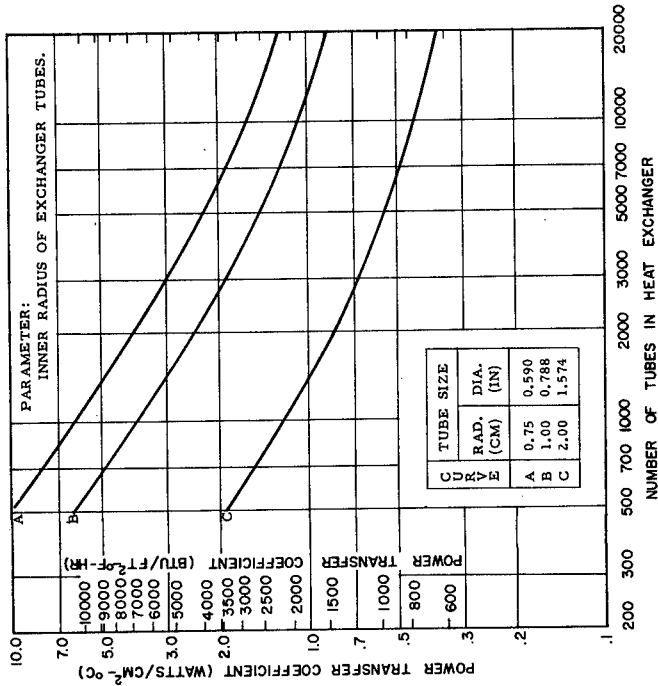


Figure 7c. Power transfer coefficient vs number of heat exchanger tubes.

Any Tubular Exchanger

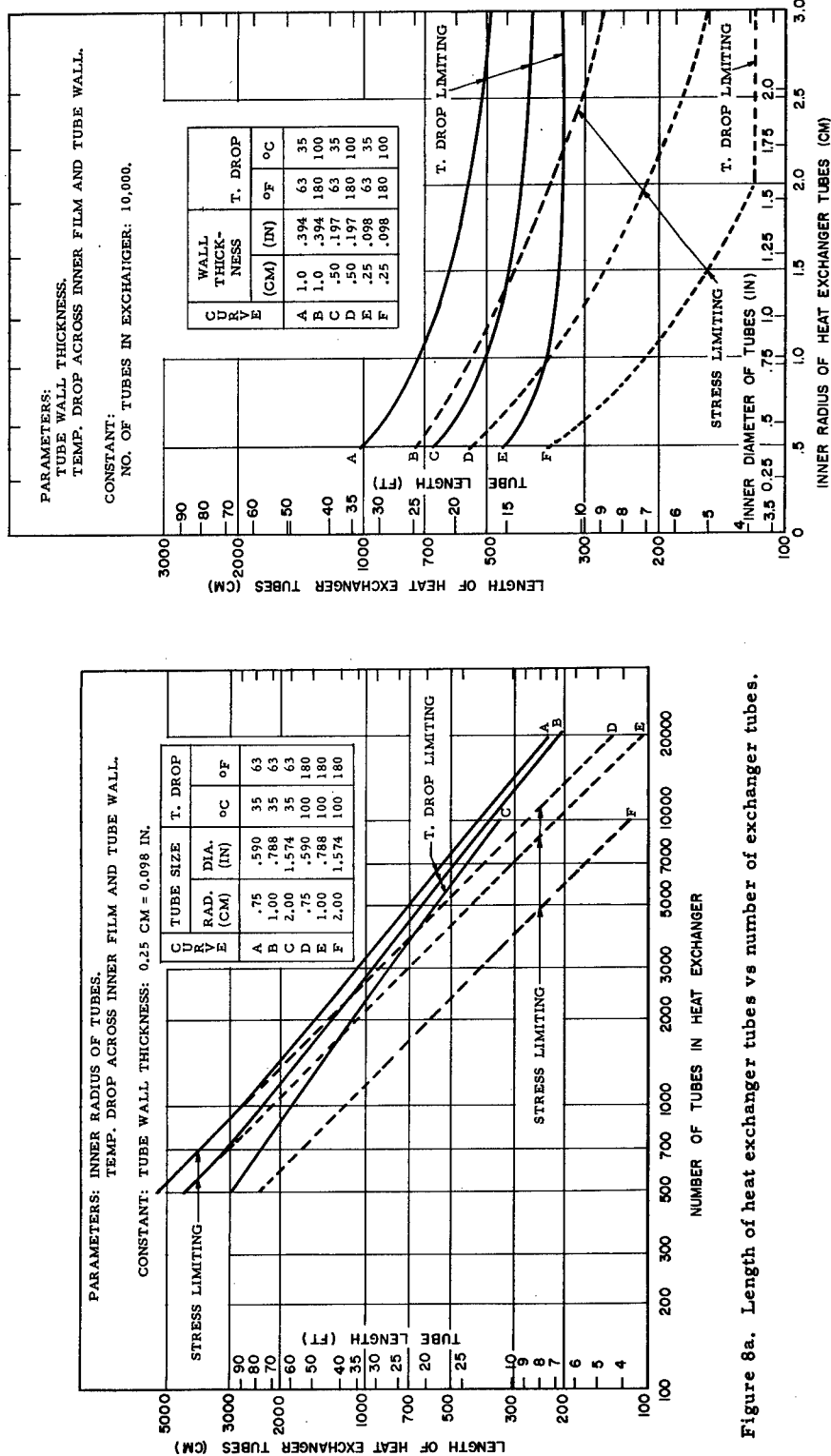


Figure 8a. Length of heat exchanger tubes vs number of exchanger tubes.

Figure 8b. Length of heat exchanger tubes vs their inner radius.

Any Tubular Exchanger

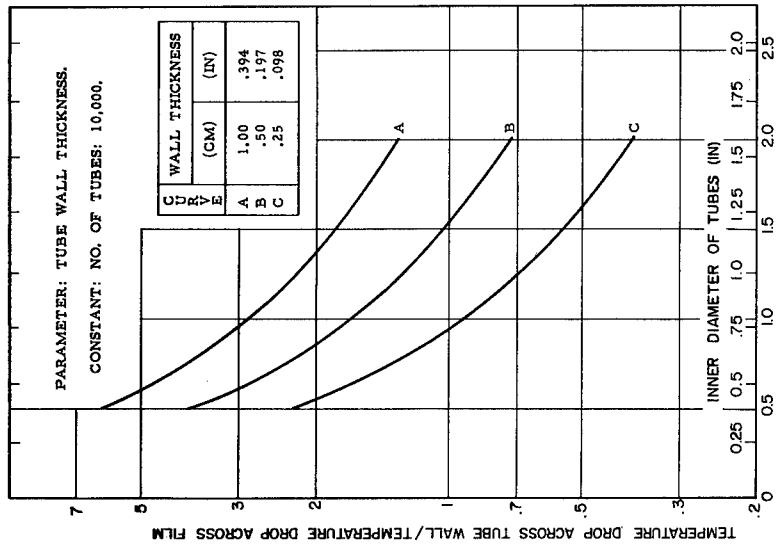


Figure 9a. Tube wall film temperature drops vs radius of heat exchanger tubes.

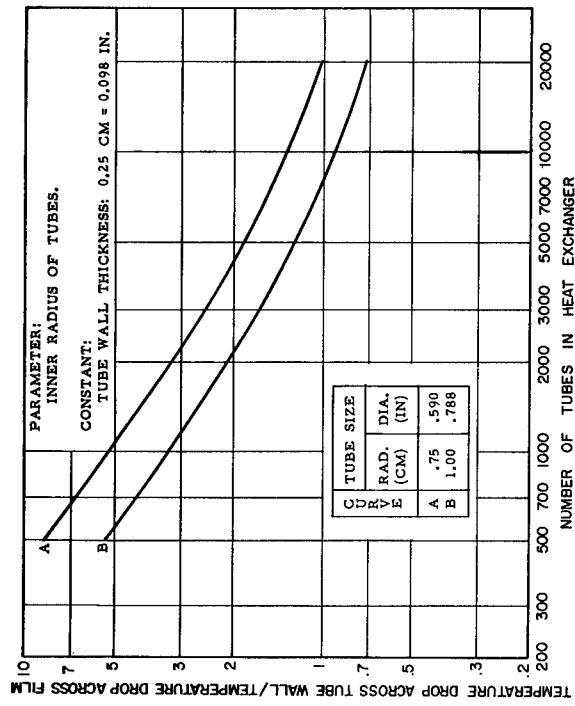


Figure 9b. Tube wall film temperature drop vs number of heat exchanger tubes.

Tubular Exchanger: Thermal Pumping

38

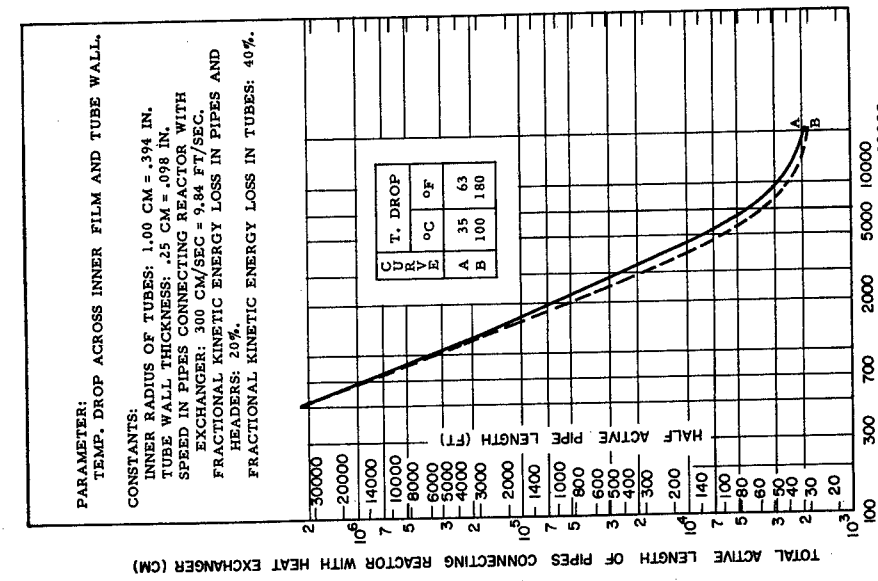


Figure 10a. Total active length of pipes connecting reactor with heat exchanger vs number of tubes.

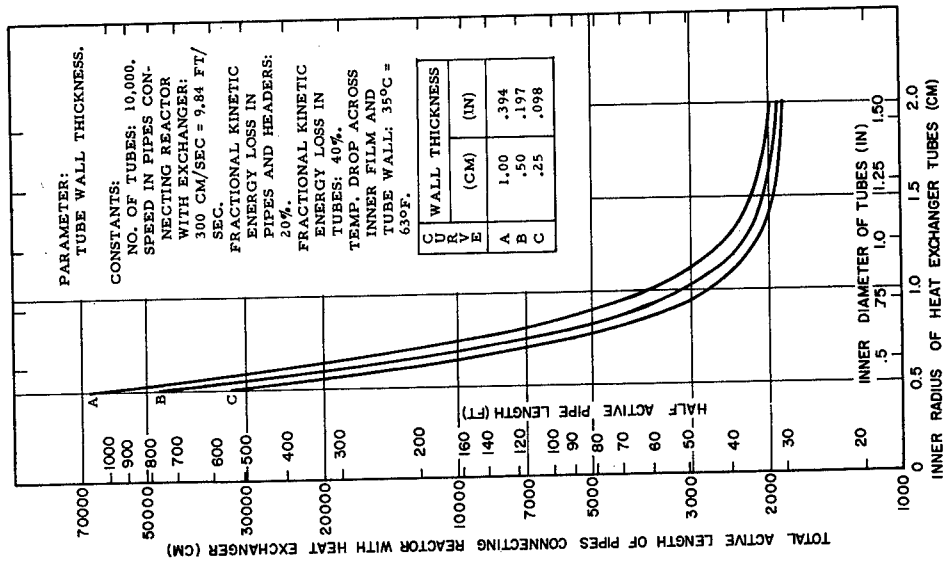


Figure 10b. Total active length of pipes connecting reactor with heat exchanger vs inner radius of tubes.

Tubular Exchanger: Thermal Pumping

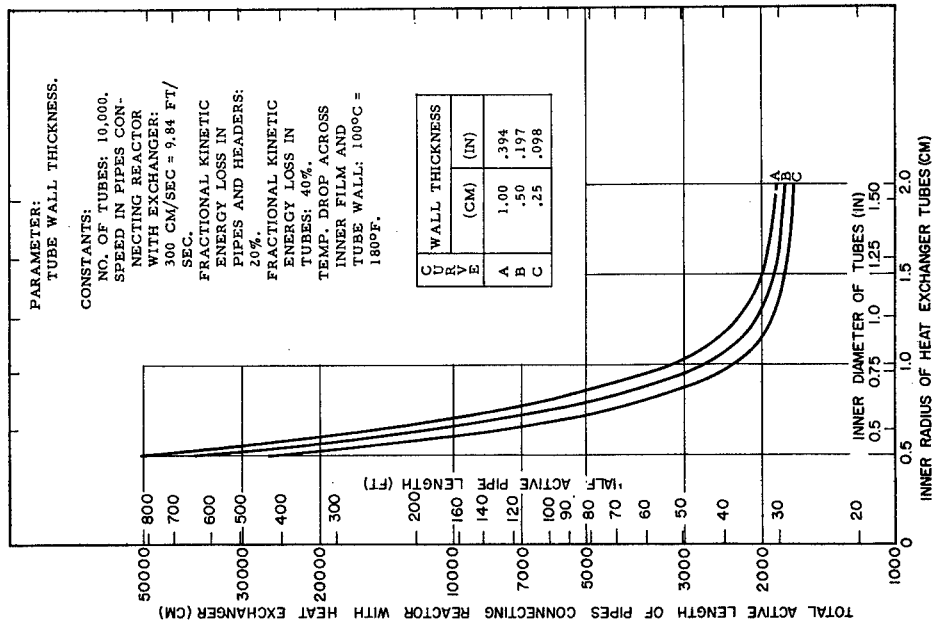


Figure 10c. Total active length of pipes connecting reactor with heat exchanger vs inner radius of tubes.

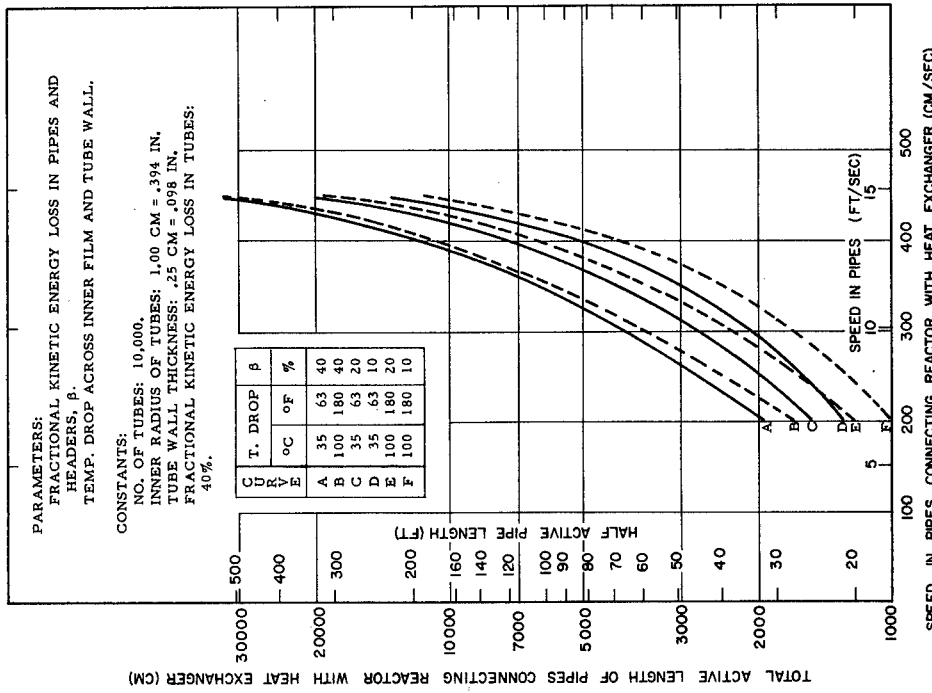


Figure 10d. Total active length of pipes connecting reactor with heat exchanger vs speed in pipes.

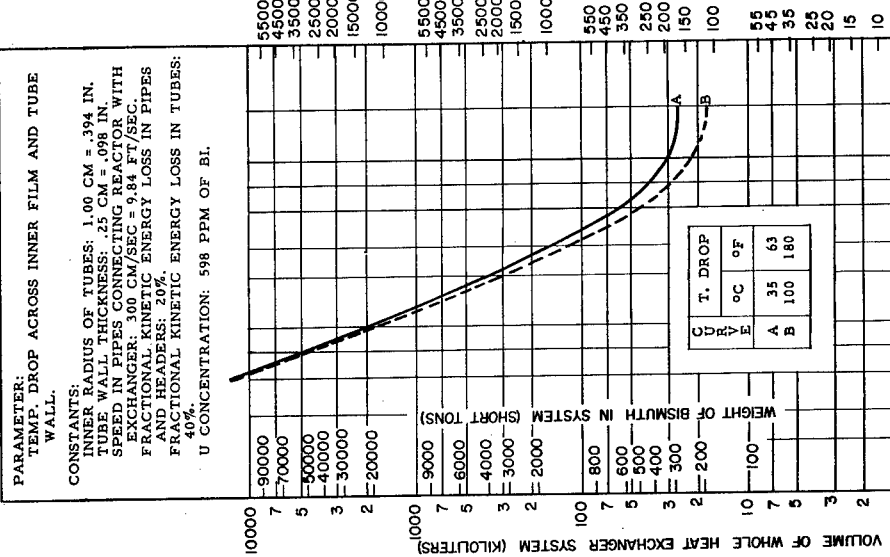


Figure 11a (Left). Mass of uranium in and volume of whole heat exchanger system vs number of exchanger tubes. BNL Log No. D-2068.

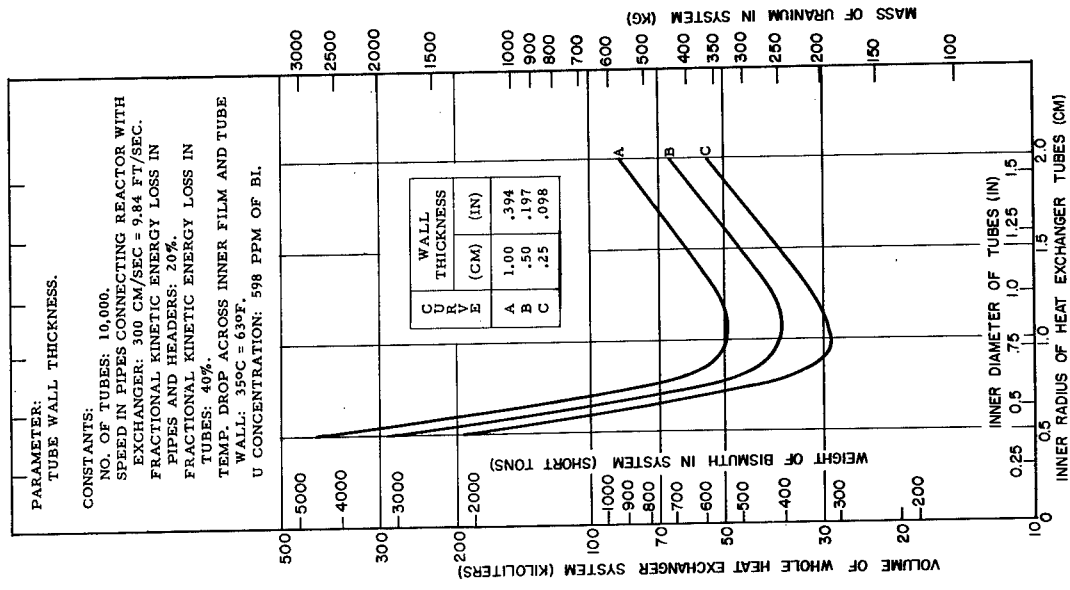


Figure 11b (Right). Mass of uranium in and volume of whole heat exchanger system vs inner radius of exchanger tubes. BNL Log No. D-2069.

Tubular Exchanger: Thermal Pumping

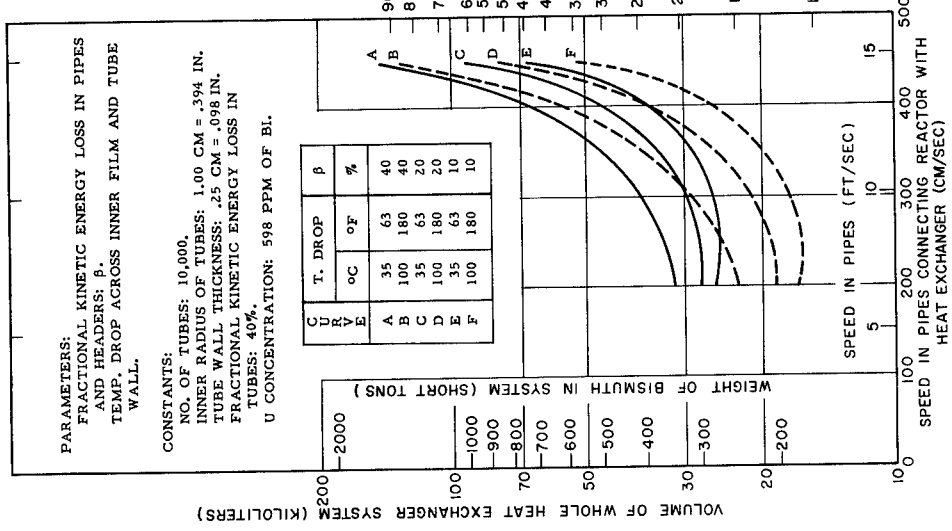
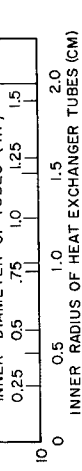
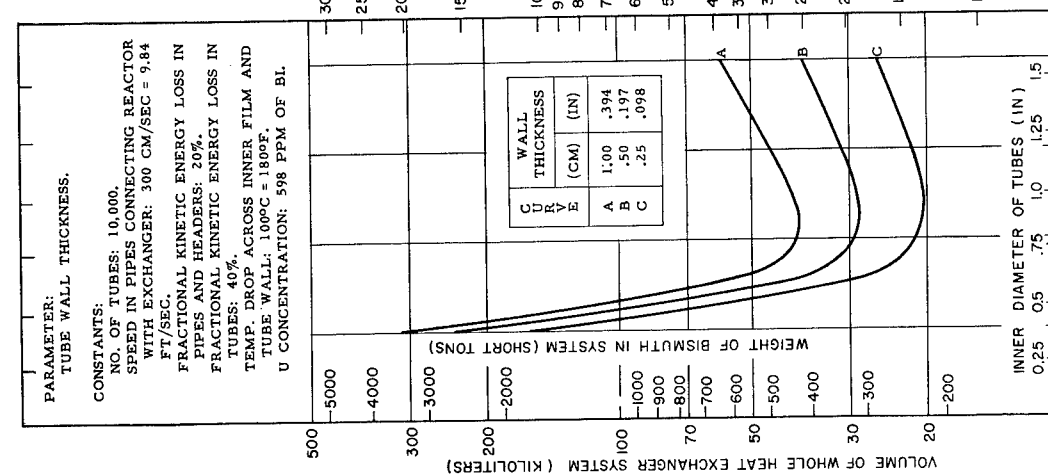


Figure 11c. (Left). Mass of uranium in and volume of whole heat exchanger system vs inner radius of exchanger tubes. BNL Log No. D-2070.

Figure 11d (Right). Mass of uranium in and volume of whole heat exchanger system vs speed in pipes connecting reactor with exchanger. BNL Log No. D-2071.

Tubular Exchanger: Thermal Pumping

42

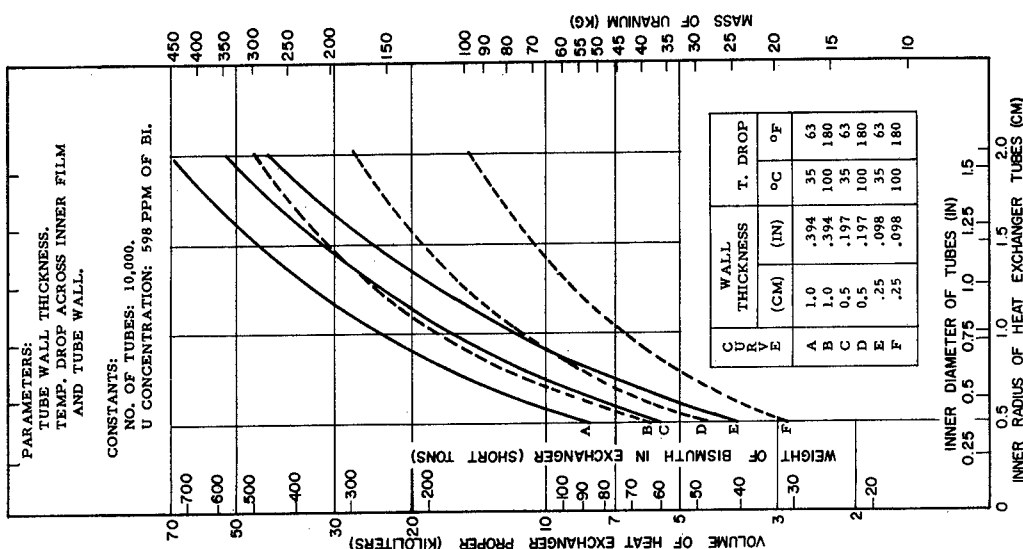


Figure 12a. Mass of uranium in and volume of heat exchanger proper vs inner radius of heat exchanger tubes. BNL Log No. D-2072.

Tubular Exchanger: Thermal Pumping

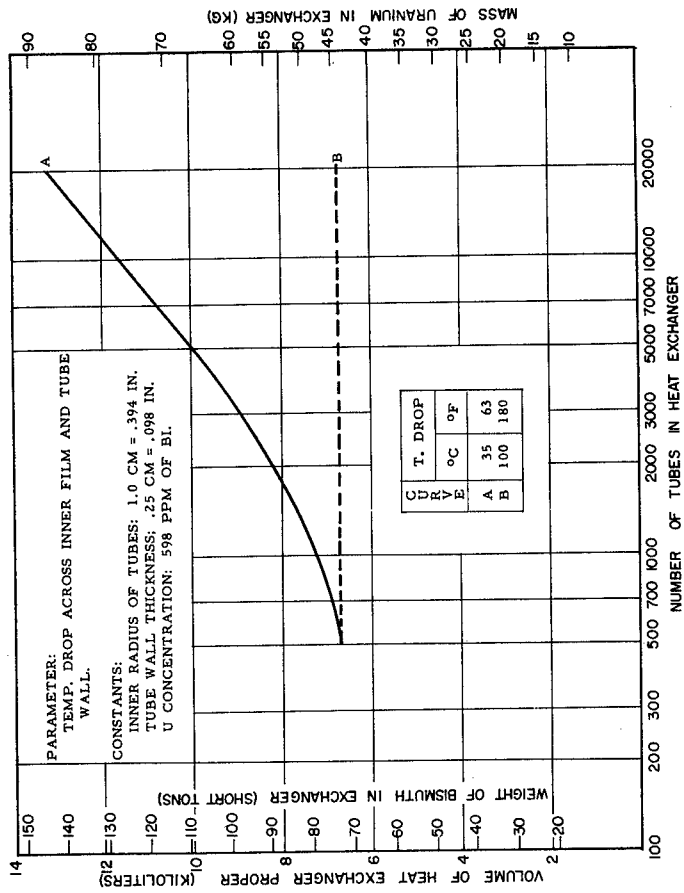


Figure 12b. Mass of uranium in and volume of heat exchanger proper vs number of exchanger tubes. BNL Log No. D-2073.

Tubular Exchanger: Thermal Pumping

44

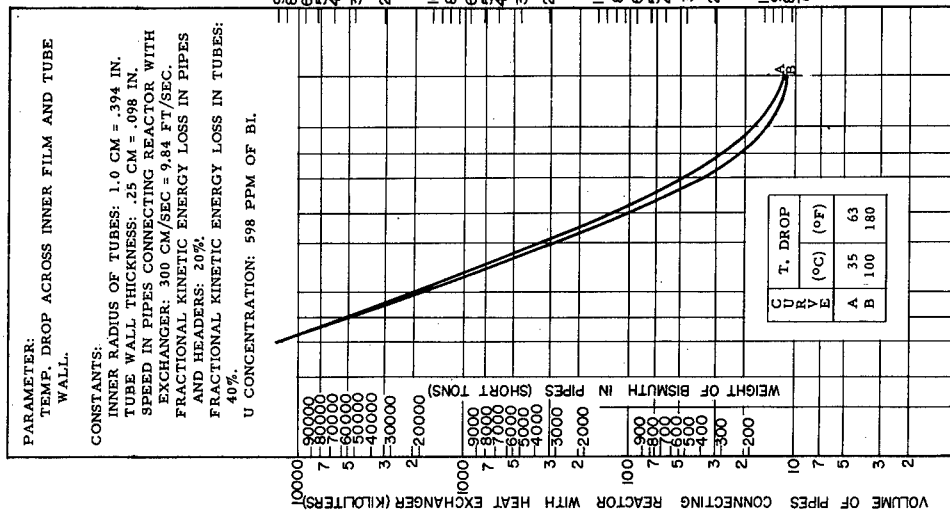


Figure 13a (Left). Mass of uranium in and volume of pipes connecting reactor with heat exchanger vs number of exchanger tubes. BNL Log No. D-2074.

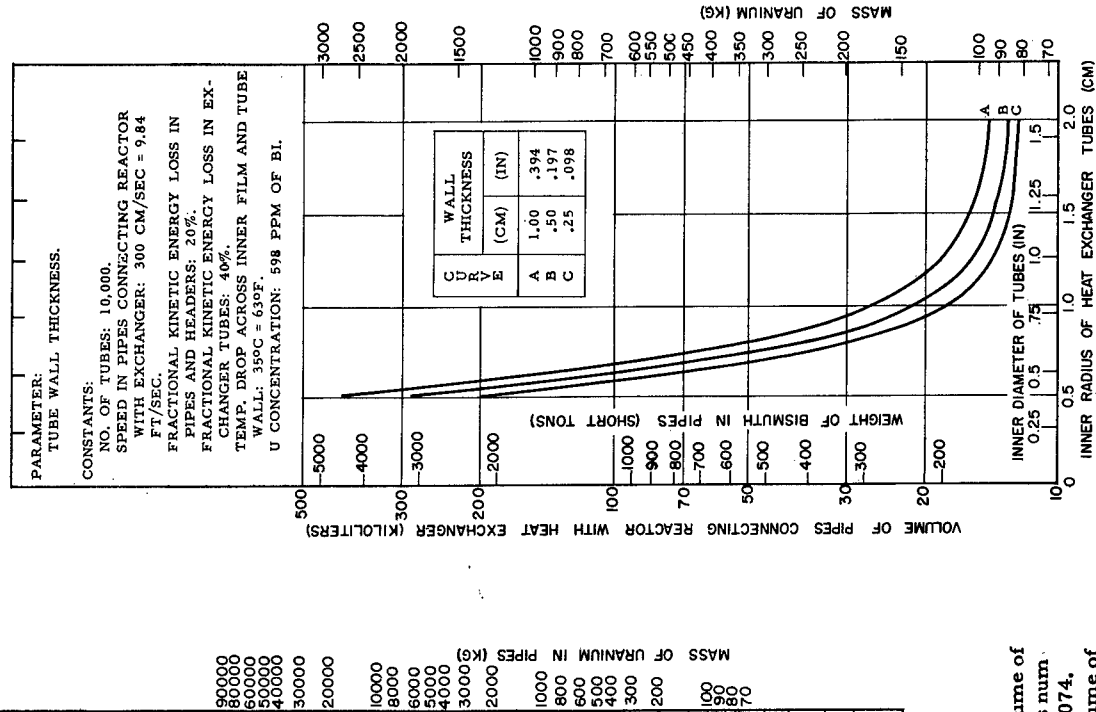


Figure 13b (Right). Mass of uranium in and volume of pipes connecting reactor with heat exchanger vs inner radius of exchanger tubes. BNL Log No. D-2075.

Tubular Exchanger: Thermal Pumping

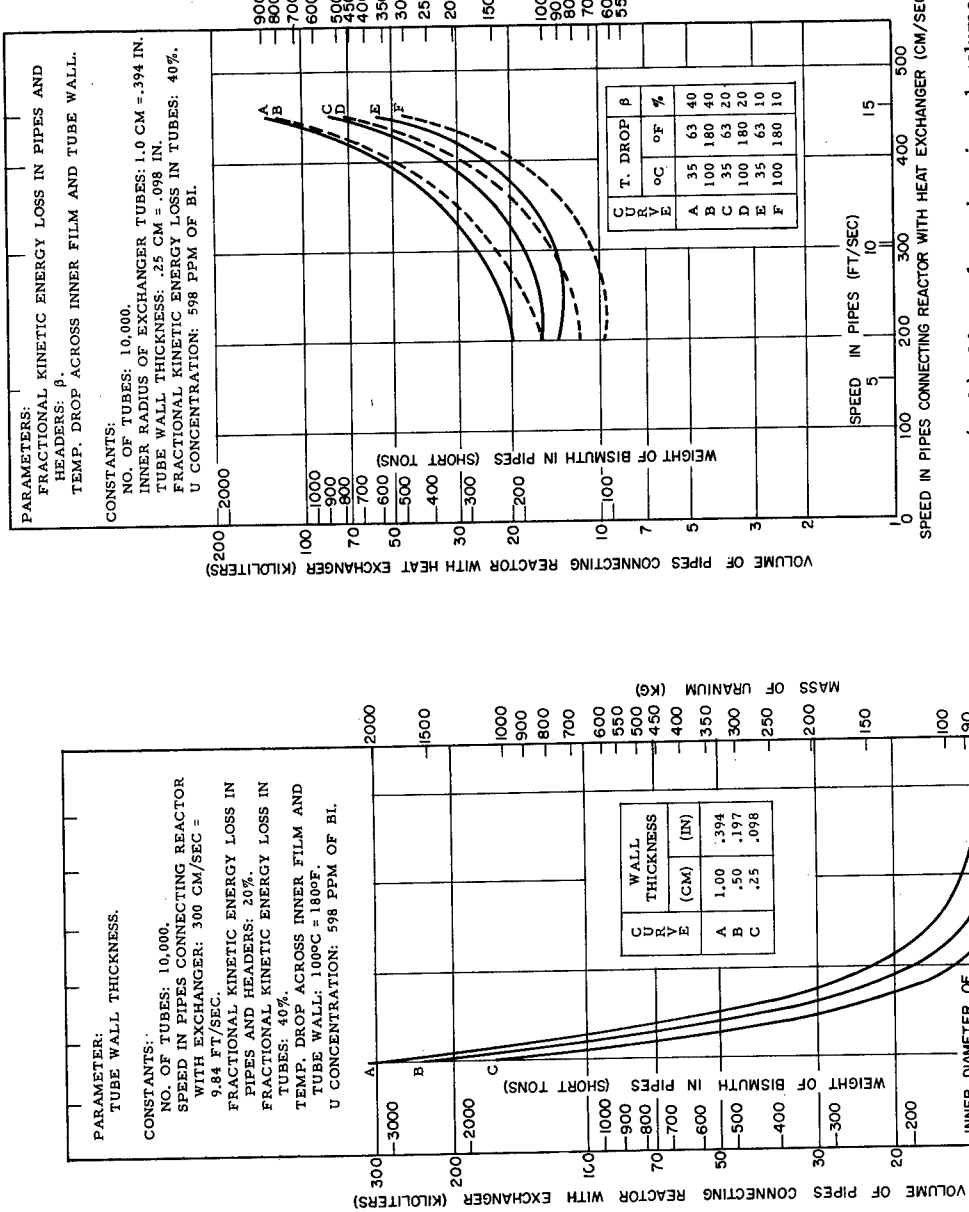


Figure 13c (Left). Mass of uranium in and volume of pipes connecting reactor with heat exchanger vs inner radius of exchanger tubes. BNL Log No. D-2076.

Figure 13d (Right). Mass of uranium in and volume of pipes connecting reactor with heat exchanger vs speed in pipes. BNL Log No. D-2077.

Tubular Exchanger: Mechanical Pumping.

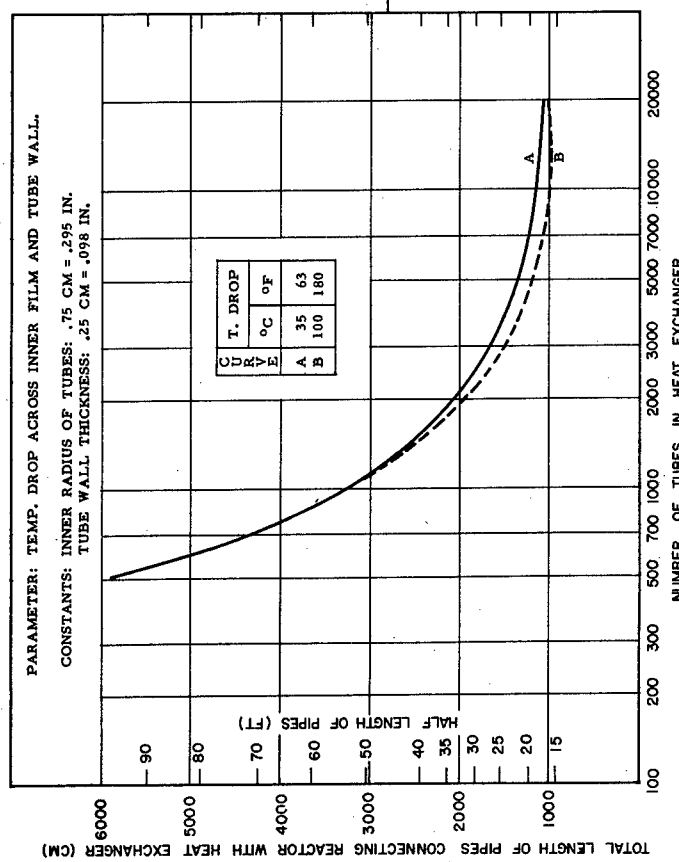


Figure 14a. Length of pipes connecting heat exchanger and reactor vs number of tubes in heat exchanger.

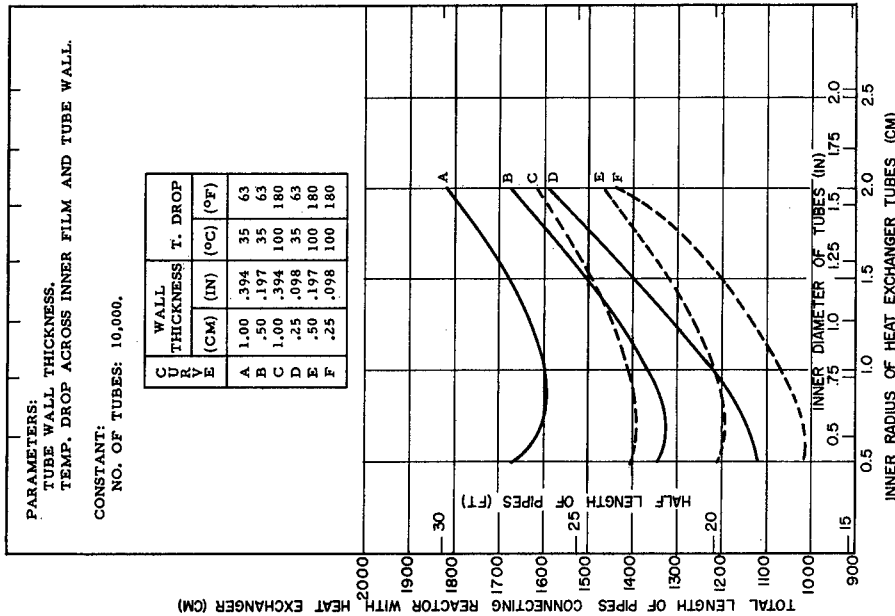


Figure 14b. Length of pipes connecting reactor with heat exchanger vs inner radius of tubes.

Tubular Exchanger: Mechanical Pumping

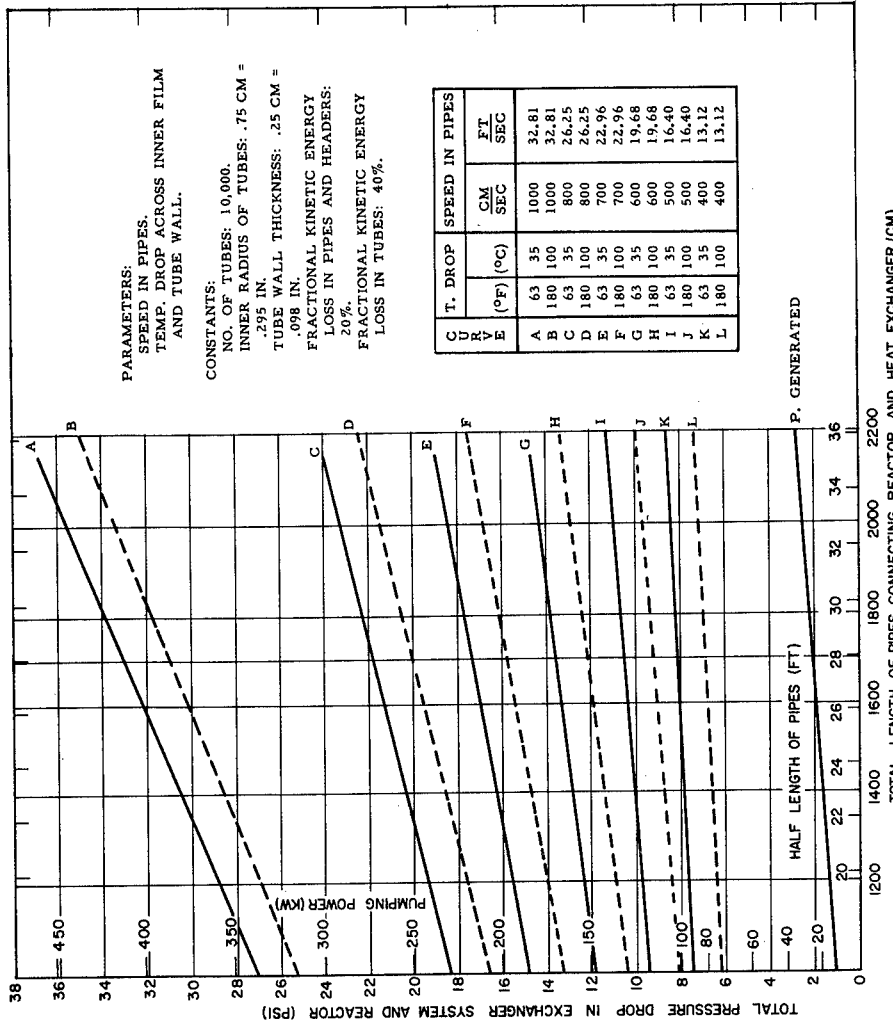


Figure 15a. Total pressure drop in heat exchanger system and reactor vs length of pipes connecting reactor with exchanger.

Tubular Exchanger: Mechanical Pumping

48

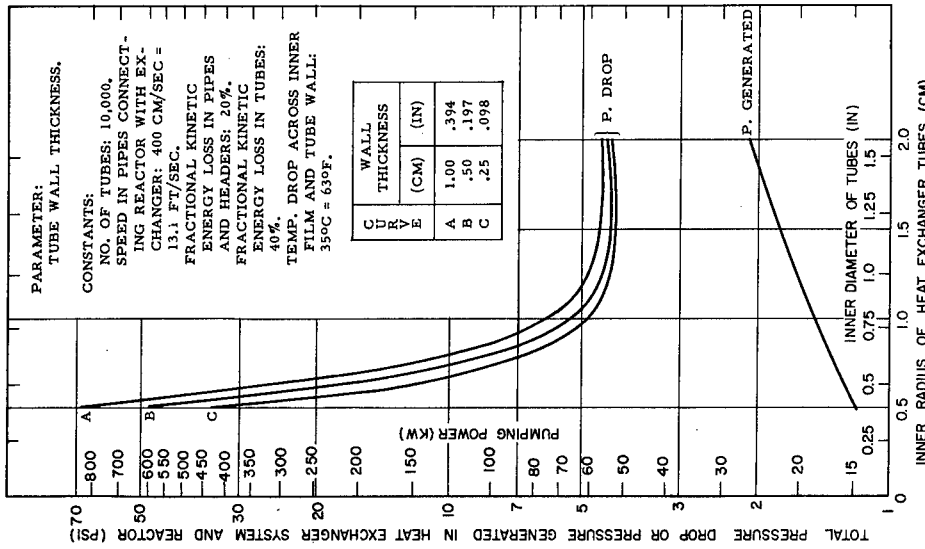


Figure 15b. Total pressure drop and pumping power in heat exchanger system and reactor vs inner radius of tubes. Pressure and pumping power generated by active part of pipes connecting reactor with heat exchanger tubes.

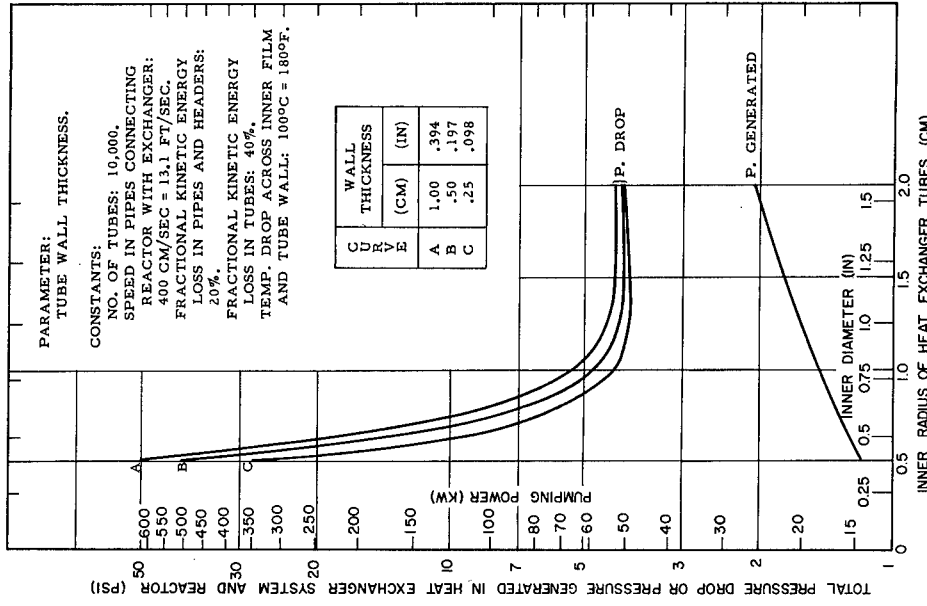


Figure 15c. Total pressure drop and pumping power in heat exchanger system and reactor vs inner radius of tubes. Pressure and pumping power generated by active part of pipes connecting reactor with heat exchanger vs inner radius of tubes.

Tubular Exchanger: Mechanical Pumping

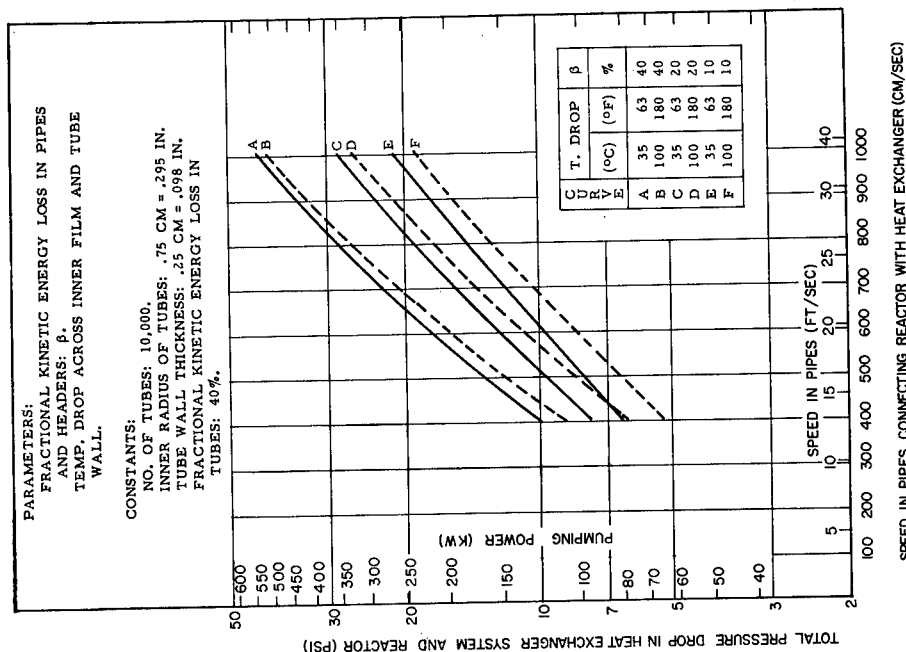
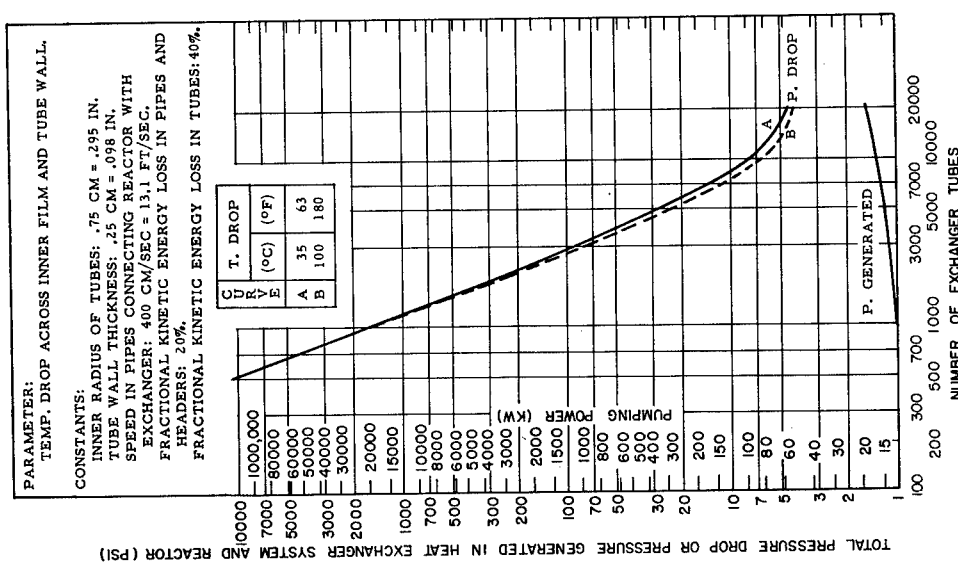


Figure 15d. Total pressure drop and pumping power in heat exchanger system and reactor vs number of exchanger tubes.

Figure 15e. Total pressure drop and pumping power in heat exchanger system and reactor vs speed in pipes connecting reactor with exchanger system.

Tubular Exchanger: Mechanical Pumping

50

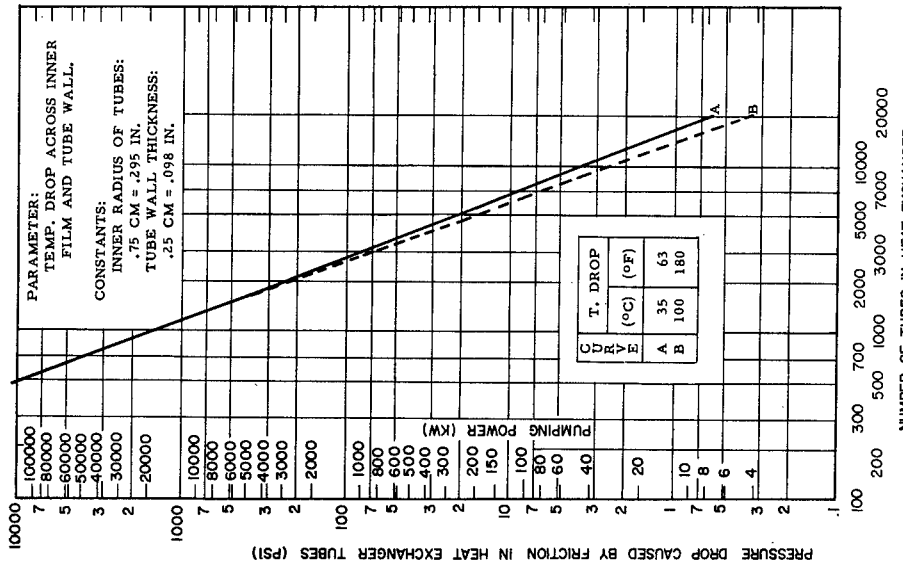


Figure 16a. Pressure drop caused by friction in heat exchanger tubes vs number of exchanger tubes.

Tubular Exchanger: Mechanical Pumping

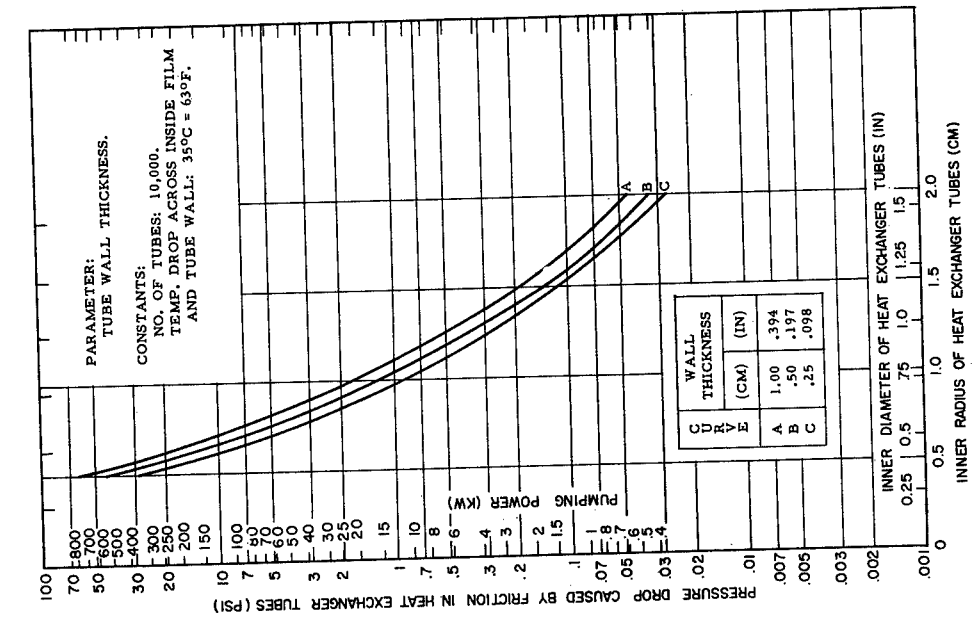


Figure 16b. Pressure drop in heat exchanger tubes caused by friction vs inner radius of heat exchanger tubes.

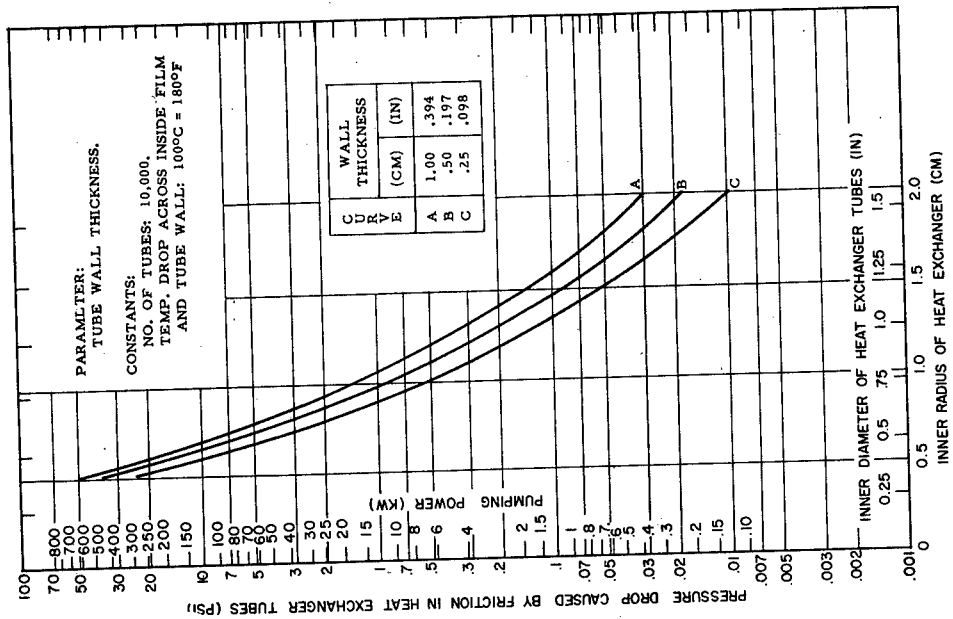


Figure 16c. Pressure drop in heat exchanger tubes caused by friction vs inner radius of heat exchanger tubes.

Tubular Exchanger: Mechanical Pumping

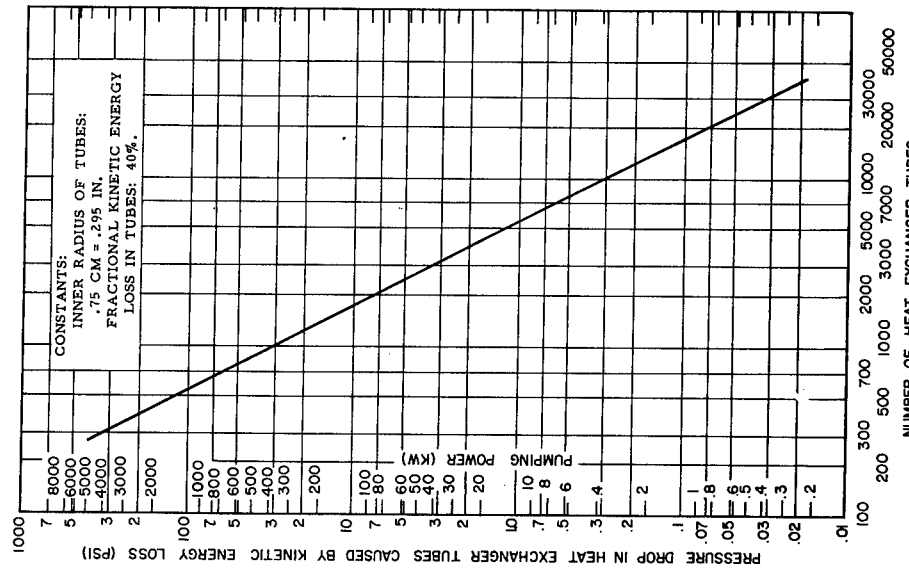


Figure 17a. Pressure drop in tubes caused by kinetic energy loss vs number of tubes.

Tubular Exchanger: Mechanical Pumping

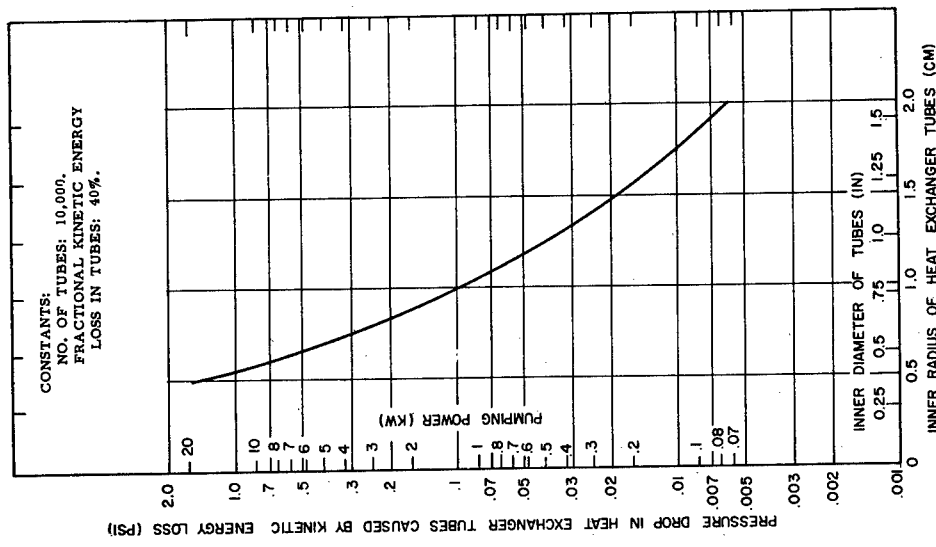


Figure 17b. Pressure drop in heat exchanger tubes caused by kinetic energy loss vs inner radius of tubes.

Tubular Exchanger: Mechanical Pumping

54

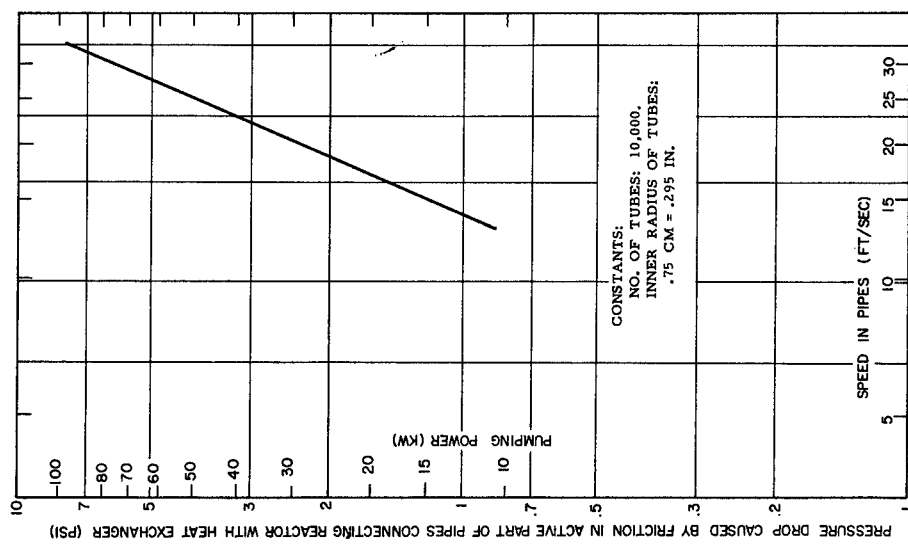


Figure 18a. Pressure drop caused by friction in active part of pipes connecting reactor with heat exchanger vs speed in pipes.

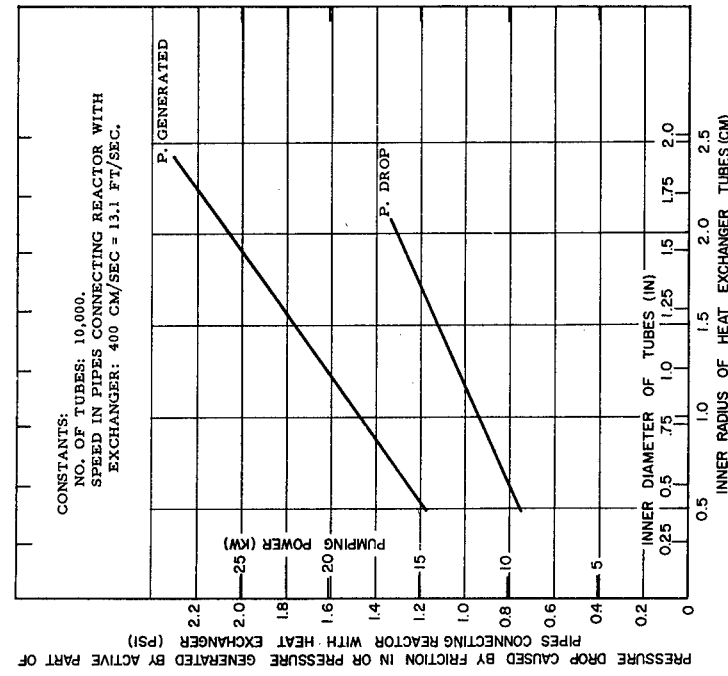


Figure 18b. Pressure drop caused by friction in active part of pipes connecting reactor with heat exchanger vs inner radius of heat exchanger tubes.

Tubular Exchanger: Mechanical Pumping

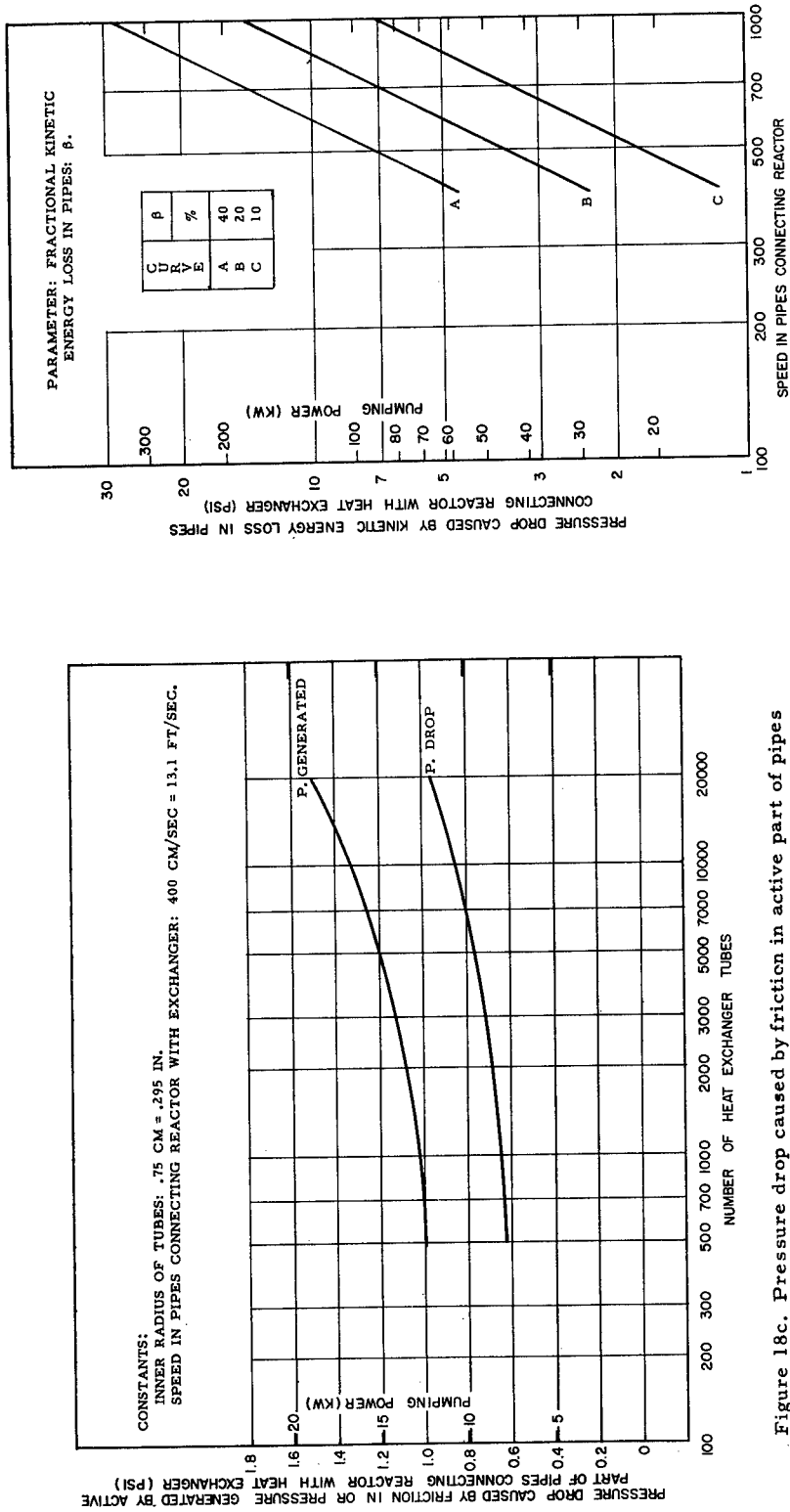


Figure 18c. Pressure drop caused by friction in active part of pipes connecting reactor with heat exchanger vs number of exchanger tubes.
Pressure generated by active part of pipes connecting reactor with heat exchanger vs number of exchanger tubes.

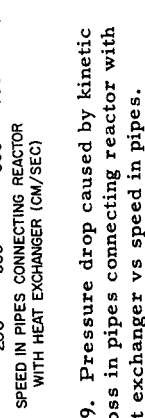


Figure 19. Pressure drop caused by kinetic energy loss in pipes connecting reactor with heat exchanger vs speed in pipes.

Tubular Exchanger: Mechanical Pumping

56

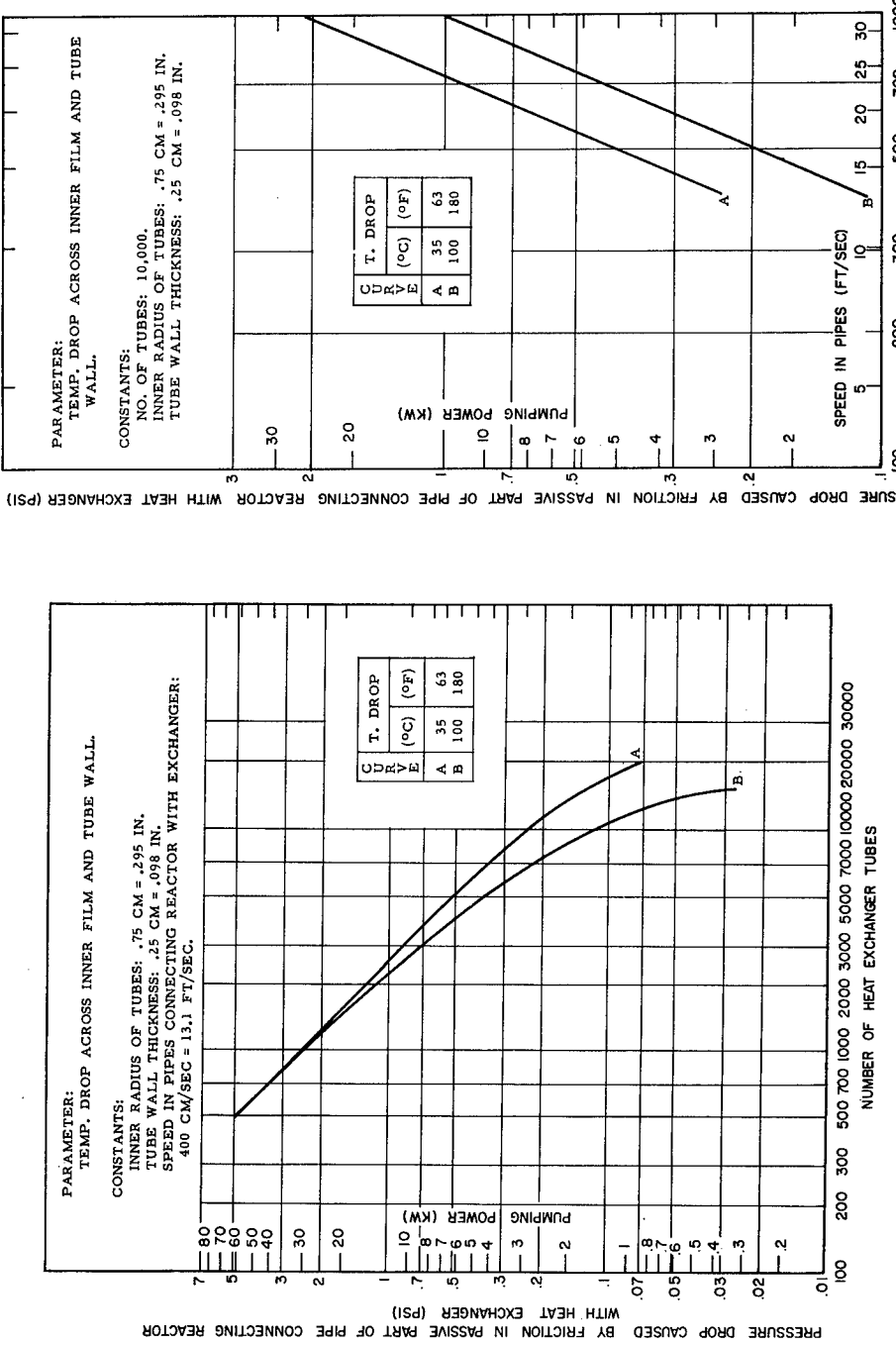


Figure 20a. Pressure drop caused by friction in passive part of pipe connecting reactor with heat exchanger vs number of exchanger tubes.

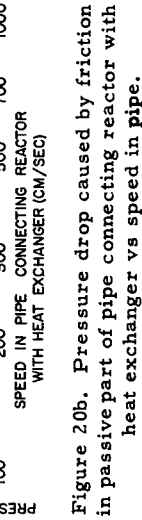


Figure 20b. Pressure drop caused by friction in passive part of pipe connecting reactor with heat exchanger vs speed in pipe.

Tubular Exchanger: Mechanical Pumping

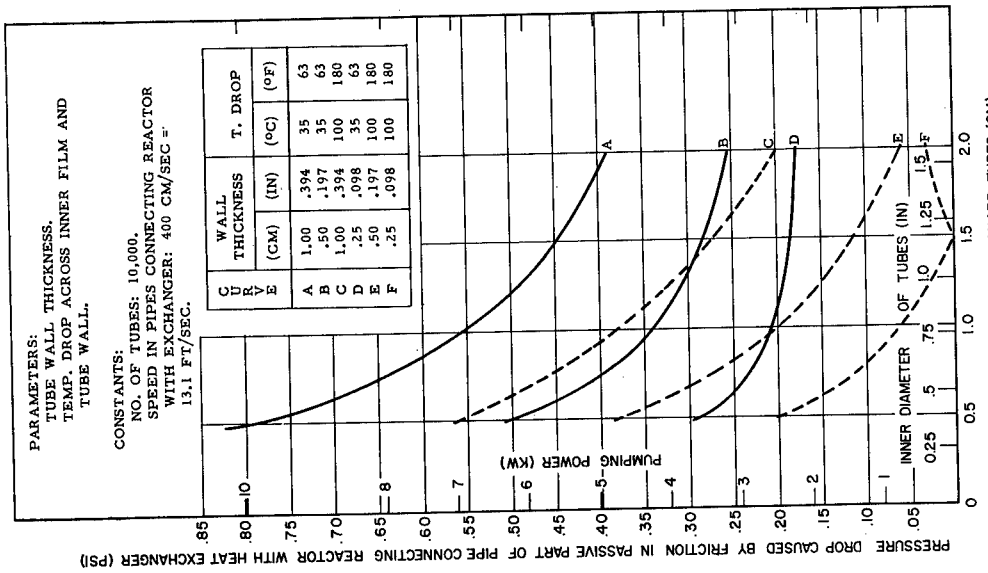


Figure 20c. Pressure drop caused by friction in passive part of pipe connecting reactor with heat exchanger vs inner radius of heat exchanger tubes.

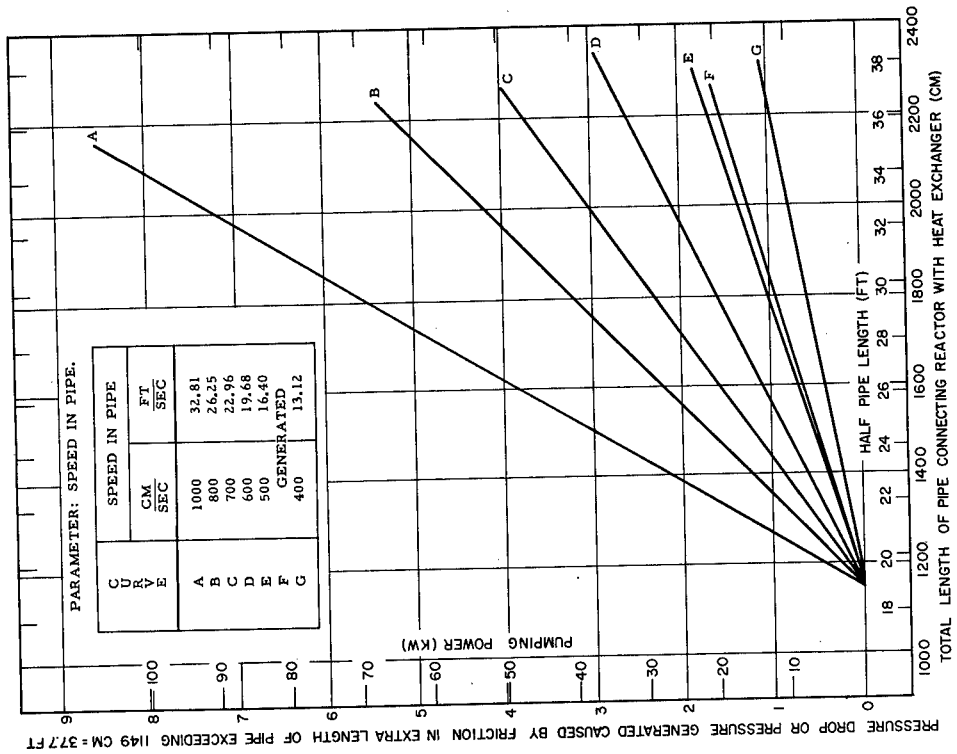


Figure 20d. Pressure drop caused by friction in extra lengths of pipe connecting reactor with heat exchanger vs length of pipe.

Tubular Exchanger: Mechanical Pumping

58

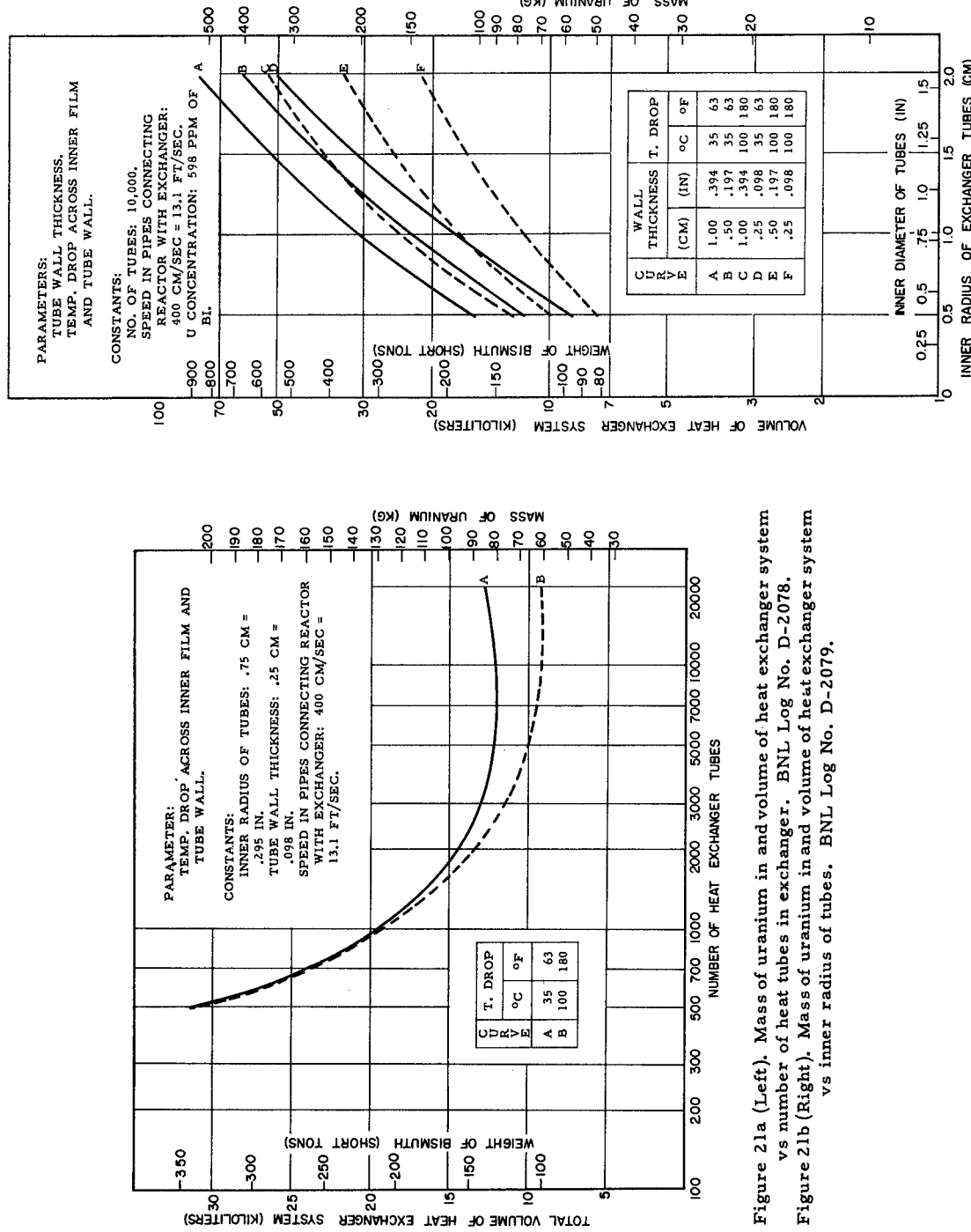


Figure 21a (Left). Mass of uranium in and volume of heat exchanger system vs number of heat tubes in exchanger. BNL Log No. D-2078.

Figure 21b (Right). Mass of uranium in and volume of heat exchanger system vs inner radius of tubes. BNL Log No. D-2079.

Tubular Exchanger: Mechanical Pumping

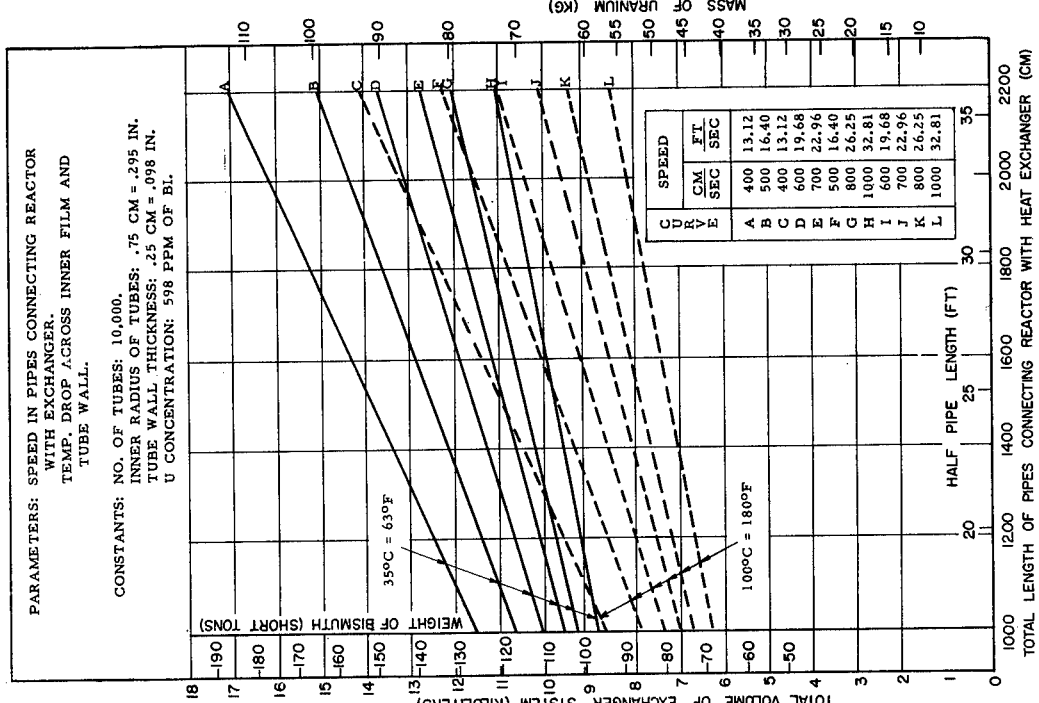
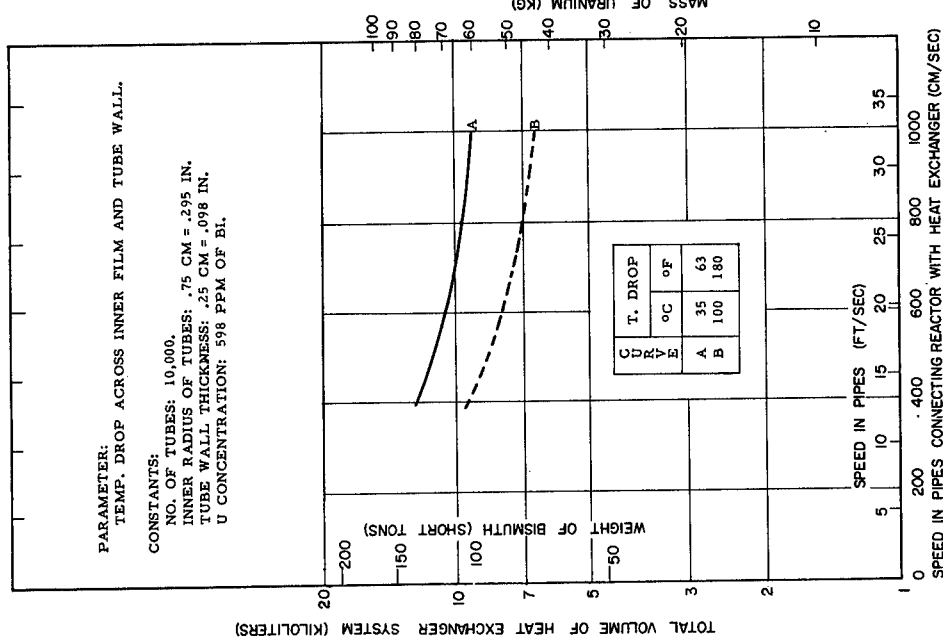


Figure 21c (Left). Mass of uranium in and volume of heat exchanger system vs speed in pipes connecting reactor with exchanger. BNL Log No. D-2080.
 Figure 21d (Right). Mass of uranium in and volume of heat exchanger system vs length of pipes connecting reactor with exchanger. BNL Log No. D-2081.

Tubular Exchanger: Mechanical Pumping

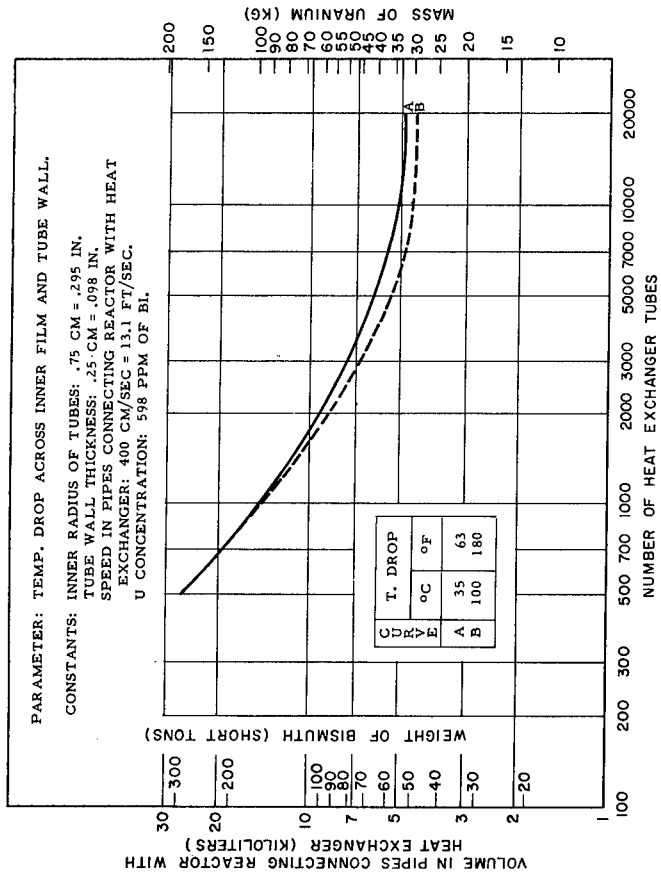


Figure 22a. Mass of uranium in and volume of pipes connecting reactor with heat exchanger vs number of exchanger tubes. BNL Log No. D-2083.

Tubular Exchanger: Mechanical Pumping

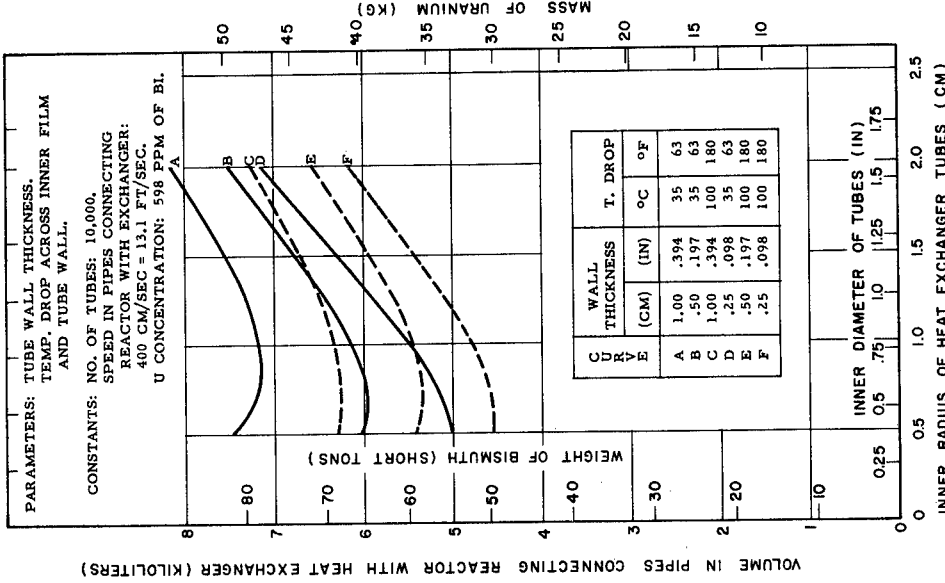
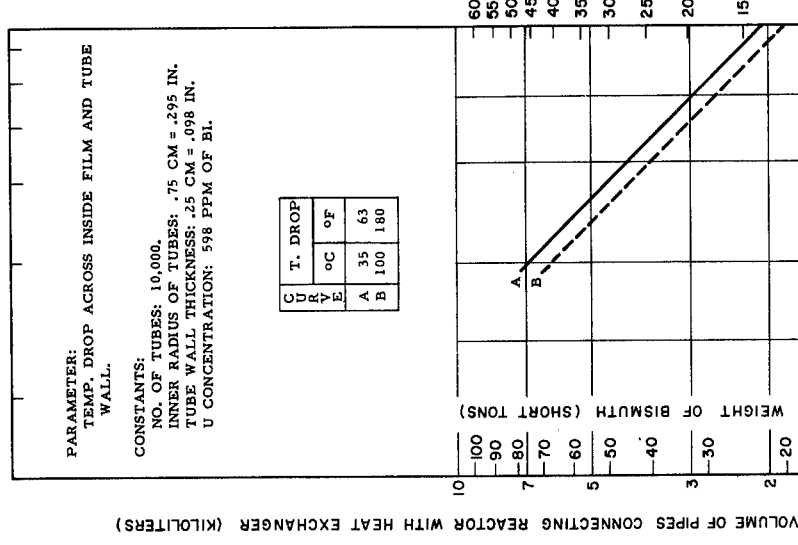


Figure 22b. Mass of uranium in and volume of pipes connecting reactor with heat exchanger vs inner radius of heat exchanger tubes. BNL Log No. D-2082.

Figure 22c. Mass of uranium in and volume of pipes connecting reactor with heat exchanger vs inner radius of heat exchanger tubes. BNL Log No. D-2084.

Tubular Exchanger: Mechanical Pumping

62

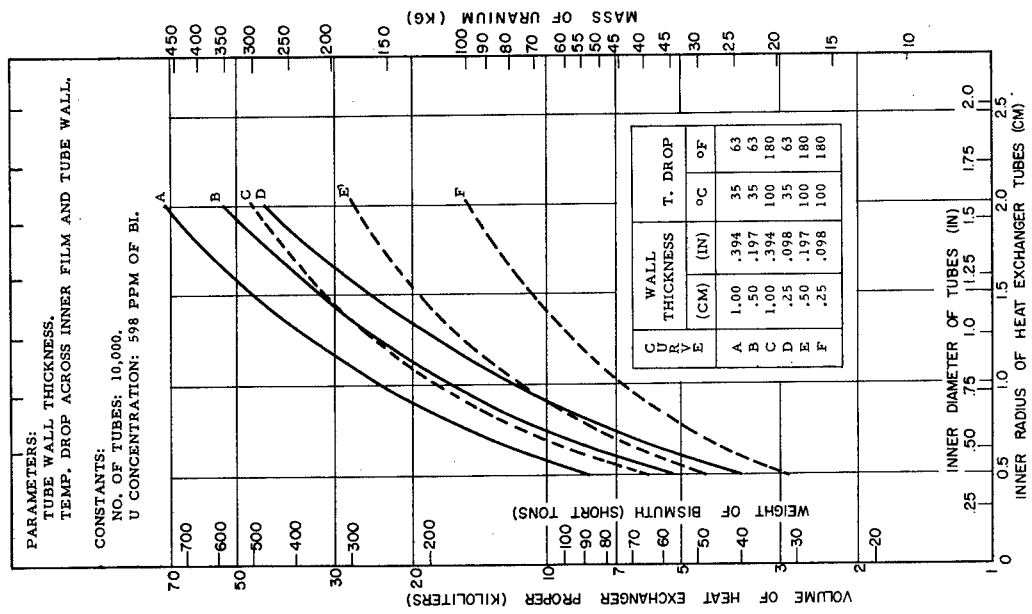


Figure 23a. Mass of uranium in and volume of heat exchanger proper vs inner radius of tubes.
BNL Log No. D-2085.

Tubular Exchanger: Mechanical Pumping

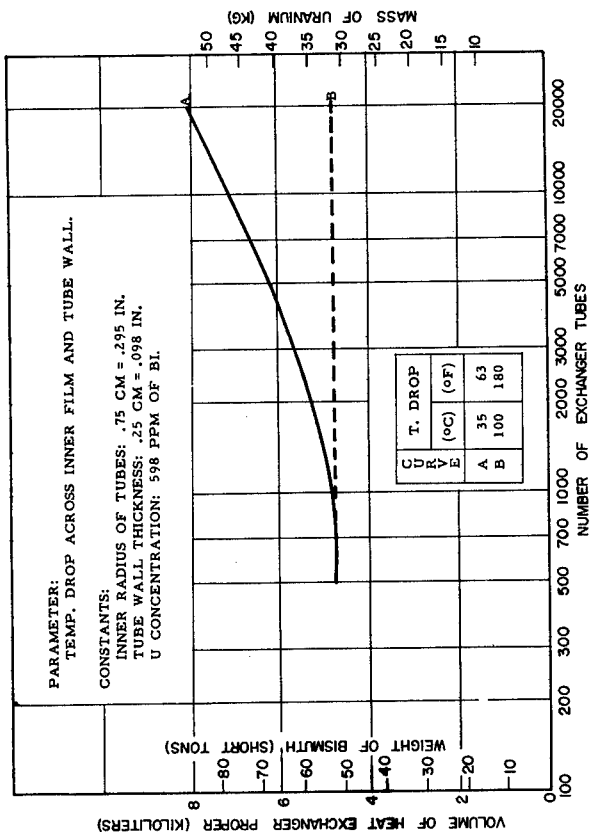


Figure 23b. Mass of uranium in the volume of heat exchanger property vs number of tubes in exchanger. BNL Log No. D-2086.

Tubular Exchanger: Mechanical Pumping

64

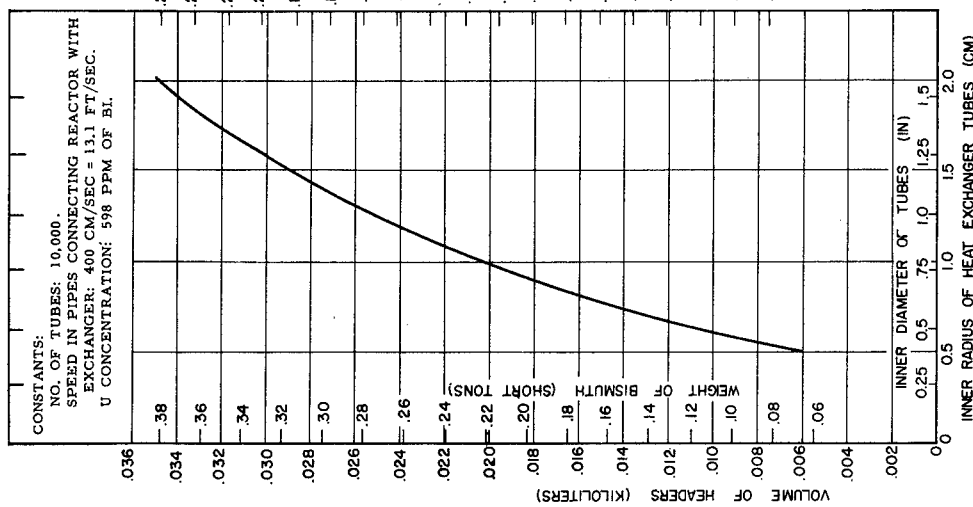


Figure 24a. Mass of uranium in and volume of headers vs inner radius of tubes.
BNL Log No. D-2087.

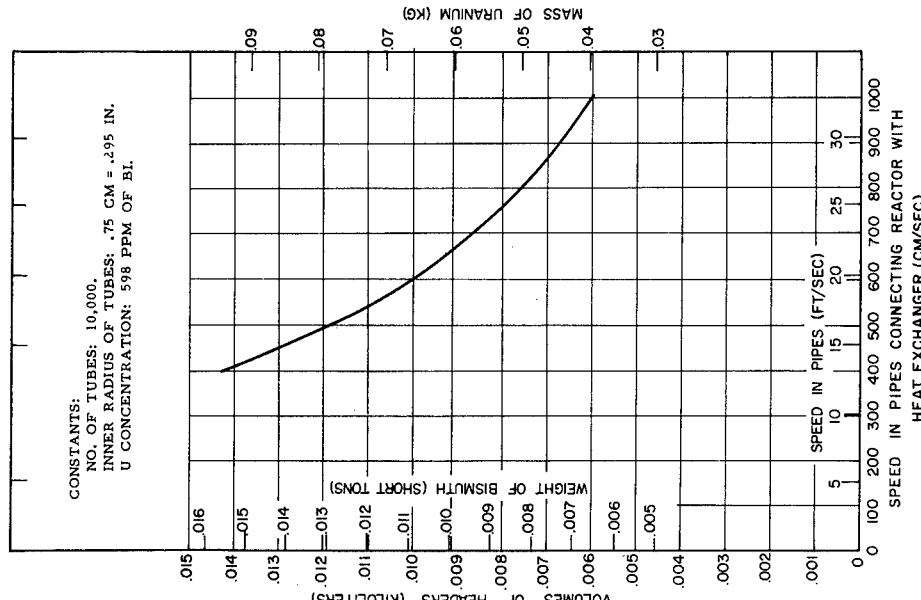


Figure 24b. Mass of uranium in and volume of headers of pipes connecting reactor with heat exchanger. BNL Log No. D-2089.

Tubular Exchanger: Mechanical Pumping

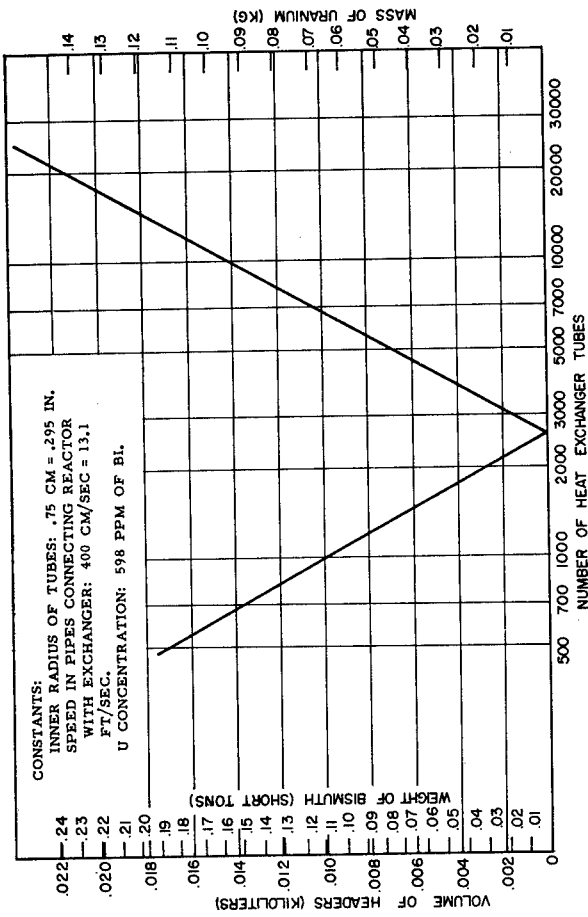


Figure 24c. Mass of uranium in and volume of headers v number of tubes.
BNL Log No. D-2088.

Spray Exchanger: Mechanical Pumping

66

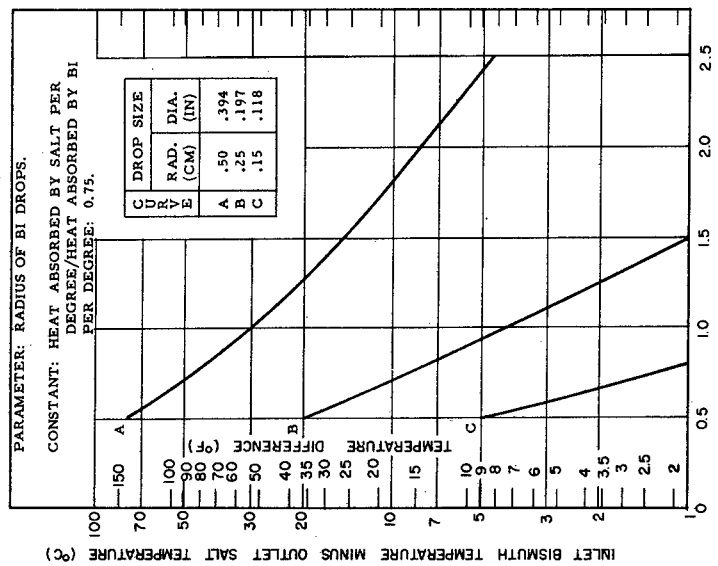


Figure 25a. Temperature drop between inlet bismuth and outlet salt vs time bismuth drops fall.

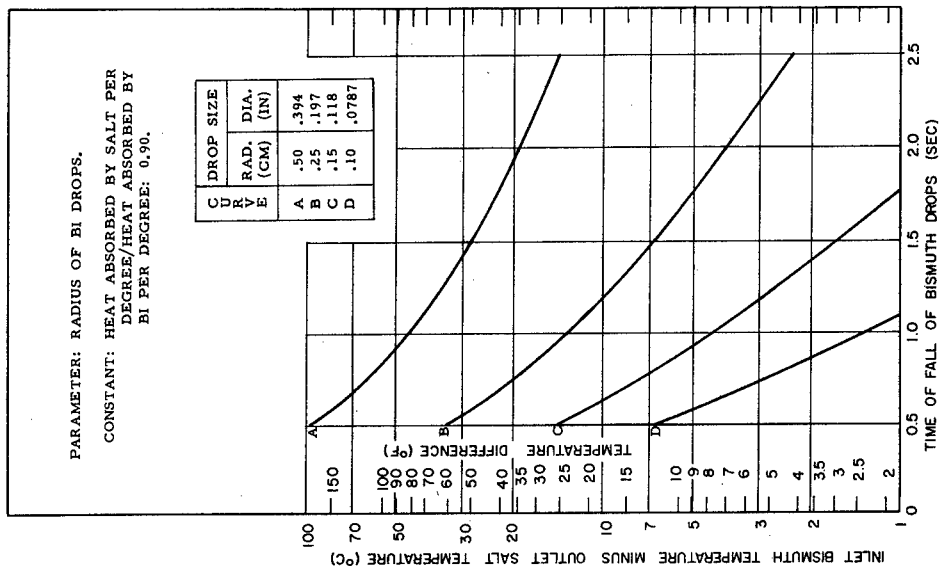


Figure 25b. Temperature drop between inlet bismuth and outlet salt vs time bismuth drops fall.

Spray Exchanger: Mechanical Pumping

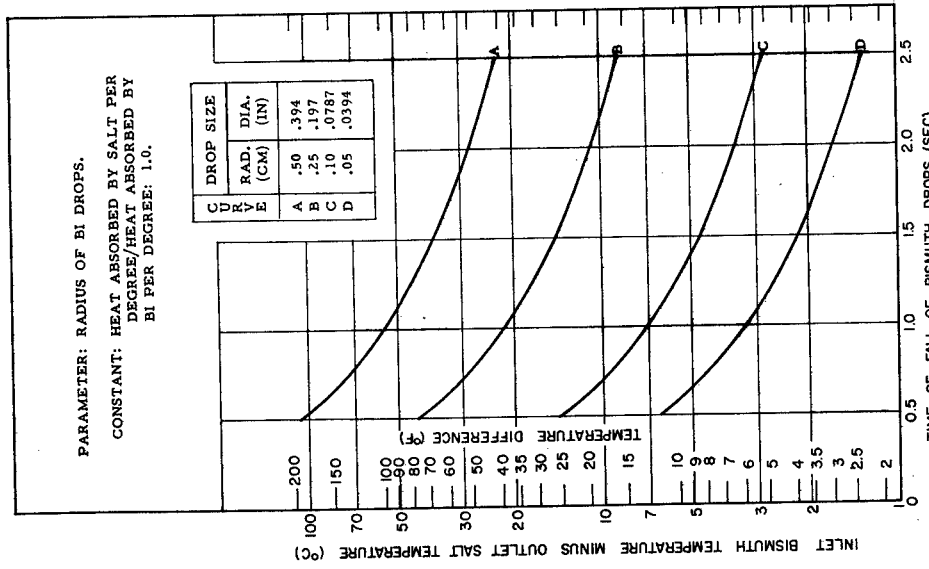


Figure 25c. Temperature drop between inlet bismuth and outlet salt vs time bismuth drops fall.

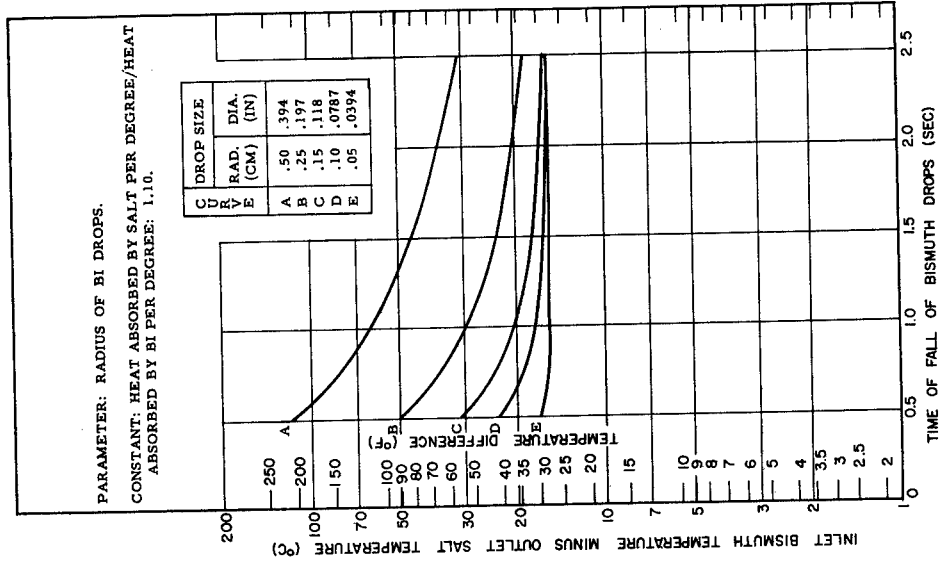


Figure 25d. Temperature drop between inlet bismuth and outlet salt vs time bismuth drops fall.

Spray Exchanger: Mechanical Pumping

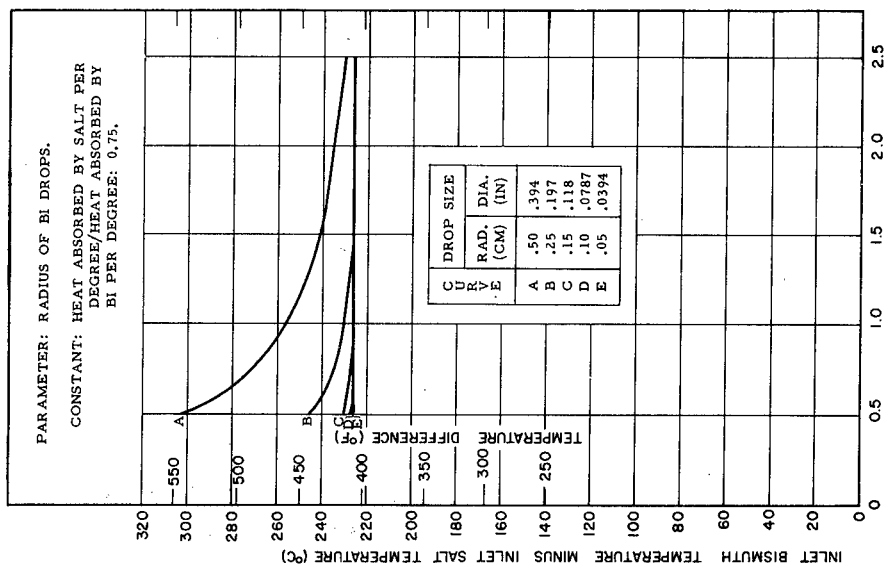


Figure 26a. Temperature drop between inlet bismuth and inlet salt in heat exchanger vs time bismuth drops fall.

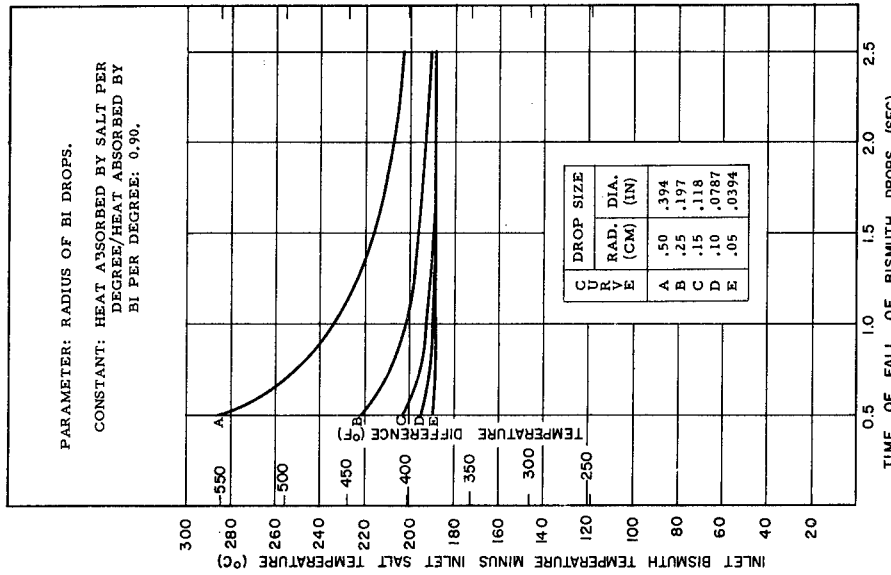


Figure 26b. Temperature drop between inlet bismuth and inlet salt in heat exchanger vs time bismuth drops fall.

Spray Exchanger: Mechanical Pumping

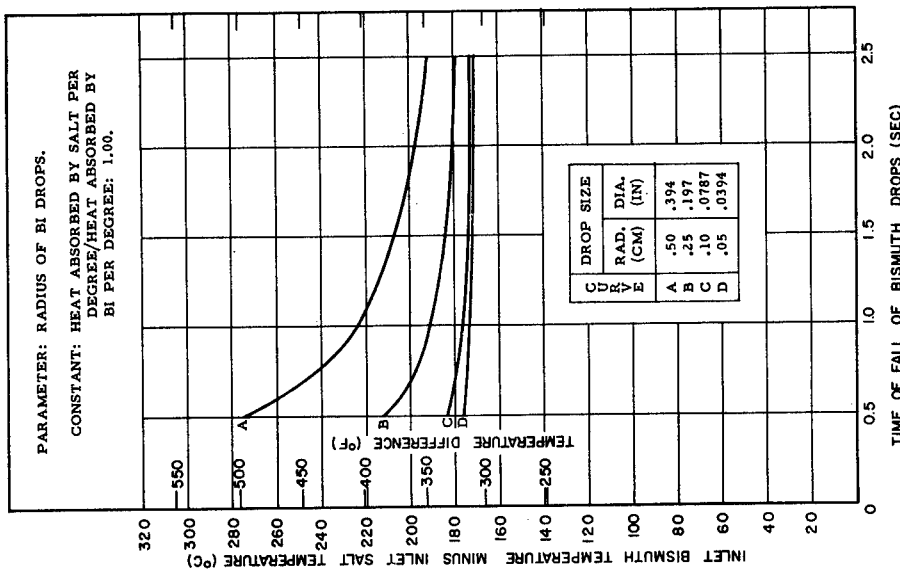


Figure 26c. Temperature drop between inlet bismuth and inlet salt in heat exchanger vs time bismuth drops fall.

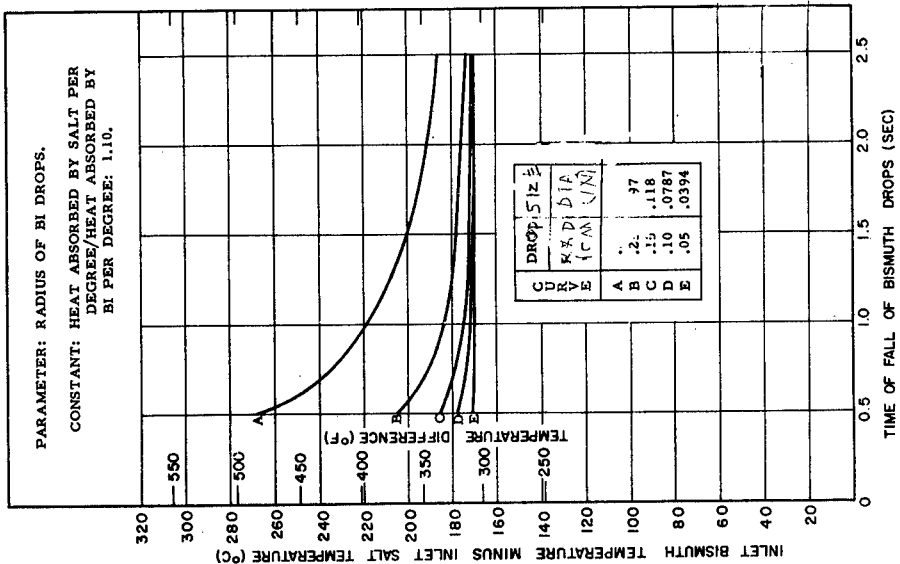


Figure 26d. Temperature drop between inlet bismuth and inlet salt in heat exchanger vs time bismuth drops fall.

Spray Exchanger: Mechanical Pumping

70

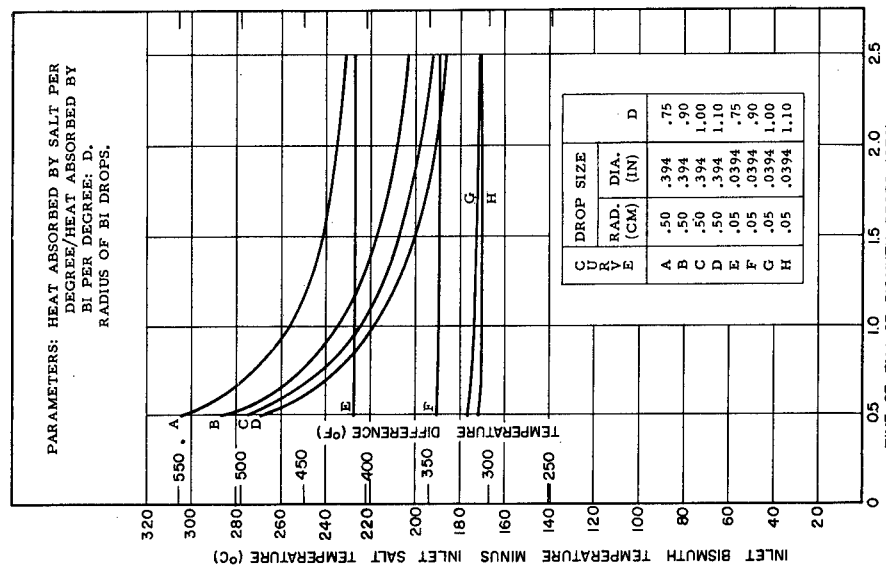


Figure 26e. Temperature drop between inlet bismuth and inlet salt in heat exchanger vs time bismuth drops fall.

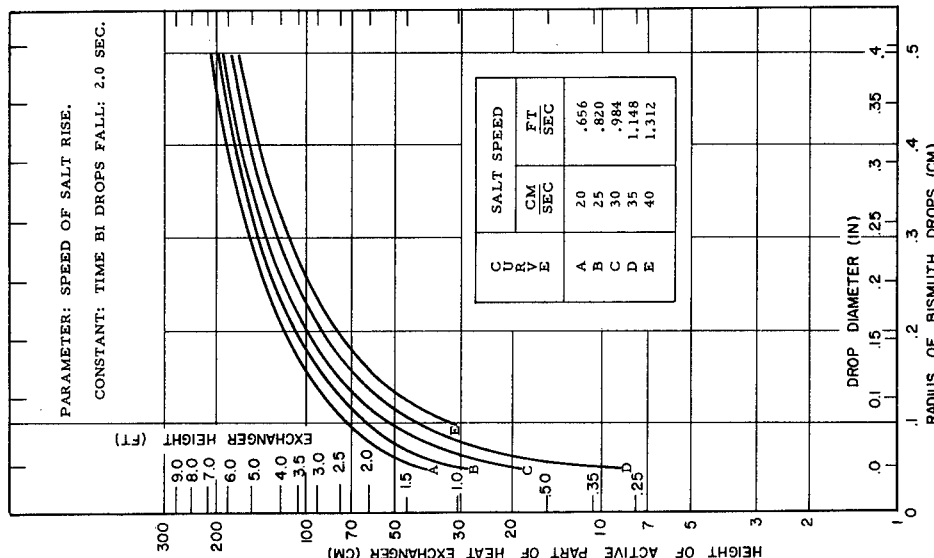


Figure 27a. Height of active part of heat exchanger vs time bismuth drops fall.

Spray Exchanger: Mechanical Pumping

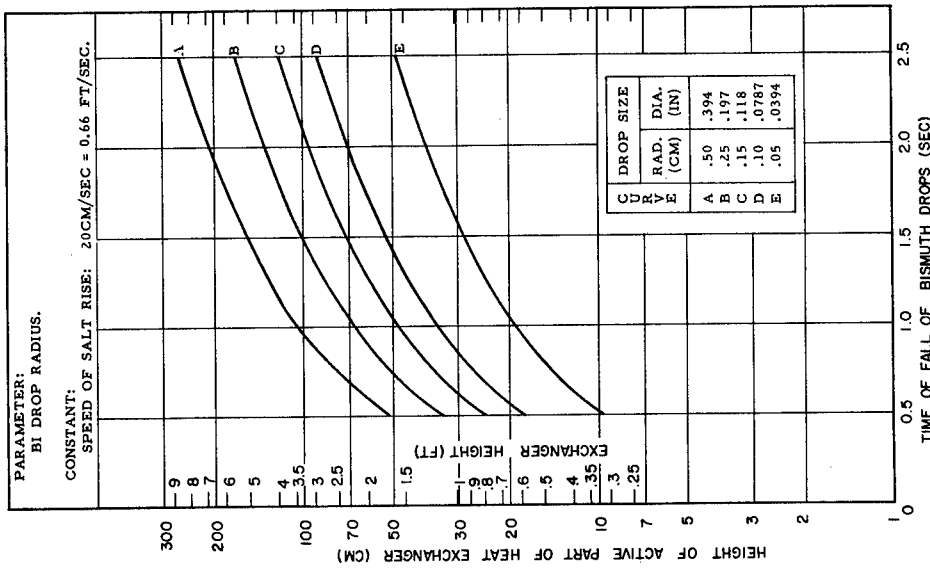


Figure 27b. Height of active part of heat exchanger vs time bismuth drops fall.

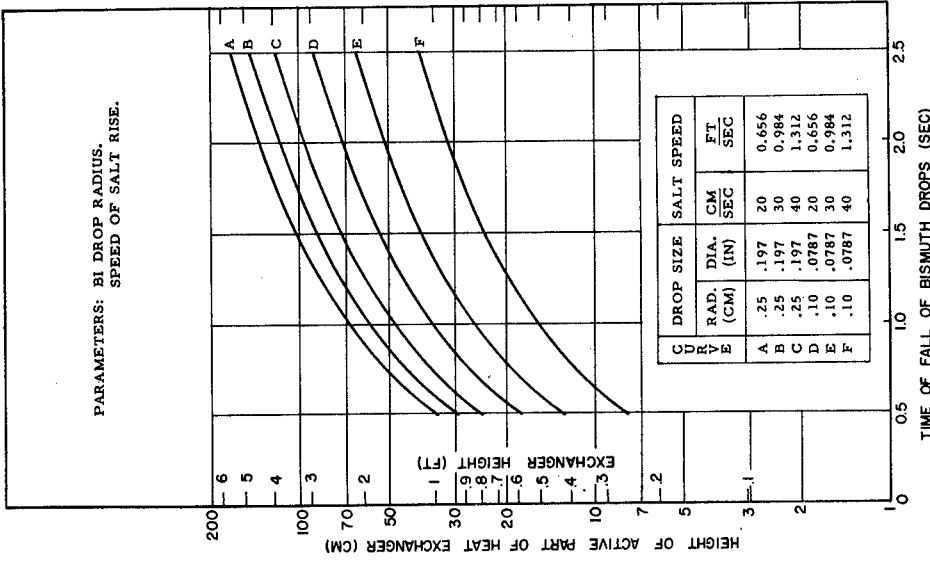


Figure 27c. Height of active part of heat exchanger vs time bismuth drops fall.

Spray Exchanger: Mechanical Pumping

72

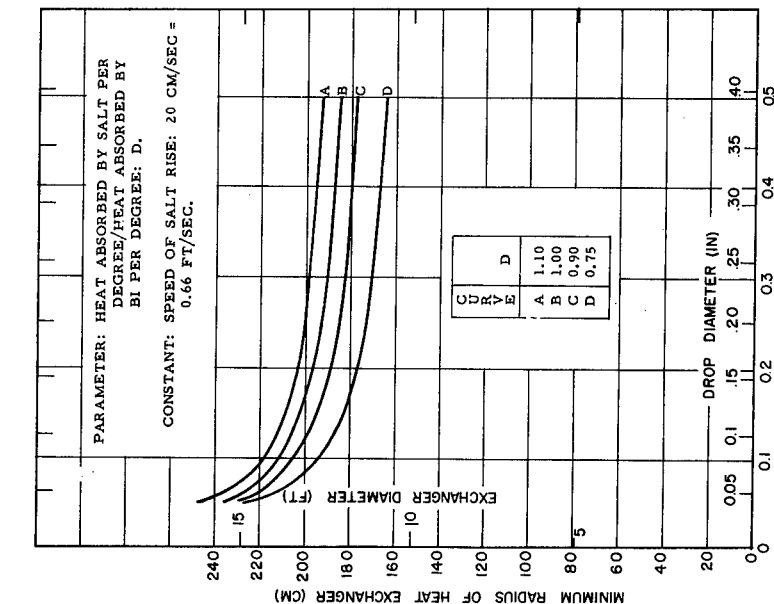


Figure 28a. Minimum radius of heat exchanger vs radius of bismuth drops.

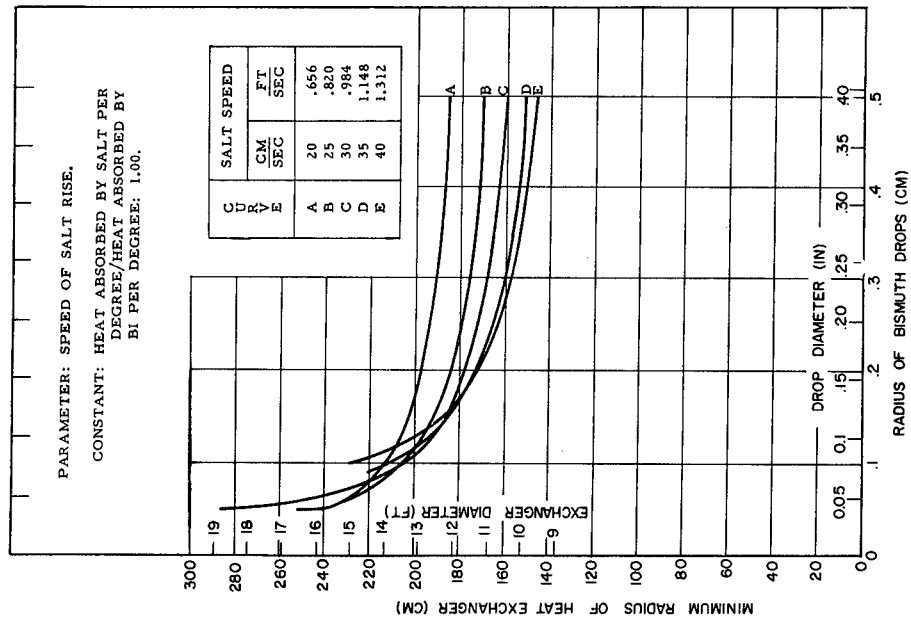


Figure 28b. Minimum radius of heat exchanger vs radius of bismuth drops.

Spray Exchanger: Mechanical Pumping

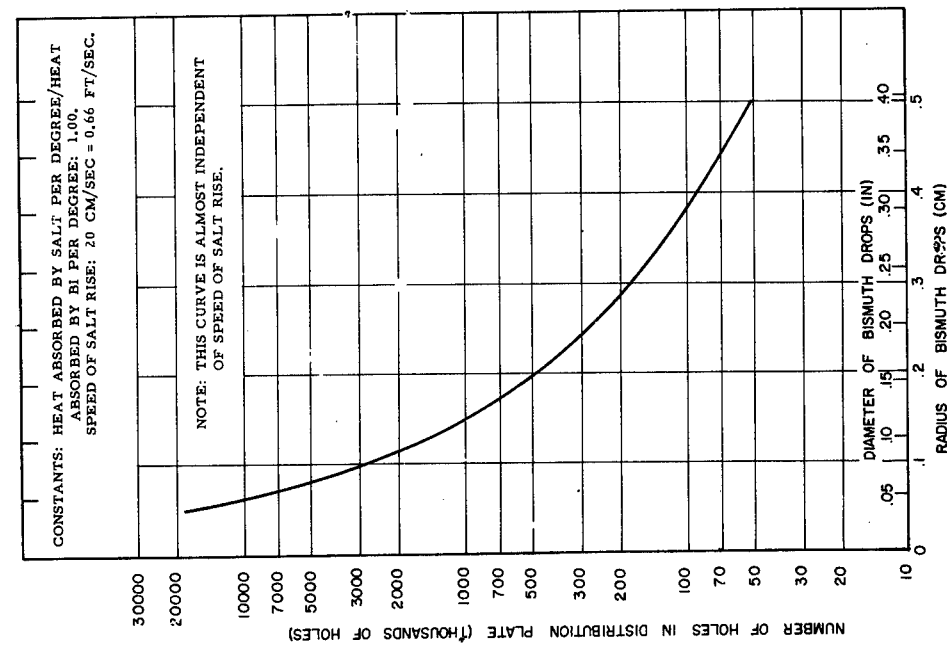


Figure 29a. Number of holes in distribution plate vs radius of bismuth drops.

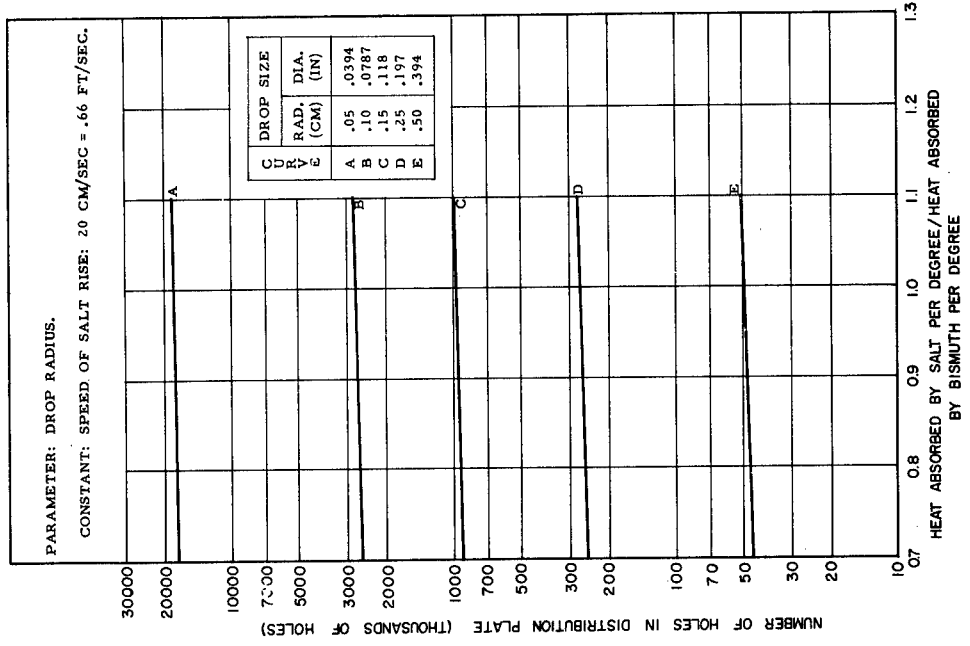


Figure 29b. Number of holes in distribution plate vs ratio of heat absorbed by salt per degree to heat absorbed by bismuth per degree.

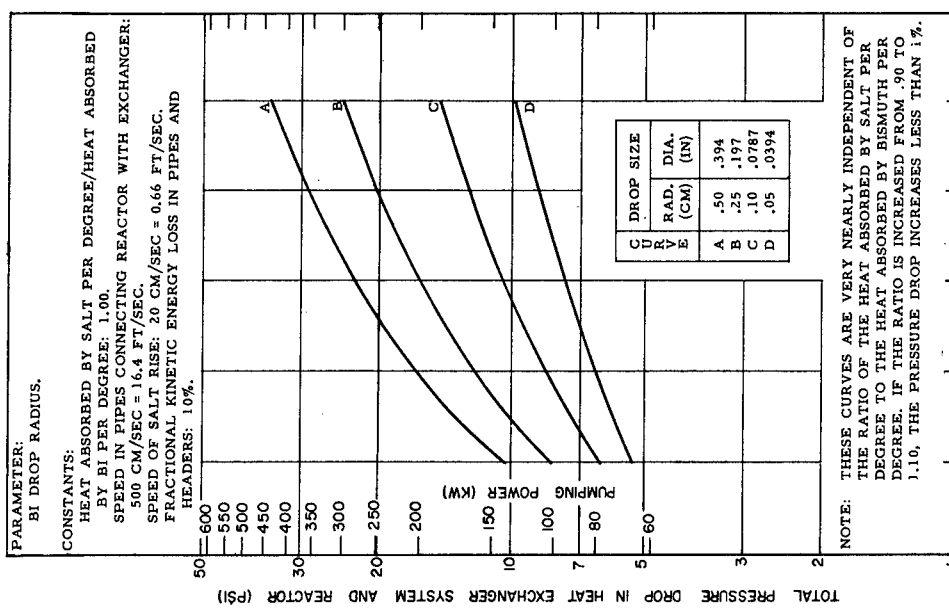


Figure 30a. Total pressure drop and pumping power in heat exchanger system and reactor vs time bismuth drops fall.

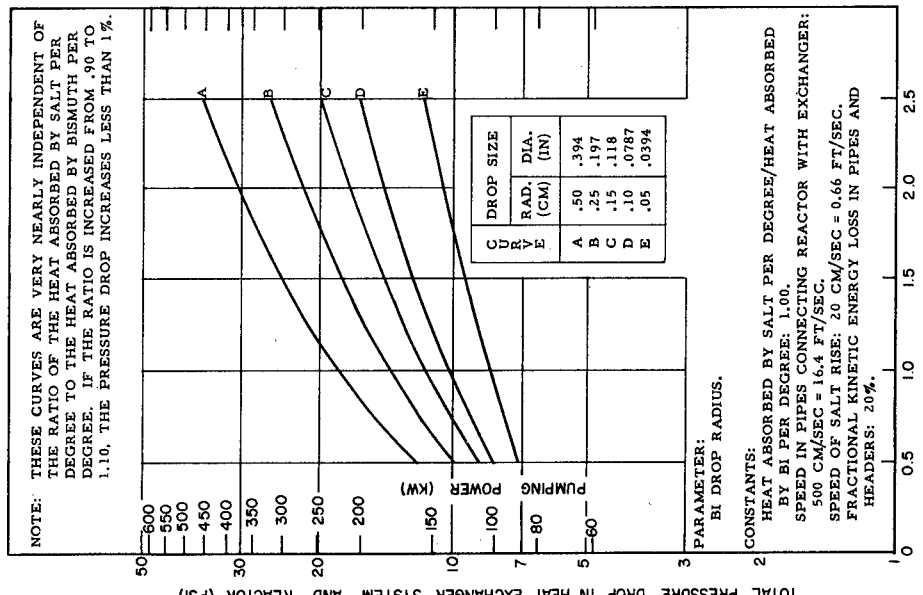


Figure 30b. Total pressure drop and pumping power in heat exchanger system and reactor vs time bismuth drops fall.

Spray Exchanger: Mechanical Pumping

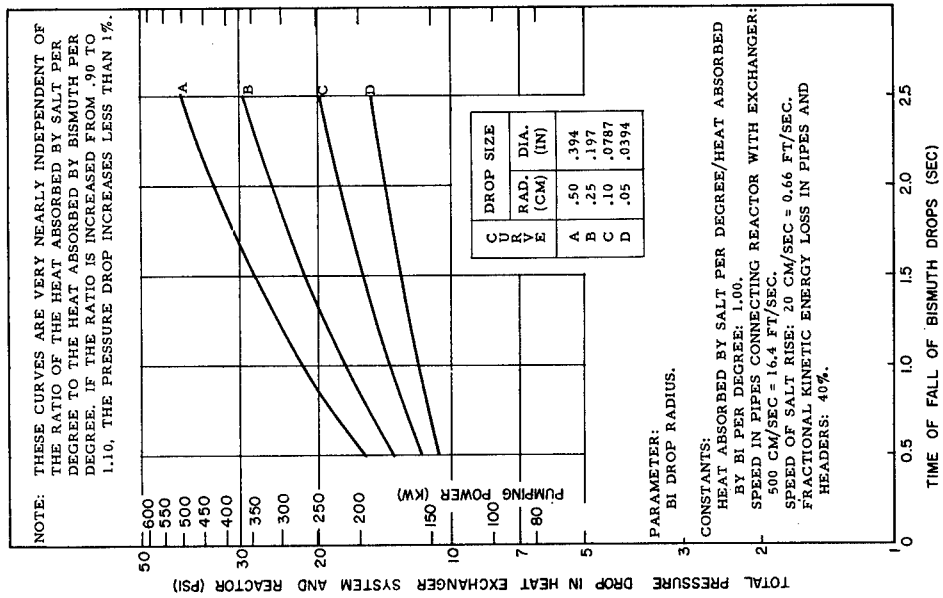


Figure 30c. Total pressure drop and pumping power in heat exchanger system and reactor vs time bismuth drops fall.

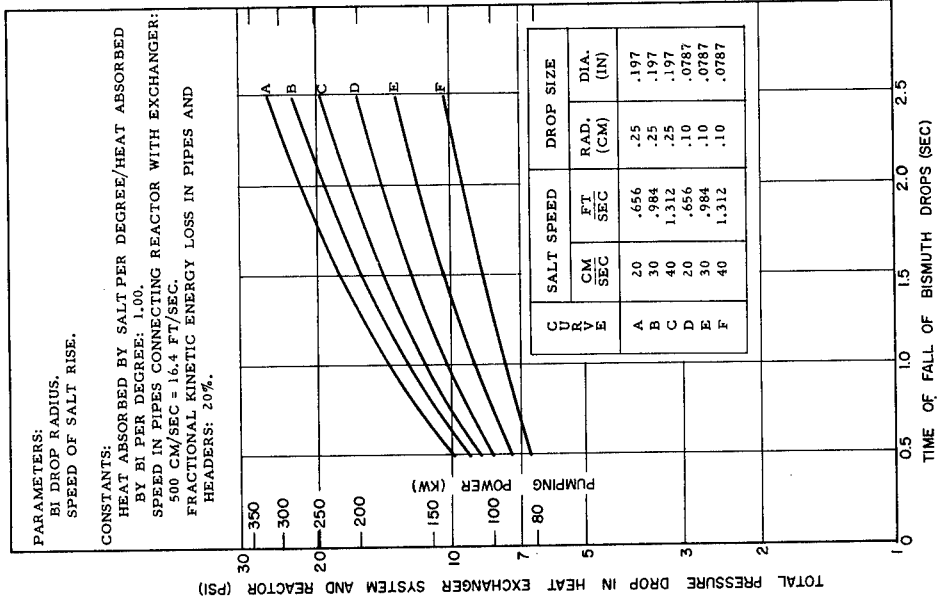


Figure 30a. Total pressure drop and pumping power in heat exchanger system and reactor vs time bismuth drops fall.

Spray Exchanger: Mechanical Pumping

76

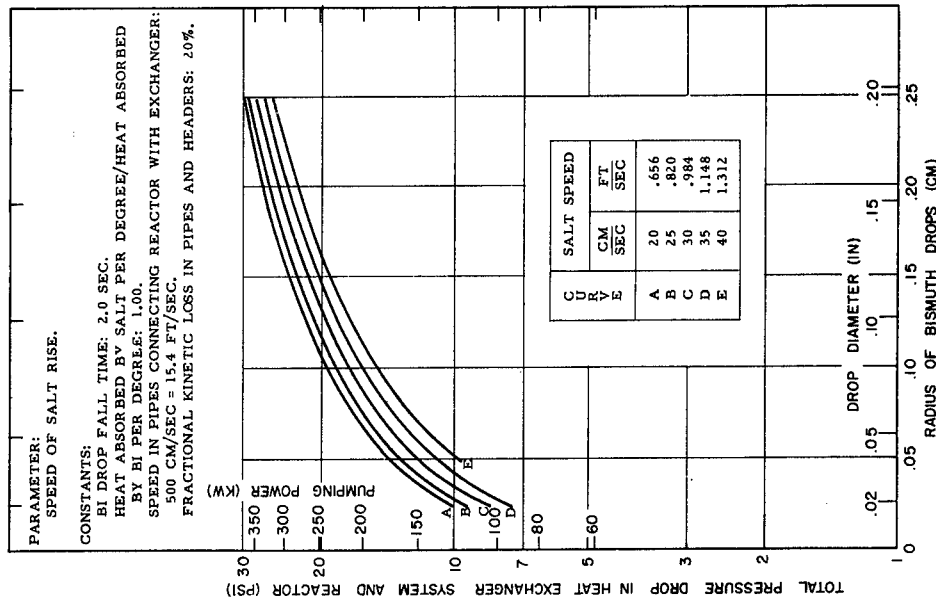


Figure 30e. Total pressure drop and pumping power in heat exchanger system and reactor vs. radius of bismuth drops.

Spray Exchanger: Mechanical Pumping

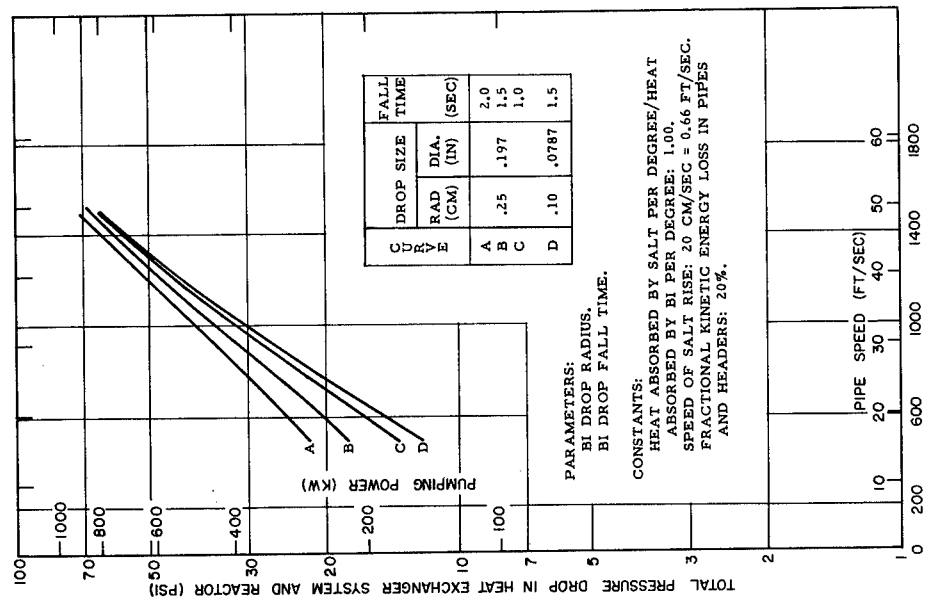


Figure 30f. Total pressure drop and pumping power in heat exchanger system and reactor vs speed in pipes connecting reactor with heat exchanger.

Spray Exchanger: Mechanical Pumping.

78

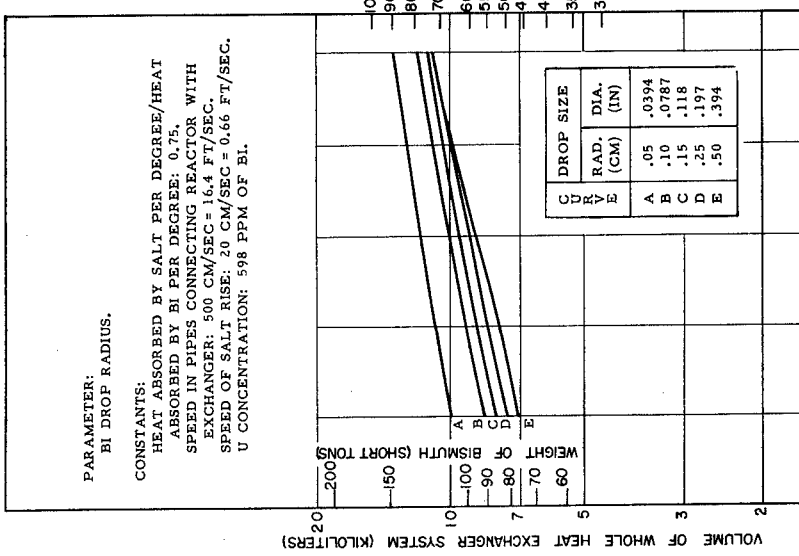


Figure 31a. Mass of uranium in and volume of whole heat exchanger system vs time bismuth drops fall.
BNL Log No. D-2090.

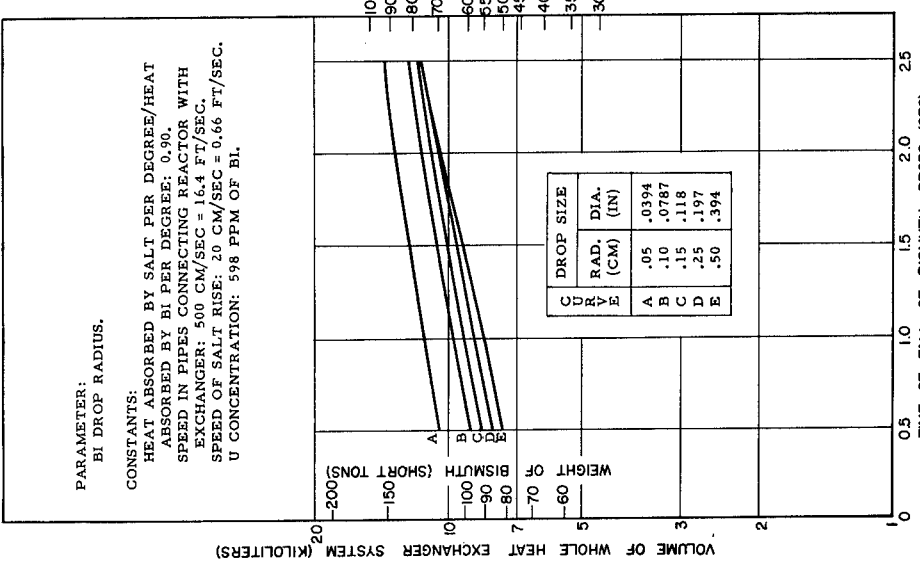


Figure 31b. Mass of uranium in and volume of whole heat exchanger system vs time bismuth drops fall.
BNL Log No. D-2091.

Spray Exchanger: Mechanical Pumping

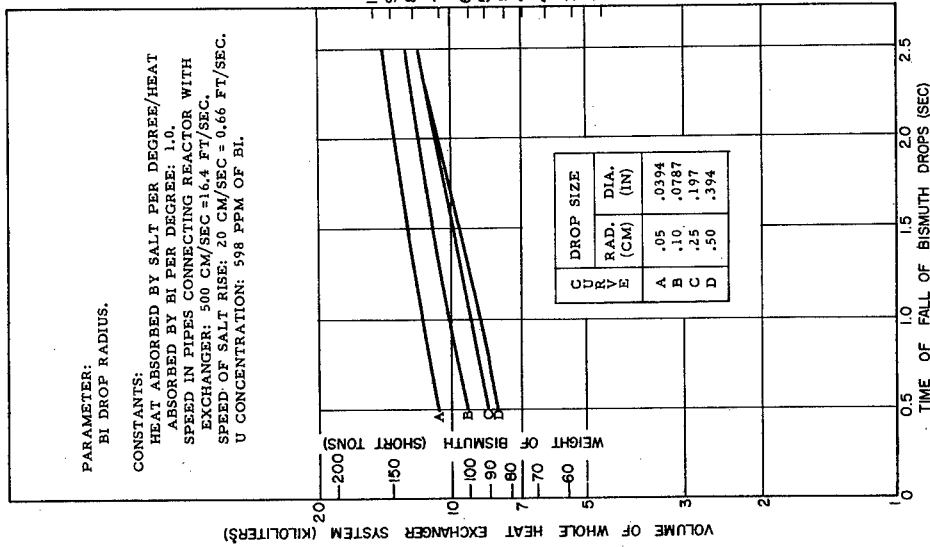


Figure 31c. Mass of uranium in and volume of whole heat exchanger system vs time bismuth drops fall.
BNL Log No. D-2092.

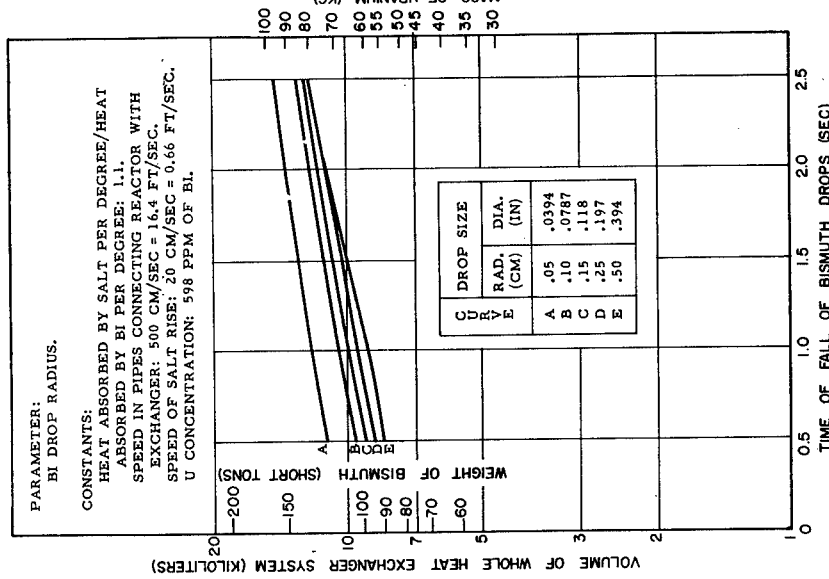


Figure 31d. Mass of uranium in and volume of whole heat exchanger system vs time bismuth drops fall.
BNL Log No. D-2093.

Spray Exchanger: Mechanical Pumping

80

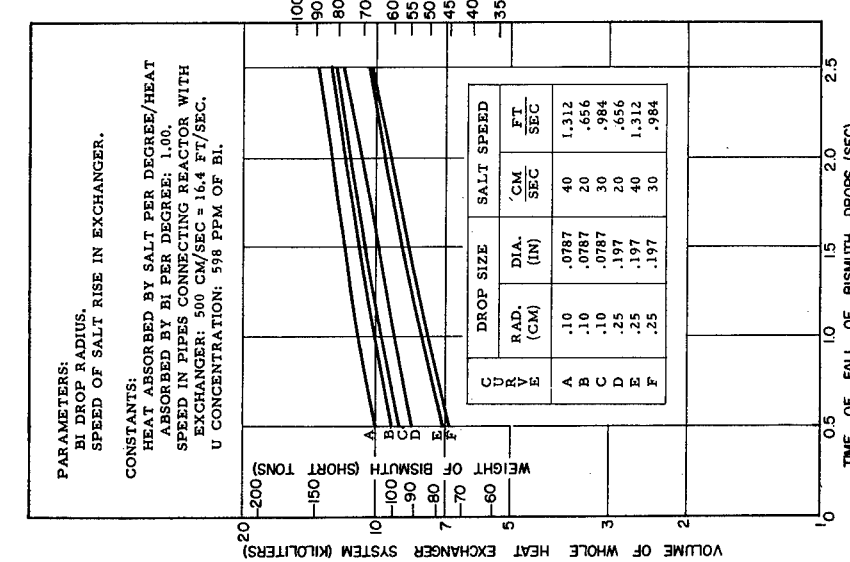


Figure 3le. Mass of uranium in and volume of whole heat exchanger system vs time bismuth drops fall.

BNL Log No. D-2095.

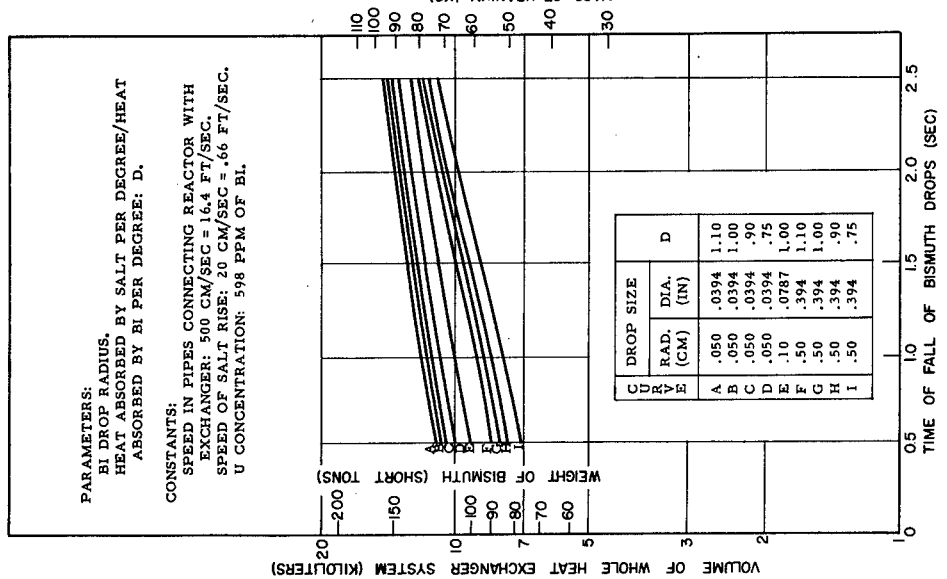


Figure 3lf. Mass of uranium in and volume of whole heat exchanger system vs time bismuth drops fall.

BNL Log No. D-2096.

Spray Exchanger: Mechanical Pumping

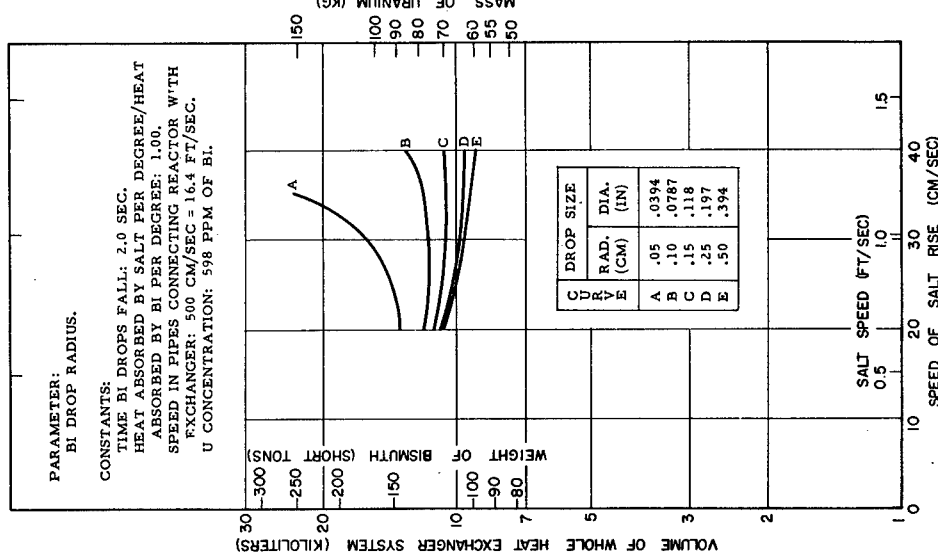


Figure 31g. Mass of uranium in and volume of whole heat exchanger system vs speed of salt rise. BNL Log No. D-2094.

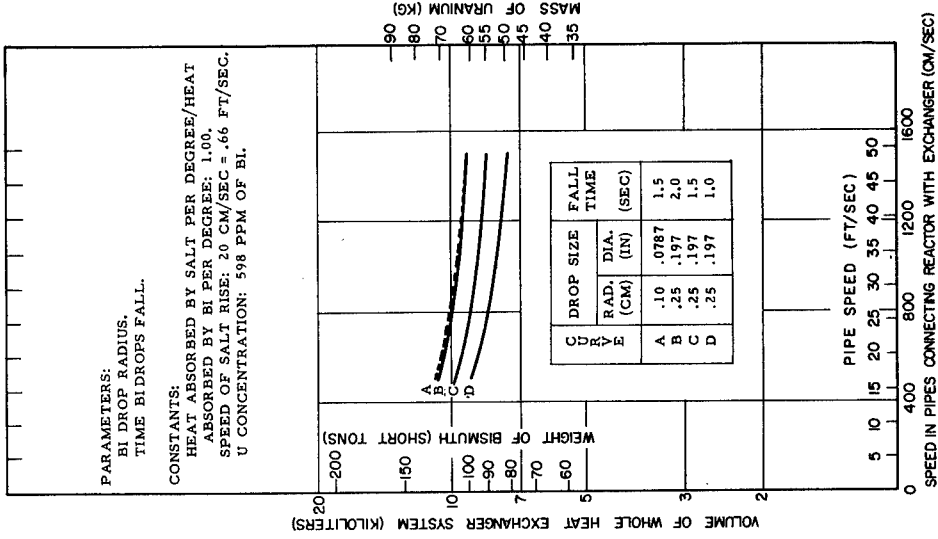


Figure 31h. Mass of uranium in and volume of whole heat exchanger system vs speed in pipes connecting reactor with heat exchanger. BNL Log No. D-2097.

Spray Exchanger: Mechanical Pumping

82

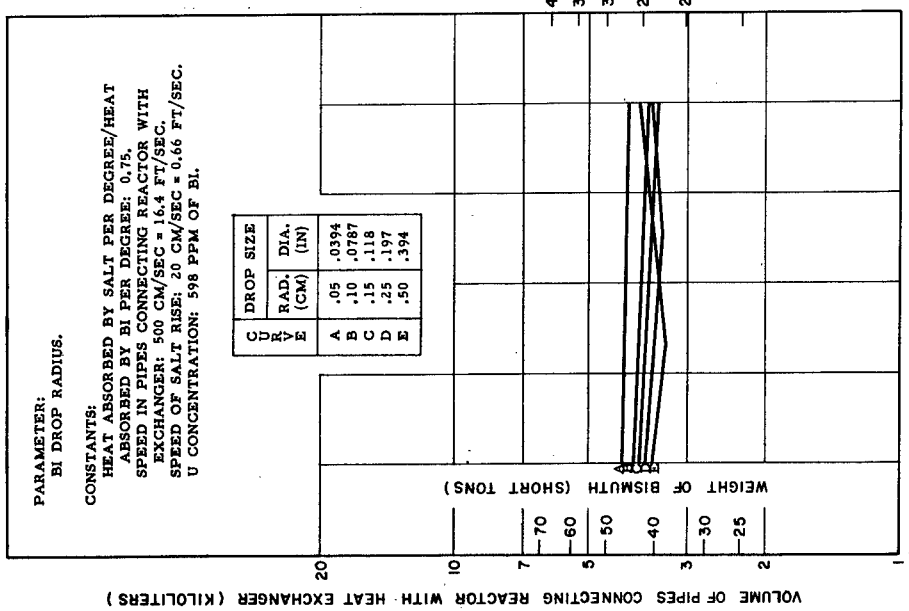


Figure 32a. Mass of uranium in and volume of pipes connecting reactor with heat exchanger vs time bismuth drops fall. BNL Log No. D-2098.

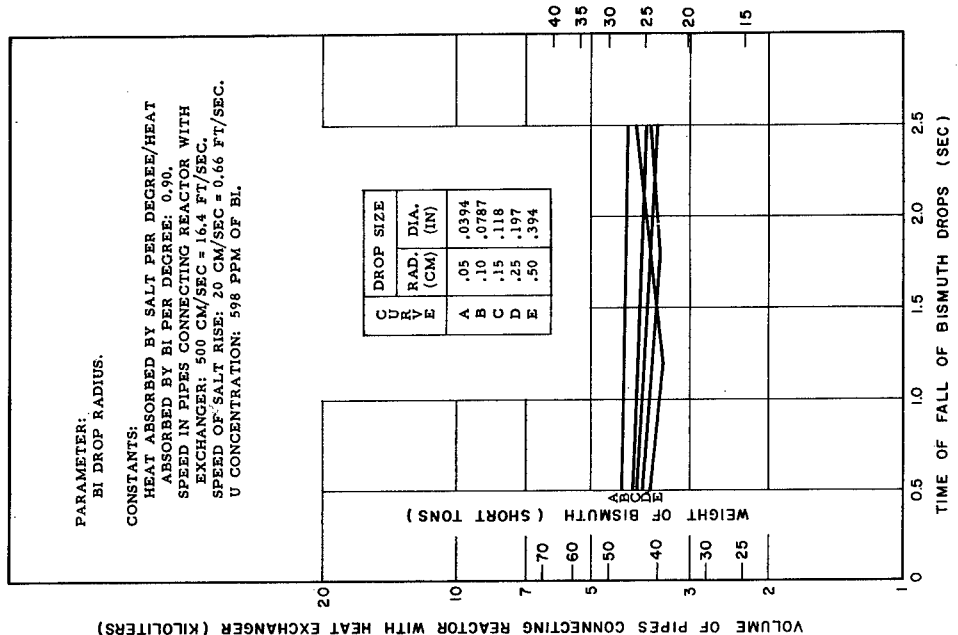


Figure 32b. Mass of uranium in and volume of pipes connecting reactor with heat exchanger vs time bismuth drops fall. BNL Log No. D-2099.

Spray Exchanger: Mechanical Pumping

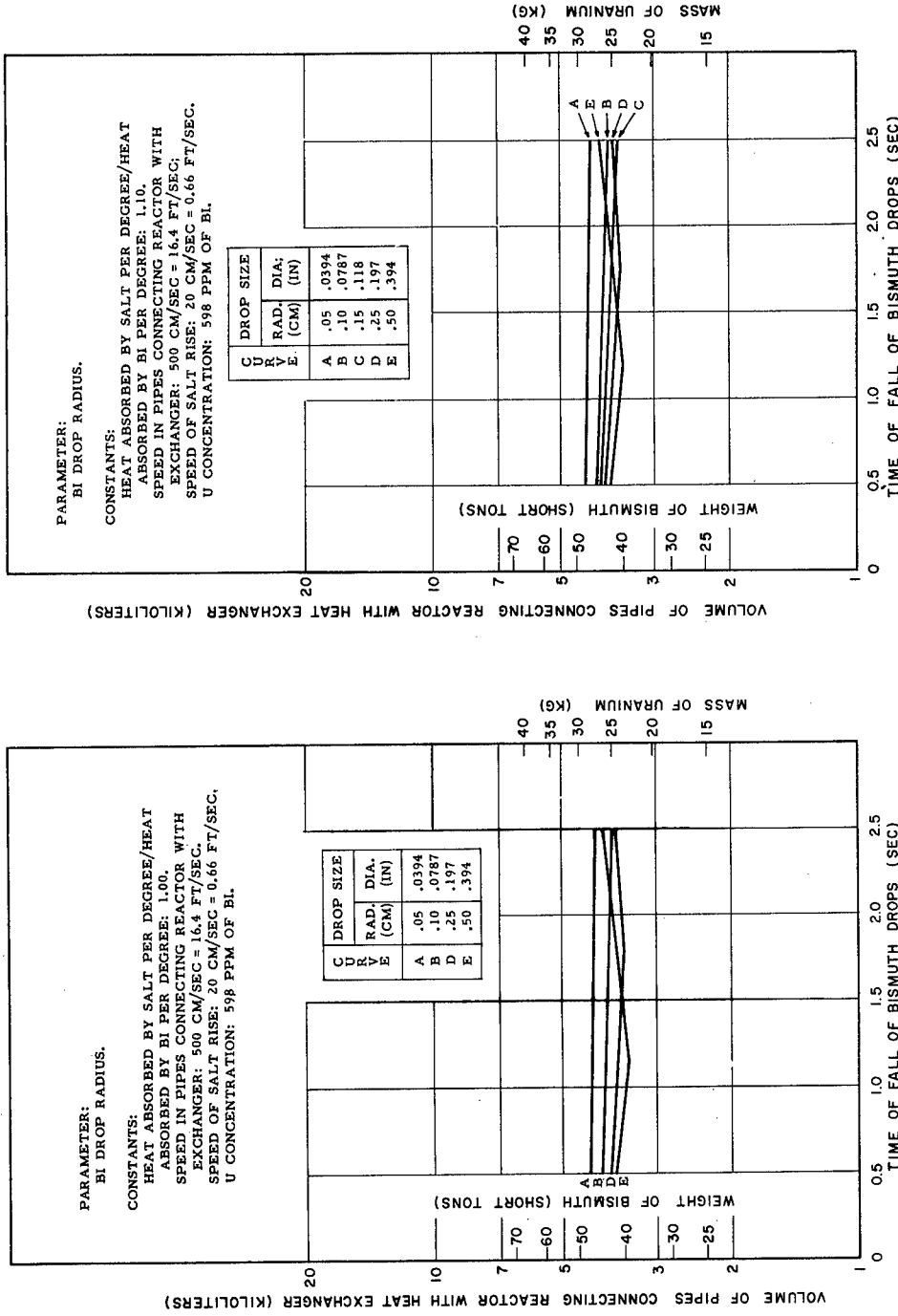


Figure 32c. Mass of uranium in and volume of pipes connecting reactor with heat exchanger vs time bismuth drops fall. BNL Log No. D-2100.

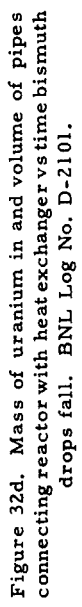


Figure 32d. Mass of uranium in and volume of pipes connecting reactor with heat exchanger vs time bismuth drops fall. BNL Log No. D-2101.

Spray Exchanger: Mechanical Pumping

84

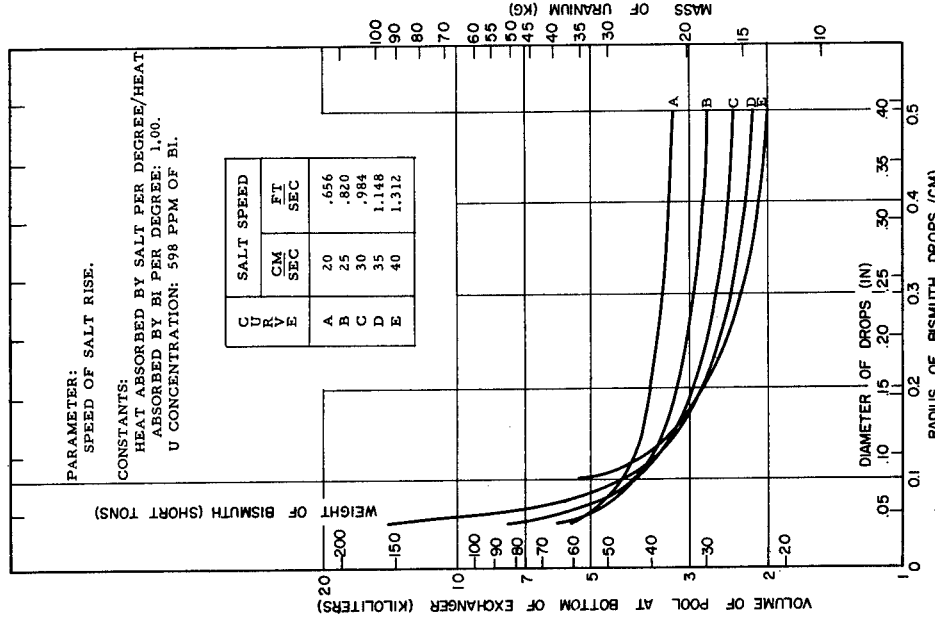
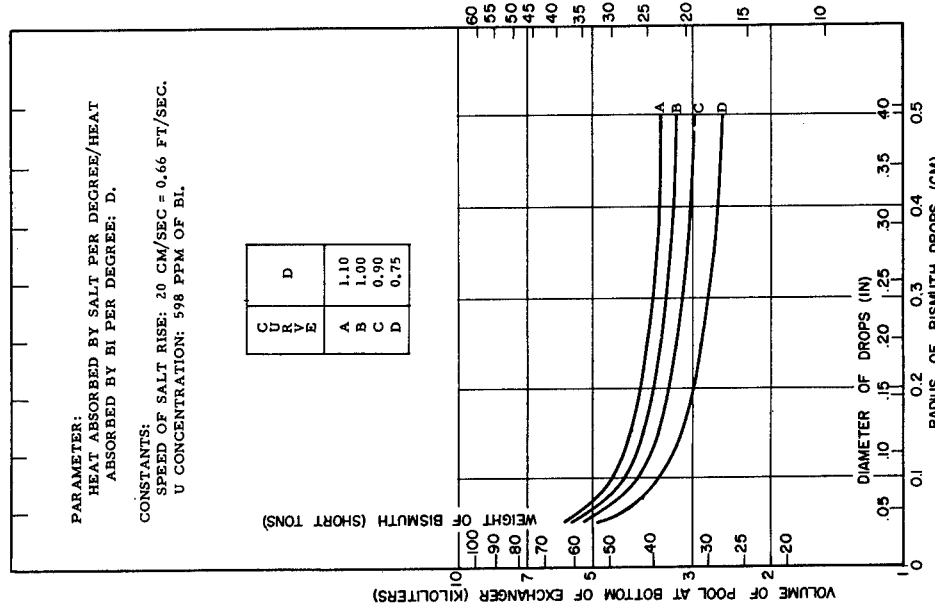
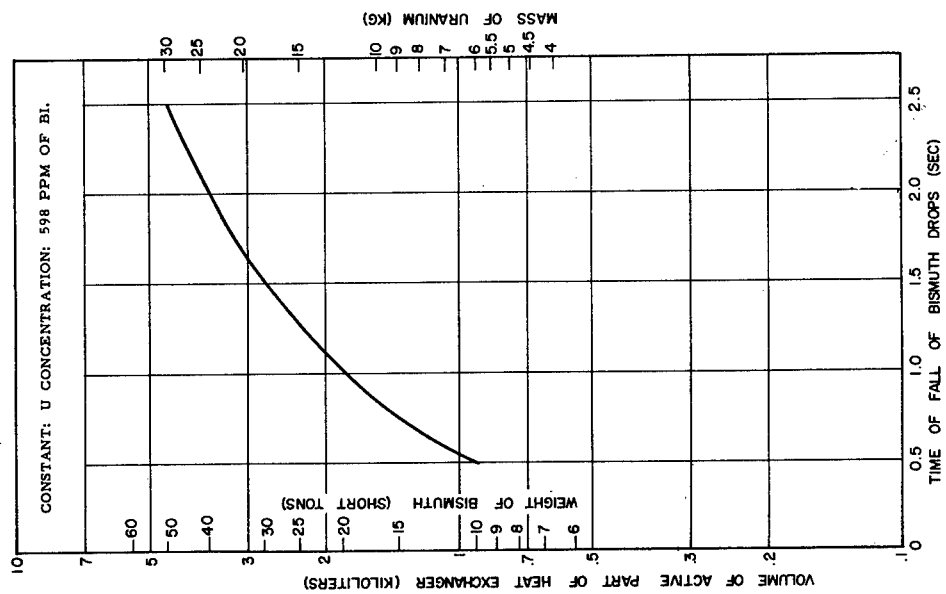


Figure 33a. Mass of uranium in and volume of pool at bottom of heat exchanger vs radius of bismuth drops. BNL Log No. D-2102.

Figure 33b. Mass of uranium in and volume of pool at bottom of heat exchanger vs radius of bismuth drops. BNL Log No. D-2103.

Spray Exchanger: Mechanical Pumping



★ U. S. GOVERNMENT PRINTING OFFICE: 1956 O— 376513

Figure 34. Mass of uranium in and volume of active part of heat exchanger vs time bismuth drops fall. BNL Log No. D-2104.